Ecological and environmental controls on the fine-scale distribution of cold-water corals in the North-East Atlantic

Laurence Hélène De Clippele

Submitted for the degree of Doctor of Philosophy

Heriot-Watt University

The School of Energy, Geoscience, Infrastructure and Society

February 2018

ABSTRACT

This thesis integrated acoustic, high-definition video and hydrodynamic data to study the distribution, morphology and ecology of cold-water corals (CWC) in the Mingulay Reef area (Chapter 2), the Tisler Reef area (Chapter 3) and the Logachev Mound area (Chapter 4). A new British Geological Survey (BGS) ArcGIS seabed mapping toolbox was developed and quantified semi-automatically the morphometric and acoustic characteristics of CWC reefs. Over 500 *Lophelia pertusa* reef mounds were delineated and characterised at the Mingulay Reef Complex (Chapter 2), 14 at the Tisler Reef (Norway) (Chapter 3) and 123 in the Logachev Area (Chapter 4). These reefs all had large amounts of small round-shaped mounds. Additionally, the Logachev area had very large dendriform-shaped mounds. A microbathymetric grid of the central area of the Mingulay Reef was used to identify individual live coral colonies (1-7 m) that provided data to predict the likelihood of presence of live coral colonies on biogenic reef mounds (Chapter 2). The distribution and morphology of *L. pertusa* colonies and the sponges *Mycale lingua* and *Geodia* sp. within the Tisler Reef, revealed the importance of local hydrodynamics and substrate availability (Chapter 3). Non-scleractinian corals associated with the Logachev mounds (Chapter 4) proved to be abundant, biodiverse and function as a habitat for associated organisms. Differences in their distribution were found to be related to food supply, the availability and stability of settling substrates. This thesis showed that the BGS Seabed Mapping Toolbox is useful to study the ecology and morphology of reef mounds within and between reefs. Studies on the fine-scale spatial distribution of corals within reefs provided information on the ecology of CWCs.

ACKNOWLEDGEMENTS

I would like to start by thanking my academic supervisor Murray Roberts for broadening my expertise, always enthusiastically introducing me to the wider scientific community and allowing me to take up "non-academic" opportunities which prepared me for post-PhD life. I would also like to thank my second supervisor Veerle Huvenne for being a great inspiration, giving endless amounts of feedback, kind words and for encouraging my critical thinking. I'm also immensely grateful for the Heriot-Watt University James Watt Scholarship which funded my PhD. Doing this PhD, moving to Edinburgh and meeting wonderful people along the way has truly been the best thing that has ever happened to me, and for this I am eternally grateful.

My great thanks go to Lene and Pål Buhl-Mortensen, Tomas Lundälv, Susanna Strömberg and Ann Vanreusel. Thank you for taking me under your wings at the beginning of my career and introducing me to the beauty and science of cold-water coral habitats. I also owe thanks to Seb, Fiona, Lea-Anne, Alan, Laura, Katherine, Kat, Laure, Johanne, Afiq and Lissie. Thank you for being amazing colleagues and friends, and for supporting me throughout the good and more difficult times. I treasure the laughs and experiences from Skye, Boston, Portugal, Southampton, Tjärnö and the Celtic Explorer. Special thanks go to Joanna and Cova, for their kindness, critical thinking and for sharing their wisdom and skills which have helped me a lot throughout writing this PhD and publishing papers.

I am blessed to have the family I do and couldn't be more grateful to them. Thank you for being supportive of my career, life choices and for sending me endless amounts of *Chokotoffs*! I am grateful for my incredible friends Jennie, Nikki, Heather, Hannah MC, Anna, Leila, Loris, Jon, Mounsey and Swany. I would like to offer my special thanks to Hannah I. for being an amazing friend, inspiration and stimulation during my PhD. Thank you all for being so supportive at all times. Deep gratitude is reserved for my *schattie* Jack, who I would like to thank for all the stimulating discussions and feedback but especially for the love, silliness and laughter which added much happiness throughout this adventure.

DECLARATION STATEMENT

ACADEMIC REGISTRY

Research Thesis Submission

Name*:*	Laurence De Clippele		
School:	The School of Energy, Geoscience, Infrastructure and Society		
Version:	First	Degree Sought:	Doctor of Philosophy

Declaration

In accordance with the appropriate regulations I hereby submit my thesis and I declare that:

1) the thesis embodies the results of my own work and has been composed by myself
2) where appropriate, I have made acknowledgement of the work of others and have made reference to work carried out in collaboration with other persons
3) the thesis is the correct version of the thesis for submission and is the same version as any electronic versions submitted*.
4) my thesis for the award referred to, deposited in the Heriot-Watt University Library, should be made available for loan or photocopying and be available via the Institutional Repository, subject to such conditions as the Librarian may require
5) I understand that as a student of the University I am required to abide by the Regulations of the University and to conform to its discipline.
6) I confirm that the thesis has been verified against plagiarism via an approved plagiarism detection application e.g. Turnitin.

* *Please note that it is the responsibility of the candidate to ensure that the correct version of the thesis is submitted.*

Signature of Candidate*:*		Date:	

Submission

Submitted By *(name in capitals):*	
Signature of Individual Submitting:	
Date Submitted:	

For Completion in the Student Service Centre (SSC)

Received in the SSC by *(name in capitals):*			
Method of Submission *(Handed in to SSC; posted through internal/external mail):*			
E-thesis Submitted (mandatory for final theses)			
Signature:		Date:	

CONTENT

LIST OF PUBLICATIONS BY THE CANDIDATE

Chapter 2 has been published as:

De Clippele LH, Gafeira J, Robert K, Hennige S, Lavaleye MS, Duineveld GCA, Huvenne VAI, Roberts JM (2016) Using novel acoustic and visual mapping tools to predict the small-scale spatial distribution of live biogenic reef framework in cold-water coral habitats. Coral Reefs 36(1): 255-268

Chapter 3 has been published as:

De Clippele LH, Lundälv T, Huvenne VAI, Hennige SJ, Fox A, Orejas C, Roberts JM (2017). The effect of the local hydrodynamics on the spatial extent and morphology of cold-water coral habitats at the Tisler Reef, Norway. Coral Reefs 37(1): 253-266

Other publications and co-authorships:

De Clippele LH, Buhl-Mortensen P, Buhl-Mortensen L (2015) Fauna associated with cold water gorgonians and sea pens. Continental Shelf Research 105: 67-78

Henry L-A, Stehmann M, De Clippele LH, Golding N, Roberts JM (2016) Seamount egg-laying grounds of the deepwater skate *Bathyraja richardsoni* (Garrik 1961). Journal of Fish Biology 89: 1473-1481

Hummel H, Frost M, Juanes JA, Kochman J, Castellanos Perez Bolde CF, Aneiros F, Vandenbosch F, Franco JN, Echavarri B, Guinda X, Puente A, Fernández C, Galván C, Merino M, Ramos E, Fernández P, Pitacco V, Alberte M, Wojcik D, Grabowska M, Jahnke M, Crocetta F, Carugati L, Scorrano S, Fraschetti S, Pérez García P, Sanabria Fernández JA, Poromov A, Iurchenko A, Isachenko A, Chava A, Pavloudi C, Bordeyne F, Andersen SF, Tunka Eronat EC, Cakmak T, Louizidou Pm, Rico J, Ruci S, Corta Diego D, Mendez S, Rousou M, De Clippele L, Eriksson A, Van Zanten W, Diamant A, Fernández De Matos VK (2015) A comparison of the degree of implementation of marine biodiversity indicators by European countries in relation to the Marine Strategy Framework Directive (MSFD). Journal of the Marine Biological Association of the United Kingdom p 1-13

Vansteenbrugge L, Hostens K, Vanhove B, De Backer A, De Clippele LH, De Troch M (2016) Erratum to: Trophic Ecology of *Mnemiopsis leidyi* in the southern North Sea; a biomarker approach. Marine Biology 163: 25

AUTHOR CONTRIBUTIONS

De Clippele LH, Gafeira J, Robert K, Hennige S, Lavaleye MS, Duineveld GCA, Huvenne VAI, Roberts JM (2016) Using novel acoustic and visual mapping tools to predict the small-scale spatial distribution of live biogenic reef framework in cold-water coral habitats. Coral Reefs 36(1): 255-268

Design of the work: De Clippele LH and Gafeira J designed the presented work. The work was based on Gafeira J her previous work on pockmarks for which she developed an ArcGIS toolbox to study pockmarks using a bathymetry map. Together with De Clippele LH, Gafeira J adjusted the toolbox to map coral reef mounds.

Data collection: Roberts M, Huvenne VA, Lavaleye MS and Duineveld GCA provided the HD-video data and the bathymetry maps for this article.

Data analyses and interpretation: De Clippele LH performed the data analyses. Robert K provided an R script for the statistical analyses. Gafeira J assisted with the interpretation of the results from the BGS Seabed Mapping Toolbox.

Drafting the article: De Clippele LH wrote the article.

Critical revision of the article: All the co-authors critically revised the article. Roberts JM and Huvenne VAI are the supervisors of this thesis that is funded by the James Watt Studentship at Heriot-Watt University.

De Clippele LH, Lundälv T, Huvenne VAI, Hennige SJ, Fox A, Orejas C, Roberts JM (2017) The effect of the local hydrodynamics on the spatial extent and morphology of cold-water coral habitats at the Tisler Reef, Norway. Coral Reefs 37(1): 253-266

Design of the work: De Clippele LH designed the presented work.

Data collection: De Clippele LH, Cova Orejas and Lundälv T collected the HD video data. Lundälv T provided the bathymetric data. The hydrodynamic data used in this study is with the courtesy of White M and Guihen D.

Data analyses and interpretation: Fox A analysed the hydrodynamic data. De Clippele LH analysed the remaining data.

Drafting the article: De Clippele LH wrote the article.

Critical revision of the article: All the co-authors critically revised the article. Roberts JM and Huvenne VAI are the supervisors of this thesis that is funded by the James Watt Studentship at Heriot-Watt University.

CHAPTER 1 - INTRODUCTION

1.1 General Introduction

Cold-water corals occur throughout the world's oceans (Figure 1.1) where the benthic habitats they form are constructed by only a handful of scleractinian coral species (Roberts et al. 2009a, Roberts and Cairns 2014). Cold-water coral reefs are ecologically important as they are hotspots of biomass and biodiversity (Costello et al. 2005, Buhl-Mortensen et al. 2010), function as breeding and nursing grounds for fish (Baillon et al. 2012) and sharks (Henry et al. 2013), are paleoclimatic archives (Douarin et al. 2014) and recycle carbon along continental margins (van Oevelen et al. 2009).

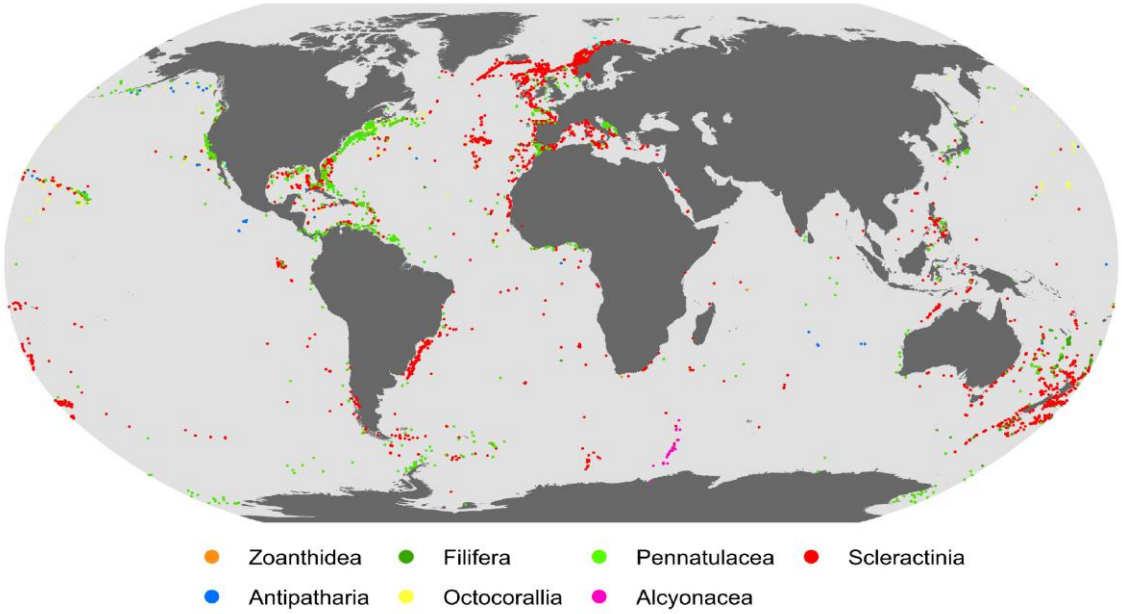

Figure 1.1 Global distribution of cold-water corals, which include records for the subclass Octocorallia and four Orders (in Class Anthozoa): Scleractinia (reef-forming corals), Antipatharia (black corals), Zoanthidae (encrusting or button polyps), and Pennatulacea (sea pens). Occurrence records are also available for the order sub-Order Filifera (lace corals) in Class Hydrozoa. Figure by Freiwald et al. (2017)

Humans have increasingly caused ecological changes in the whole marine environment (Halpern et al. 2008). The reasons for changes in marine ecosystems are varied and complex, but can be split into direct anthropogenic influences such as coral exploitation and trade (Grigg 1965, Bruckner 2001), pollution (Purser and Thomsen 2012, Cordes et al. 2016), habitat destruction by bottom fishing activities (Althaus et al. 2009, Clark et al. 2016) or indirect influences which include climate change and related disturbances to ocean biogeochemistry involving ocean warming, altered stratification and food supply, ocean acidification and de-oxygenation (Ruhl and Smith 2004,

Keeling et al. 2010, Mora et al. 2013, Long et al. 2016). These changes extend now to great depths affecting cold-water coral habitats. In the 1990s, advances in technology allowed us to explore the deeper parts of our oceans with camera systems which showed us severe damage and habitat losses worldwide (Freiwald et al. 2004). Because cold-water corals are of great ecological importance but are sensitive to anthropogenic impacts and climate change they are considered as Vulnerable Marine Ecosystems by OSPAR (Duran Munoz and Sayago-Gil 2011). Therefore, cold-water coral ecosystems are protected in national and international waters.

This PhD-project aims to increase the understanding on the effect of environmental forces on the fine-scale spatial distribution, morphology and ecology of live and dead cold-water coral colonies within reefs and cold-water coral carbonate mounds. By increasing the knowledge on cold-water corals, their importance becomes clearer, and new methods to monitor them can be developed. This provides policymakers with the necessary information to protect cold-water coral reefs in a changing ocean.

1.2 What are cold-water coral reefs?

A reef is defined as a submerged structure that rises from the surrounding seafloor (Bosence 1979, EC 1996, Birkeland 1997, Wood 1999). Corals form biogenic reefs, as they are built up from the skeletal remains of the reef organism themselves and other organisms such as the tubes of serpulid polychaete worms (EC 1996, Roberts 2005), the skeletons of other scleractinian corals and siliceous sponges (Douarin et al. 2014). Cold-water coral habitats are benthic habitats that are physically distinct areas of seabed, associated, with in this case, a diverse range of coral species (Harris and Baker 2012a). However, among the 17 stony cold-water coral species (Scleractinia, Cnidaria) (Cairns 2007) that produce skeletal frameworks, only six (*Enallopsammia profunda*, *Goniocorella dumosa*, *Lophelia pertusa*, *Madrepora oculata*, *Oculina varicosa* and *Solenosmilia variabilis*) are currently known to form important cold-water coral reef habitats (Roberts et al. 2009a). In the study areas discussed in this thesis, which are located in the northeast Atlantic and northeastern part of the Skagerrak (Norway), the dominant reef-framework building coral is *L. pertusa*, with *M. oculata* as an important secondary species (Rogers 1999, Roberts et al. 2003, Freiwald et al. 2004). Other cold-water corals such as gorgonians, antipatharians (black corals), and hydrocorals, can develop dense aggregations that also provide significant structural habitat for other species (e.g. Bo et al. 2012, De Clippele et al. 2015).

The cold-water coral *L. pertusa* was first described by Linnaeus (1758) and is mentioned in other early works (Pontoppidan 1755, Gunnerus 1768, Fleming 1846, Gosse 1860). The preferred

temperature range of *L. pertusa* seems to be between 6-8 ◦C (Frederiksen et al. 1992, Freiwald 1998). However, this species has been recorded in reefs with temperatures varying from 4 to 14 °C (Zibrowius 1980, Freiwald 1998, Fosså et al. 2002). Studies have shown that *L. pertusa's* metabolism increases with increasing temperatures (Dodds et al. 2007, Davies et al. 2009). When food supply meets the needs to support an increase in its metabolism, the coral will grow. If not, the coral will reduce its growth and can starve (Dodds et al. 2007, Davies et al. 2009). *Lophelia pertusa* is commonly found at depths between 200 and 1000 m, but also as shallow as 39 m in Trondheimsfjorden in Norway (Mortensen et al. 2000) and has been found as deep as 3000 m in the Atlantic (Squires 1959). The majority of *L. pertusa* records in the northeast Atlantic coincide with zones of relatively low dissolved oxygen of 3-5 mL L^{-1} and a salinity of 35-37 (Rogers 1999, Taviani et al. 2005). Globally, the depth of the aragonite saturation horizon (ASH) is also a limiting factor for this coral's occurrence. Aragonite is the primary form of calcium carbonate which is secreted by the scleractinian coral during coral growth (Clode et al. 2010). Sea water below the ASH is undersaturated with respect to calcium carbonate (Orr et al. 2005). Near this depth, the calcification of cold-water corals is hampered, and gradually their aragonite framework begins to dissolve (Guinotte et al. 2006, Cairns 2007, Lunden et al. 2013). The calcite or carbonate compensation depth (CCD) is similar to the ASH but is located at a deeper depth as calcite is less soluble than aragonite (Berger 2016). Scleractinian corals do not use calcite as a primary material to build their skeleton, but can under certain circumstances be produced as a secondary material to fill pore space (Houck et al. 1975, Higuchi et al. 2014). Even though *L. pertusa* is able to grow at broad temperature, salinity, oxygen and depth ranges, its ability to do so varies on the combination of these variables and with food availability (Dodds et al. 2007, De'ath et al. 2012).

Unlike many warm-water scleractinian corals, *L. pertusa* is azooxanthellate and thus not living in association with micro-algal endosymbionts (*Symbiodinium*). This lack of an algal symbiosis allows for a species distribution outside of the photic zone (Zibrowius 1980). In the 1990s it was speculated that some of the deep-water coral reefs are associated with the areas affected by submarine hydrocarbon seepage (the '*hydraulic theory'*). A direct dependence of cold-water corals on locally increased nutrient fluxes associated with methane emissions is here assumed (Hovland 1990, Hovland et al. 1998). However, to date, researchers failed to find any indications of fluid seepage in the majority of the deep-water coral reefs (Duineveld 2004, Etiope et al. 2010). Instead, *L. pertusa* appears to be an opportunistic feeder capable of taking a variety of food. Data obtained so far indicate that cold-water coral communities rely on the delivery of phytoplankton, organic matter, and/or zooplankton derived from near-surface primary productivity (Heinrich and Freiwald 1997, Mortensen et al. 2001, Roberts and Anderson 2002, Dodds et al. 2009). Food supply to reef

sites varies considerably both spatially and temporally (Duineveld et al. 2004, Duineveld et al. 2007, Davies et al. 2009, section 1.3).

1.3 Why are cold-water coral reefs important?

The human population size is currently around 7.6 billion and is growing by 1.10 % per year, adding 83 million people annually (United Nations 2017). Biodiversity is essential to ensure human wellbeing as it sustains all life processes and supports the production of food, fuels, fibres, medicine and genetic material (Millennium Ecosystem Assessment 2005, Harris and Baker 2012b). Biological diversity is defined by the Convention on Biological Diversity (CBD) as 'the variability among living organisms from all sources including … terrestrial, marine and other aquatic ecosystems and the ecological complexes of which they are part: this includes diversity within species, between species and of ecosystems'. Species are interdependent components of ecosystems, and when removing any one species the ecosystem's resilience and functioning decreases (Harris and Baker 2012b).

Tropical rain forests and coral reefs are the most species rich and diverse ecosystems in the world (Millennium Ecosystem Assessment 2005, Knowlton and Jackson 2008). The total area of coral reefs in the world's oceans is estimated to be about 255,000 km^2 (Spalding and Greenfell 1997, Freiwald et al. 2017) (Figure 1.1). The diversity in the ocean is much greater compared to the terrestrial ecosystems (28 of 35 animal phyla with one-third only to be found in the marine environment) (Primack 2006). This difference is likely a consequence of the older age of the ocean, the fact that it covers a much greater volume, the degree of isolation of certain seas, the relative environmental stability and specialization. Studies have showed that species richness in samples is greater than in shallow water (Gage 1996, Levin and Gage 1998, Gray et al. 1997, Gray 2001, Levin et al. 2001). However, there are also areas where species richness is low, and dominance is high such as in oxygen minimum zones, below upwelling regions, in isolated basins, hydrothermal vents. Here hypoxia and organic matter enrichment are believed to lower the diversity (Sanders 1969, Levin et al 1997, Grassle et al 1985, Grassle 1989).

1.4 Environmental controls on cold-water coral reefs

The initiation and development of coral reefs become possible when cold-water coral colonisation and growth happen under favourable environmental regimes (Freiwald et al. 1997, Kenyon et al. 2003, de Haas et al. 2009). The 'environmental control theory', assumes that environmental factors control the distribution of cold-water corals. These environmental factors include temperature, salinity and oxygen availability (Roberts et al. 2009a). The availability of hard substrates like worm tubes, coral rubble, or mollusc shells is also necessary for corals to settle (Wilson 1979).

Cold-water corals are found to grow in regions with a relatively high surface productivity and enhanced hydrodynamic energy (e.g. Genin et al. 1986, Frederiksen et al. 1992, Rogers 1999, White 2005, De Mol et al. 2012a), delivering food particles through a variety of hydrodynamic mechanisms including strong bottom currents (Mienis et al. 2007), retention within Taylor columns (White et al. 2005), tidal downwelling and breaking internal waves (Frederiksen et al. 1992, Mienis et al. 2007, Davies et al. 2009, van Haren et al. 2014).

Living coral polyps feed on particles suspended in the water and their encounter rate with food increases when current speeds are higher (Frederiksen et al. 1992, Mortensen 2001, Thiem et al. 2006). In particular, phytoplankton is predominantly captured at higher flow velocities of 0.5 cm s^{-1}, but zooplankton is successfully captured at lower flow velocities of 0.2 cm s^{-1} (Purser et al. 2010). When the flow velocities become higher than 0.5 cm s^{-1}, prey capture efficiency drops (Chamberlain and Graus 1975, Sebens and Johnson 1991). These hydrodynamic systems are pathways in which currents can deliver regularly pulses of warm, nutrient-rich water to the corals in the deep sea. Local hydrodynamics are also crucial for coral larval dispersal and recruitment, and it keeps the corals free from smothering sediments (Brooke et al. 2009, Larsson and Purser 2011). Another mechanism to supply the corals with food is through the redistributing of suspended particles in near-bed mixing layers (Frederiksen et al. 1992, White et al. 2005, Thiem et al. 2006, Mueller et al. 2014). The roughness of the topography of a coral reef and the framework of individual coral colonies, can affect the degree of turbulence in and around the reef (Reidenbach et al. 2006). The food capture of corals and the delivery of food, dissolved gases and larvae to the boundary layer can be impacted by the level of turbulence for both an individual coral and the reef (Chamberlaine and Graus 1975, Reidenbach et al. 2006).

To summarise, the presence, distribution and abundance of cold-water corals depends on the temperature, salinity, oxygen, hydrodynamics, the supply of larvae, the availability of settling substrate and food supply. However, anthropogenic impacts such as trawling, and climate change can also affect the corals distribution (see section 1.7).

1.5 Morphology of cold-water coral reefs

During the last glacial, the range of cold-water corals was restricted to more temperate zones due to ice-sheet discharge and grounding, cooler surface temperatures and reduced surface water productivity (Frank et al. 2011). Since the beginning of the current interglacial, the Holocene, cold-water coral reef growth has generally increased as ice sheets retreated, sea surface temperatures increased and ocean circulation recovered (Douarin et al. 2013, Henry et al. 2014). Almost all of the

world's continental shelves were emergent 20,000 years ago during the last ice age, when global sea level was around 120 m below its present position (Harris and Baker 2012a). Therefore, all species found on continental shelves today are relatively recent arrivals who were able to colonize the shelf as sea level rose and created new habitat (Harris 2012). Reefs which have developed after the last glacial are typically smaller in size, have a strong substrate control and owe their overall morphology to the features they colonised (e.g. Sula Ridge, Mingulay Reef Complex, Tisler Reef), and are therefore classified by Wheeler et al. 2007 as having an 'inherited' morphology (Freiwald et al. 1999, van Weering et al. 2003, Wheeler et al. 2007).

In some cases, a topography supporting live cold-water corals is the result of the growth of the corals themselves, giving rise to cold-water coral carbonate mounds. When the morphology of a mound reflects that of the dominant hydrodynamic controls, Wheeler et al. 2007 classified these mounds as having a 'developed' morphology (Darwin Mounds, Logachev Mounds). These large mound structures (Chapter 4) have developed over glacial-interglacial time periods (Kenyon et al. 2003, van Weering et al. 2003, Mienis et al. 2007). A recent publication from the Rockall Bank (North East Atlantic) showed that there is a significant interaction between tidal currents and cold-water coral formed mounds which induce downwelling events of surface water that brings the organic matter to 600 m deep (Soetaert et al. 2016). The influence of topography on current patterns, and consequently on the food supply, is thought to determine the distribution of cold-water corals and their associated fauna on both broader and finer scales (Sebens 1998, Mortensen et al. 2001, Davies et al. 2009, Soetaert et al. 2016).

Local hydrodynamics can also determine the coral's colony morphology (Chamberlain and Graus 1975, Wheeler et al. 2007, Chindapol et al. 2013, Chapter 3). Like sponges (Bell and Barnes 2001), corals have different growth forms as they have a high level of phenotypic variation (Todd 2008). When corals occur in an area with strong uni-directional currents, the resulting corals respond by growing assymetrically with their branches growing in the upstream direction (Chindapol et al. 2013). Additionally the coral colonies will appear more compact as their branch thickness increases to avoid branches breaking off (Chindapol et al. 2013, Hennige 2016). The size of a colony can also be influenced by the mechanical strength of living, growing branches of coral (Sherwood and Edinger 2009), extent of inter-colony fusion (Hennige et al. 2014), the impact of the water flow that passes trough a colony in relation to its access to food (Chamberlain and Graus 1975) and the speed at which dead parts of a coral colony are weakened by bioeroders, such as clinoid sponges (Grehan et al. 2004), or low pH water from regional upwellings or ocean acidification (Hennige et al. 2015).

1.6 Cold-water corals as ecosystem engineers

Ecosystem engineers are organisms that can modulate the availability of resources, in a direct or indirect way to other species. They can do this by causing physical state changes in biotic or abiotic materials. In doing so, they modify, maintain and create habitats (Jones et al. 1997). If a coral reef becomes large enough, it can engineer an ecosystem that can alter the hydrodynamic and sedimentary processes and form structurally complex habitats for other species (Noé et al. 2006, Wheeler et al. 2007, Mortensen et al. 2010, Soetaert et al. 2016).

Tropical and cold-water corals are autogenic engineers, like trees, they change the physical, chemical and biological environment by modifying their own living and dead structures (Jones et al. 1997, Bellwood and Hughes 2001)). Their arborescent architecture provides biomass, structural complexity, modifies the seascape and produces a great diversity of microhabitats. They provide shelter, food sources and spawning habitats to deep-sea fish and shark communities and a wide range of other organisms, ranging from micro- to megafauna (e.g. Jensen and Frederksen 1992, Rogers 1999, Roberts et al. 2008, Raes and Vanreusel 2006, Van Soest et al. 2007, Henry et al. 2010, De Clippele et al. 2015).

Three succeeding habitats can be observed when crossing a reef: a zone containing small pieces of coral skeleton referred to as coral rubble, followed by an area with large blocks of coral skeleton, and ending up in an area with the live coral reef (de Haas et al. 2009, Buhl-Mortensen et al. 2010). Four different microhabitats can be recognised within the coral colonies of the live reef: the tissue of living corals, detritus-laden surfaces of dead corals, cavities inside coral skeletons, and free space between coral branches (Buhl-Mortensen et al. 2010). This complex reef structure can significantly influence the local hydrodynamics in the reef vicinity, providing further diversity in habitat niches (Dorschel et al. 2007).

Corals also act as allogenic engineers because they can generate and transform inorganic and organic materials biophysically (Glynn 1997, Hallock 1997). Coral skeletons can be turned into calcareous reef sands by bioeroding organisms and by other biological, physical, and chemical erosion processes (Glynn 1997, Hallock 1997, Roberts 2005) so that corals, through the production of inorganic materials, influence the composition of their surrounding sediments. Corals also continuously release significant amounts of dissolved and particulate organic materials, especially as mucus which may function as a substrate for microbial communities. These microbial communities increase the nutritional value of the mucus and the sedimentation rates of these

organic materials (Wild et al. 2008, 2009). Consequently, how a reef function is directly controlled by the corals capacity as ecosystem engineers.

1.7 Threats

The most prominent threats to coral ecosystems are bottom trawl fishing (Hall-Spencer et al. 2001, Althaus et al. 2009), exploration and extraction of fossil fuels (Larsson and Purser 2011, Purser and Thomsen 2012, Cordes et al. 2016) and anthropogenic changes in ocean conditions (Ruhl and Smith 2004, Keeling et al. 2010, Findlay et al. 2013, Mora et al. 2013, Long et al. 2016, Sweetman et al. 2017).

As shelf fisheries collapsed in the mid-twentieth century, the fishing industry has progressively fished deeper targeting long-lived, slow-growing deep-water species (Norse 1993, Butman and Carlton 1995, Pauly et al. 1998, Roberts 2009a). This trend has brought fishing activity to the continental shelves, slopes, offshore banks and seamounts that support cold-water coral habitats (Koslow et al. 2000, Roberts 2002). Bottom-trawl fishing uses nets that are dragged along the seabed and are known as an extremely effective way of catching bottom-living organisms (Watling 2005). However, video surveys have recorded the remains of fishing gear such as gillnets, anchors, and trawl nets among corals, together with furrows or scars in the sea bottom which are all the unmistakable evidence of the damage from trawling activity (Fosså et al. 2002, Roberts et al. 2009b, Guihen et al. 2012).

Deeper waters have also been a promising source for oil and gas extraction (Davies et al. 2007). Corals, as suspension feeders, are sensitive to the effects of sedimentation which is increased around the extraction sites (Larsson and Purser 2011, Purser and Thomson 2012). Siltation and sand deposition caused by bottom-trawl fishing and drill cutting may clog the coral's polyps (Watling and Norse 1998, Brooke et al. 2009, Larrson and Purser 2011). However, *L. pertusa* has been discovered growing on oil rigs, and therefore it has been promoted by the Oslo-Paris Convention (OSPAR decision 98/3) that the 'footings' of large platforms might be left in place after the rig is decommissioned. Such an option would preserve existing colonies and might allow *L. pertusa* to spread in the North Sea (Bell and Smith 1999). However, those observed growing close to discharge chutes have shown signs of contamination with some colonies suffering upwards of 30% polyp mortality (Gass and Roberts 2006).

Anthropogenic carbon dioxide produced through fossil fuel burning, cement production, agriculture and deforestation has increased the concentration of atmospheric CO_2 from pre-industrial levels of

about 280 ppm to about 407 ppm today with projections to over 900 ppm by 2100 unless emissions are substantially reduced (under Representative Concentration Pathway 8.5, Sweetman et al. 2017). These rising atmospheric greenhouse gas concentrations have led to an increase in global average temperatures of ~ 0.2°C over a period of ten years. The oceans absorb CO_2 (Pauchauri et al. 2014) and heat (Glecker et al. 2016), leading to a change in the surface ocean pH (Byrne et al. 2010), temperature (Purkey and Johnson, 2010), oxygen minimum zones (Stramma et al. 2008, 2010, 2012, Keeling et al. 2010, Helm et al. 2011) and particulate organic carbon flux to the seafloor (Ruhl and Smith 2004). As a consequence of changes in the pH of the seawater, models predict a dramatic shallowing of the aragonite saturation horizon (Orr et al. 2005, Guinotte et al. 2006). Therefore, the calcification of cold-water corals may be hampered, and their aragonitic framework could begin to dissolve, causing the reefs to collapse posing an additional threat to the cold-water coral's associated fauna (Maier et al. 2009). An increase in seawater temperature can increase the metabolic rate of *L. pertusa* (Dodds et al. 2007). If the food input doesn't compensate the increased metabolic demand of the coral, it can starve. Ocean acidification can also directly affect the physiology, reproduction, behaviour, neuronal functions and survival of many groups of organisms (De'ath et al. 2012). Sensitivities to these disturbances vary between groups and can lead to shifts in food webs, can alter competitive advantages and functional replacements in reef communities (De'ath et al. 2012). However, to be able to detect anthropogenic impacts, measurements must first account for the natural variability that affect any signal (See introduction sections in Chapter 2,3,4).

1.8 Policy and management

Global declines in biodiversity have ignited responses from local to international scales, aiming to establish management methods (e.g. Ottersen et al. 2011, Nybø et al. 2011, Zhang 2015, Mortensen et al. 2015) for the effective protection of species and ecosystems, and limiting human impact on the environment (Ross and Howell 2013). Cold-water coral habitats are recognised by the United Nations (U.N. 2007) as Vulnerable Marine Ecosystems (VMEs) and meet the criteria of Ecologically and Biologically Significant Areas under the Convention on Biological Diversity (CBD) (CBD 2008). International, European, and national (UK) initiatives are responding to global calls for improved spatial management of the marine environment, and the establishment of networks of marine protected areas (MPAs) for the purpose of protecting marine habitats from ongoing anthropogenic damage, and conservation of marine biodiversity (IUCN 2003, CBD 2008). In addition to protecting important species or ecosystems, MPAs also act as propagule sources that could be located where they can produce and receive larval out and influxes, so they can act to buffer species against local extinctions and allow genetic mixing (Bell 2008).

1.9 Studying cold-water coral reefs

Since the late eighteenth century, cold-water corals have been a subject of interest. Notes from fishing records already indicated where cold-water corals could be found, but since the 1990s, advances in deep-sea technology are allowing us to explore the deep sea with more accuracy (Roberts et al. 2009a). There are four broad approaches that are used to survey cold-water coral reefs and the seabed in general: (1) acoustic, sonar technology (2) remote sensing (3) underwater photography and video (4) direct sampling of sediment and biota (Harris and Baker 2012a). Here, a general overview of the approaches relevant to this thesis are given.

Ships, remotely operated vehicles (ROV) or autonomous underwater vehicles (AUV) can all deploy a variety of acoustic devices operating at different frequencies. When low-frequency sonar pulses are used, the sonar can penetrate deeper into the sea floor than when high-frequency pulses are used (Harris and Baker. 2012a). Choosing the right frequency depends on the purpose of the data collection but also on the depth of the acoustic device to the sea floor below it (Lurton 2002, Harris and Baker 2012a). In this thesis, acoustic data collected with multibeam sonars were used. Multibeam sonars have their transmitting and receiving transducers attached to the hull of the vessel (ship, ROV) and provide next to backscatter maps also bathymetry maps. Backscatter data gives information on the physical attributes of the seabed (Todd et al. 1999, Kostylev et al. 2001). Soft substrates such as mud give weak signals, while hard substrates such as rock give strong signals (Harris and Baker 2012a). A bathymetry map gives you information on the depth of the seabed. From the bathymetry, other variables such as slope, eastness, northness, bathymetric positioning index and rugosity can be extracted (e.g. Wilson et al. 2007, Henry et al. 2010, Guinan et al. 2009). Using several complimentary technologies to map and sample an environment is key when surveying the seabed (Harris and Baker 2012a).

Grab sampling, box coring and trawling have confirmed the presence of a high number of species at many cold-water coral reefs (Gass and Roberts 2006, Henry and Roberts 2007, Cordes et al. 2008). Such sampling is, however, very costly. time-consuming and destructive, so limiting the number of investigations and making the few samples highly valuable. This thesis analysed video surveys which have been collected with ROVs as they have the advantage of sampling large areas without affecting benthic communities. The development of ROVs has also allowed quantitative sampling and detailed observations in areas that could not be sampled using traditional methods (scuba, trawl) due to the depth or the roughness of the terrain. Sampling over a larger spatial extent is essential for a correct estimation of the overall patterns of species distributions, because observations conducted over smaller extents may not accurately reflect the patterns and processes

occurring over larger scales (Gotelli and Ellison 2004). The maps created from sonar together with information on species distributions from video surveys are essential in conservation and resource management.

1.10 Aims of this thesis

This thesis aimed to increase the understanding on differences in the distribution, morphology and ecology of cold-water corals within and between the Mingulay Reef Complex (Chapter 2), the Tisler Reef (Chapter 3) and the Logachev Mounds (Chapter 4) by integrating acoustic, high-definition video and hydrodynamic data. The first two results chapters, Chapter 2 and 3, focussed on the distribution of *L. pertusa*, the dominant framework forming cold-water coral in the study areas. The last result chapter, Chapter 4, is dedicated to non-scleractinian cold-water corals that are associated with *L. pertusa* reefs. Below the hypothesis addressed for each chapter are briefly summarised:

Chapter 2: Using novel acoustic and visual mapping tools to predict the small-scale spatial distribution of live biogenic reef framework in cold-water coral habitats

H_1: Small-scale spatial distribution of live *L. pertusa* can be accurately predicted from acoustic and video data

Chapter 3: Spatial extent and morphology of cold-water coral habitats in relation to local hydrodynamics at the Tisler Reef, Norway

H_1: Local hydrodynamics influence the distribution, growth and morphology of *L. pertusa.*

Chapter 4: The diversity, ecology and role of non-scleractinian corals at the Logachev carbonate mounds, south-east Rockall Bank.

H_1: Abundance and diversity of non-scleractinian corals is positively correlated with diversity of hard coral substratum types.

CHAPTER 2- USING NOVEL ACOUSTIC AND VISUAL MAPPING TOOLS TO PREDICT THE SMALL-SCALE SPATIAL DISTRIBUTION OF LIVE BIOGENIC REEF FRAMEWORK IN COLD-WATER CORAL HABITATS

Published as peer-reviewed paper: De Clippele LH, Gafeira J, Robert K, Hennige S, Lavaleye MS, Duineveld GCA, Huvenne VAI, Roberts JM (2016) Coral Reefs 36(1): 255-268

2.1 Introduction

This chapter focusses on the Mingulay Reef Complex (MRC) (Figure 2.1) located off the west coast of Scotland, where *L. pertusa* is the framework-forming coral. The MRC is a collection of several areas supporting reef mounds (Roberts et al. 2005). It is located in the Sea of Hebrides, south of the Little Minch in a passage between the Scottish mainland and the northern Inner and the Outer Hebrides.

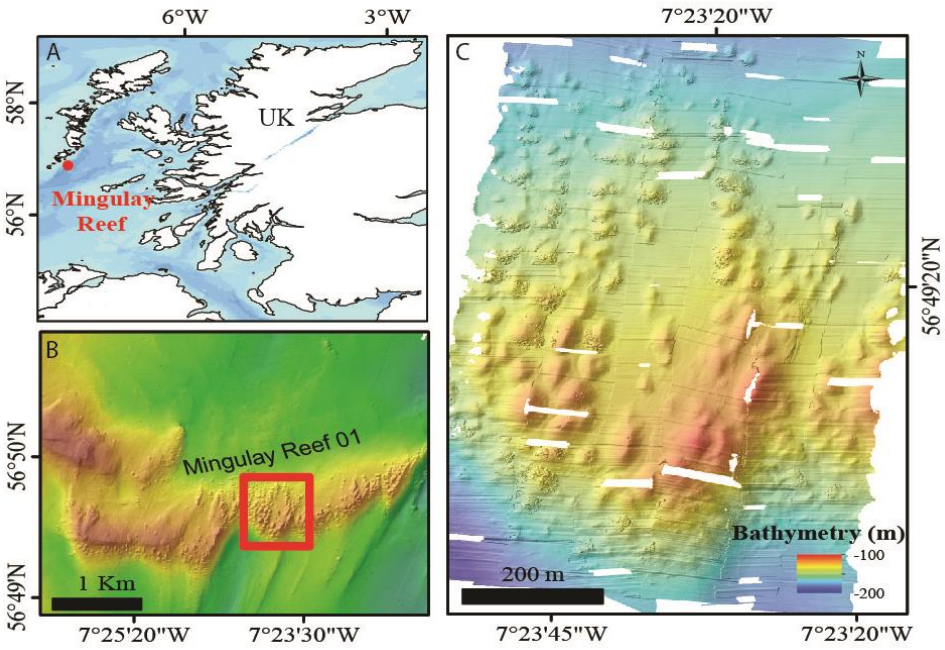

Figure 2.1 (**a**) Location of the Mingulay Reef Complex. (**b**) Mingulay Reef 01 (**c**) Microbathymetry area (location indicated by red box on panel)

The Scottish continental shelf has three water sources; (1) Atlantic water (2) Irish Sea Water and (3) coastal water (Craig 1959, Ellett 1979, Ellet and Edwards 1983). There is a net northward transport of water along the Scottish west coast (northward flux of $11x10^4$ m^3s^{-1}) flowing through the Little Minch (McKinley et al. 1981) that varies with meteorological events (Simpson 1986). In the Sea of the Hebrides, where the MRC is found, high salinity high nutrient Atlantic water flows northward from the west of Ireland (Gillibrand et al. 2003). A warm mass of the northward coastal current

(created by Scottish mainland river runoff water) passes through the Little Minch, bifurcates and recirculates southward towards Barra Head (Hill et al. 1997). Several processes are included in the recirculated current: (1) tidal rectification, (2) topographic steering of large-scale flow and (3) baroclinic pressure gradient associated with the dome of dense saline Atlantic water extending into the centre of the channel from the south (Savidge and Lennon 1987). Temperature and current data have been recorded continuously since June 1981, while salinity data have been recorded continuously since September 1993 (Tiree Passage) (Inall et al. 2009). This data indicates that the water column is well mixed or weakly stratified throughout the year, that the mean water temperature is 10.1 °C and a seasonal cycle with an amplitude of 3.2 °C. Interannual variability in the North Atlantic Oscillation (NAO) index was found to cause changes in the strength of the residual flow (Holliday 2003). A positive NAO coincides with an amplified residual flow (Inall et al. 2009). A trend of ocean temperature warming as also observed with a +0.57 °C per decade (Inall et al. 2009).

Here, the focus lies on the east-west oriented ridge of the MRC, Mingulay Reef area 01 (MR1) (Figure 2.1b), where live coral growth on the most extensive area of small *Lophelia* reef mounds in the MRC were studied. Small reef mounds, referred to as "mini-mounds", are widespread on MR1. In the spring and summer months, the water at the MRC is very turbid, caused by flocculent marine snow and some resuspension of existing seabed muddy sediments (Fyfe et al. 1993, Long and Wilson 2003), and the low visibility can interfere with the quality of video data. This near-seabed particle flux is caused by two hydrographic mechanisms. The first is a rapid downwelling motion created during the ebb and flood periods as internal wave breaks over the rock ridges associated with the largest of the five reef complexes, MR1 (Figure 2.1b) (Davies et al. 2009). The ridge of MR1 is comprised of dolerite (Roberts et al. 2005), with the reef following the gross morphology of this feature ("inherited" morphology) (Wheeler et al. 2007). The ridge is relatively shallow with the shallowest point rising to less than 100 m water depth and the deepest point reaching 260 m. Live coral can be found between 120 and 190 m depth (Roberts et al. 2009b). The hydraulic flow (or 'jump') can cause a depression of the downstream density structure which, when the tide reverses, is propagated back over the bank. This results in a supply of warmer, nutrient-rich water from the surface to MR1 (Davies et al. 2009). Organic matter resuspended from the seabed during peak tidal flows will be lower in quality but is a second mechanism of food supply to the live corals on the seabed.

To date, predictive mapping of deep-water organisms and habitats has mainly been based on video data, with or without grab or trawl samples (Roberts et al. 2009a, Henry et al. 2010, Howell et al.

2011). Despite challenges of precise taxonomic identification, the advantage of video oversampling is that it covers large areas without disturbing the habitat. The exact position and local environment of the organisms is more uncertain for grab and trawl samples taken without precise in-water positioning, but they do provide higher detail and confidence when identifying species at lower taxonomic levels (De Clippele et al. 2015). A second drawback of video material for predictive mapping is uncertainty regarding the absence of an organism in the whole area when it is not observed on the video. Even when large areas are covered with video surveys, the presence of a species that occurs outside the range of the camera's view can be missed.

To overcome these drawbacks, a high-resolution microbathymetric grid with a fine resolution of 0.35 x 0.35 m is used in this study. This grid covered a wider continuous area compared to the narrower, and discontinuous area covered by high-definition (HD) video transects. The microbathymetric grid allowed identification and mapping of individual coral colonies in their local spatial setting (Figure 2.1c). HD video transects matching the colonies on the microbathymetry confirmed that the colonies were alive. Live coral presence and absence data were integrated from the microbathymetry using a broader resolution bathymetry of 2 x 2 m) from which additional environmental variables were derived. Live coral presence data for areas outside the microbathymetry were included by using HD video transects.

A new British Geological Survey (BGS), seabed mapping toolbox, was developed in collaboration with Gefeira J. for the ArcGIS software. This toolbox allows the delineation of cold-water coral reef mounds. Here, the aim is to semi-automatically delineate biogenic 'mini-mounds' from a broader-scale bathymetry data (2 x 2 m) for the first time. Cold-water corals occur at great depth, and therefore the development of remote sensing approaches with semi-automatic systems are important. As multibeam bathymetry is commonly available for cold-water coral ecosystems, a potentially broader application of this tool is possible (Chapter 5). The characteristics of the delineated mini-mounds are extracted and integrated with live coral presence data from video data and microbathymetry. A map showing the likelihood of live coral presence on mini-mounds at the whole MR1 will be produced and will be useful for future long-term monitoring surveys and to gain insight into the impacts of global climate change.

2.2 Methods

2.2.1 Bathymetry

Multibeam bathymetry data were collected at two different resolutions. One bathymetry dataset was gathered using a Simrad EM2000 ship-mounted multibeam echosounder (MBES) as part of the MINCH project, using the RV *Lough Foyle* (28 June–5 July 2003) (Figure 2.1b). This bathymetry covered the MR1 area and was processed to a resolution of 2 x 2 m. The system has an angular coverage sector of 120°, 111 beams per ping and a 1.5° beamwidth across the track. A Seapath 200 GPS system provided real-time heading, attitude, position and velocity solutions (Roberts et al. 2004).

The second bathymetry dataset with a 0.35 x 0.35 m resolution (the microbathymetry) was acquired using the remotely operated vehicle (ROV) *Holland-1*, deployed from the RRS *James Cook* cruise 073 during the 2012 Changing Oceans Expedition (JC073, 18 May-15 June 2012) (Figure 2.1c). A Reson 7125 dual-frequency multibeam echosounder system was mounted on the ROV and used in 400 kHz mode with 512 beams. Data were recorded in the Reson software PDS2000 and were supported by the inputs of the ROV depth sensor (Digiquartz, measuring depth in dbar), Maximum Receive Unit (Phins), Doppler navigation and Ultra-Short BaseLine navigation (Sonardyne) (Roberts 2013). The microbathymetry covered only a small area (627 x 964 m) in the centre of MR1 (Figure 2.1b, c). The ROV Reson7125 bathymetry data were processed in the Caraibes software from IFREMER. Processing steps included: conversion of the bathymetry data from PDS2000 format (in which the data were recorded) to Caraibes .mbg format, smoothing of the navigation, importation of the ROV depth data to calculate absolute bathymetry (rather than depth below the vehicle), calibration for attitude offsets (pitch, roll, heading), removal of spikes and noise in the soundings, gridding to the 0.35cm x0.35cm final grid, exportation to ArcGIS. Even after processing, the dataset contains a number of errors that could not be corrected. One of these is the occurrence of across-track 'empty' strips where data are lacking. This appears to have been caused by an issue in the data recording PC during the survey. Although the real-time representation of the data coverage during the survey showed a full coverage of the study area, the high ping rate and data volume coming into the system meant that some data files became corrupted and no data was recorded for several minutes. It has proven impossible to recover these lost sections of data, hence resulting in gaps in the final map. The second issue that could not be fully corrected was the ROV navigation. During the survey, the Holland I ROV was steered manually, using the Helmsman display of the PDS2000 software. The primary navigation information source was the Ultra Short

Baseline (USBL) navigation, which has an accuracy of +/- 0.5-1% (i.e. in 100m water depth =~1-2m). In addition, a DVL (Doppler Velocity Log) system was also installed on the ROV, and the dead-reckoning measurements made with this system were used in a real-time smoothing algorithm (Kalman filter) applied to the USBL navigation. Unfortunately, this caused more problems than it solved: if the ROV pilots would be deviating from the track, the Kalman filter would smooth out those navigation points and delay the information transfer to the Helmsman display, until the ROV would be too far off the track and the pilots had to make an abrupt adjustment to the course. The end result was that the USBL navigation track of the ROV contained many irregularities, some caused by noise in the USBL, and some caused by abrupt course changes by the pilots. Application of smoothing algorithms during processing therefore would always take away some of the noise, but also some of the real course changes, because it was impossible to distinguish between both from just the USBL navigation track. Unfortunately, the setup during JC073 did not allow to record the DVL data separately, hence the data could not be reprocessed by using Doppler navigation (as is more commonly done for ROV-based bathymetry, e.g. Huvenne et al., 2018, in attachment). Taken together, the processing problems in the microbathymetry dataset were mainly caused by a less-than-ideal setup of the Reson7125 system during JC073. The Holland I ROV is not standard equipped with such a multibeam echosounder (unlike the ROV Isis), and a system had to be hired. It was installed at the very last minute, the day before sailing, and experienced several problems during the cruise (in addition to the problems outlined above). It was still deemed that the data that were recorded provided a unique insight in the morphology of the Mingulay reef complex, and therefore were worth further study. However, this restricted the use of the map for calculation of additional derived environmental variables with the BGS Seabed mapping toolbox, but its high resolution still allowed us to use the map for visual interpretation (section 2.2.4).

Additional multibeam backscatter data were collected in 2012 (JC073) using the shipboard Simrad EM710 on the RRS *James Cook*. The grid has a resolution of 2.5 x 2.5 m (Le Bas and Huvenne 2009).

2.2.2 High definition video data

High definition video data were collected in 2006 (64PE250 RV *Pelagia* cruise) and 2012 (JC073 RRS *James Cook* cruise). During the *Pelagia* cruise, two video monitoring systems were used: the Nederlands Instituut voor Onderzoek der Zee Hooper camera and the Scottish Association for Marine Science Bowtech umbilical video system. The first system consisted of a heavy drop frame holding a digital video camera with a logger, power supply, modem, underwater lights, altimeter and a set of parallel Oktopus laser pointers. The laser pointers were spaced 30 cm apart and could

be used to estimate the distance from the seafloor or the size of objects/organisms. The camera system was also connected to an electric coaxial cable that allowed real-time transmission of altimeter readings and video images. The second system consisted of a much smaller frame and could be held 1-5 m above the sea floor by a winch. The system was also fitted with a Photosea strobe and camera unit, and a set of parallel Oktopus lasers spaced 30 cm. Videos were captured to MiniDV tapes. Navigation data were collected with a Furuno DGPS system located on the bridge deck and also stored on the computer.

The second set of HD video data were collected using the ROV *Holland-1*. The data were recorded with a combination of cameras mounted on the ROV: an HD Insite mini-Zeus video camera with a direct HDSDI fibre output, a Kongsberg 14-208 digital still camera, a Kongsberg 14-366 pan and tilt camera and an Insite Pegasus-plus fixed zoom camera. Four lights were used: two 400-W deep-sea power and light SeaArc2 HMI lights and two 25,000 lumen Cathx ocean APHOS LED lights. Two deep-sea power lasers spaced 10 cm were also mounted on the HD camera. The position and depth of the ROV were determined by USBL (Sonardyne) underwater positioning system and recorded using the OFOP (Ocean Floor Observation Protocol) software.

2.2.3 Current information

Maximum current speed was obtained from the hydrodynamic model of MRC created by Moreno-Navas et al. (2014). The maximum current speed model has a lower resolution than the bathymetry and backscatter data (100 x 100 m) but provides local contextual environmental information that is not otherwise available.

2.2.4 The BGS Seabed Mapping Toolbox and visual mapping

Although subjective manual mapping is the most common approach for identifying areas of potential coral habitats (Davies et al. 2008, Ross and Howell 2013), more objective and automated approaches have been published (Salcedo-Sanz et al. 2016). However, the semi-automated mapping approach presented in this study uses a fast and consistent automatic method and allows inclusion of additional datasets that have been developed within a GIS environment. Two mapping approaches were used in this study. The first is the BGS seabed mapping toolbox which was developed in collaboration with Gafeira J. from the BGS and a second is using the microbathymetry to detect coral presence visually.

Development of the BGS Seabed Mapping Toolbox for ArcGIS started after the successful creation of a semi-automatic workflow that can map and characterise pockmarks in the seabed (Gafeira et al. 2012). To map and characterise cold-water coral mounds with this toolbox, knowledge on their

morphological features and ecology was provided by De Clippele LH. The script for the toolbox, used in this chapter, was adjusted in Phyton by Gafeira J, following a similar logic to the script developed for mapping pockmarks (Gafeira et al. 2012). This script creates a tool dialogue box which can be run as an ArcGIS tool and has a description of the individual output parameters (Table 2.1, See Gafeira et al. 2015 in Appendix). The approach by Gafeira et al. (2012) had to be reversed to map elevations (mounds) instead of depressions (pockmarks) in the seabed, by using a Bathymetric Position Index (BPI) map instead from the bathymetry map (Gafeira et al. 2012, 2015, see appendix). This was because cold-water corals preferentially develop in areas of complex and irregular topography compared to pockmarks (Gafeira et al. 2012, 2015).

Here the BPI map was created from the 2 x 2 bathymetry, instead of the fine-scale 35 x 35 cm microbathymetry, as the latter contained too many artefacts (see section 2.2.1). The BPI uses neighbourhood analyses to calculate the relative elevation of a cell compared to the surrounding cells, identifying topographic features. Positive BPI values represent locations that are shallower than the average of their surroundings (e.g., ridges). Negative BPI values represent locations that are deeper than their surroundings. BPI values near zero are either flat areas or areas of constant slope (Weiss 2001). By using the BPI values as an input, the delineation will depend dramatically on how the BPI map was calculated. Here, the BPI was calculated within ArcGIS with the land facet corridor tool (Jenness et al. 2013). The used neighbourhood's shape (annulus) and size (inner and outer radius of 8 and 24 cells respectively) were chosen based on the characteristics of the study area (e.g., typical width of the mini-mounds, distance between features).

The first tool in the toolbox was named the BPI feature delineation tool. In the BPI feature delineation tool, several thresholds are decided by the user to determine the delineation process. These are the cut-line BPI value, minimum BPI, minimum area and a minimum width/length ratio (See Gafeira et al. 2015 in Appendix). Additionally, a buffer distance can also be defined within the tool dialogue box. This buffer distance compensates for the initial feature delineation, which was based on the cut-line BPI value, that generally reaches the mound's lateral slopes rather than its actual base. The chosen buffer distance reflects therefore the distance to the actual rim of the mound. The tool's output is a polygon shapefile delineating the areas of seabed respecting the dimensions and BPI values set by the user. A cut-line BPI value of 3, minimum BPI value of 3.5, minimum area of 50 m^2 and a minimum width/length ratio of 0.2 were here used as the thresholds (Figure 2.2). A buffer distance of 4 m was chosen based on the morphological characteristics of the mounds and how they are represented in the BPI raster used as data input. Nevertheless, some degree of manual editing was required when artefacts were delineated or when adjacent mini-

mounds were inaccurately delineated as a single feature. When choosing the BPI cut-line and the buffer distance it is important to consider that the mounds, which would have been split according to the cutline, can end up being joined because of the chosen buffer distance and their closeness to a neighbouring mound. Therefore, the BPI profiles of clustered mounds were after inspection split if the BPI-value at the base of the mound was equal or smaller than the chosen cut-line value. More detailed information regarding the BPI feature delineation tool and the results of the sensitivity to the BPI input and threshold values can be found in Gafeira et al. (2015) which can be found in the appendix.

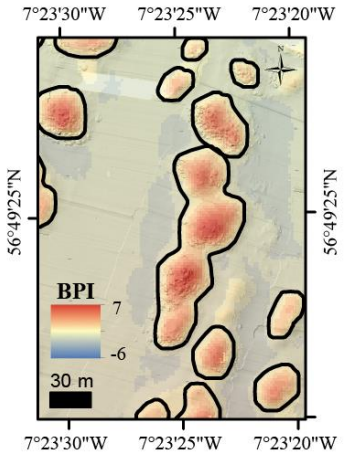

Figure 2.2 Bathymetric Positioning Index map based on the used neighbourhood's shape being an annulus and a size with an inner and outer radius of 8 and 24 cells respectively. The delineated mini-mounds have a cut-line BPI value of 3, minimum BPI value of 3.5, minimum area of 50 m^2 and a minimum width/length ratio of 0.2 were used as the thresholds with a buffer distance of 4.

The table of attributes of the output shapefile of the BPI feature delineation tool captures some characteristics of the mapped features (e.g. area, perimeter, maximum BPI value, minimum bounding geometry box (MBG) length and width). However, after manually editing the outline of some of the polygons information could be partially incorrect. The second tool in the toolbox, the feature description tool, recalculates these attribute values for each feature before adding new attribute fields with additional information. At this point of the toolbox development, the feature description tool allows extraction of information from the original digital elevation model (DEM), the BPI map, backscatter and rugosity map. Backscatter data give information on the physical attributes of the seabed (Todd et al. 1999, Kostylev et al. 2001). High values tend to represent substrates that are more reflective, like boulders or rocks. Lower values represent environments where reflection by the substrate is lower, such as muddy areas. Rugosity was calculated with the spatial analyst tool curvature in ArcGIS. It is a measure of terrain roughness and is obtained as the ratio of the 3D surface area to the planar area within a neighbourhood (3 x 3 cells) (Jenness 2002).

This tool can also calculate the assumed initial slope of the seabed surface before the development of the coral mound. The initial slope is calculated by removing the bathymetric information from inside the delineated mini-mounds and generating a new surface by interpolating from the surrounding bathymetric values. The mean value of the assumed initial slope within each mini-mound is extracted and added to the table attributes. This tool can extract 20 descriptive attributes (Table 2.1). Of these, minimum/maximum vertical relief, minimum/mean/maximum water depth, water depth of the deepest confined contour line, width, length and orientation are illustrated in Figure 2.3. Current data were not extracted automatically by the tool but added later through the joins and relates function in ArcGIS. The Area Ratio was calculated separately in Excel, by dividing the Area of the polygon with the Area of the MBG box. This value gives an indication of the shape of the mound. When the ratio is closer to 1, it means that the polygon is likely to be more round-shaped. When the ratio is closer to 0, a more dendriform-shaped mound can be expected. This ratio is used to study the variation in the mound's shapes within the studied reef area. To examine the difference in height of the mounds, the maximum water depth is retracted from the minimum water depth. Scatterplots are created in the software package R 3.2.2 (R Development Core Team 2013) to examine the relation between the Area ratio, size and height of the delineated mounds.

Table 2.1 Variables calculated by the "Feature Description Tool". The variables in bold were used in the Random Forest model (see section 2.2.5). The toolbox's output tables will give the abbreviations that are listed in the "variables" column. The explanation of the variables are listed in the "meaning" column. Maximum current speed is not listed here as it was not derived through the "Feature Description Tool".

Variables	*Meaning*
Area	**Area in square meters**
Perimeter	Length of the polygon boundary in meters
Index (BPI)	**Maximum Bathymetric (B) Positioning (P) Index (I)**
MBG_Width (m)	**Minimum (M) Bounding (B) Geometry (G) box's width**
MBG_Length (m)	**Minimum (M) Bounding (B) Geometry (G) box's length**
MBG_W_L	**MBG_Width/MBG_Length**
MBG_Orient	**Minimum (M) Bounding (B) Geometry (G) box's orientation (Orient)**
MinWD	Minimum (Min) Water (W) Depth (D) in meters
MaxWD	**Maximum (Max)Water (W) Depth (D) in meters**
MeanWD	Mean Water (W) Depth (D) in meters
ConfCL_WD	Water Depth (WD) of the deepest Confined (Conf) Contour Line (CL)
MinVRelief	**Minimum (Min) Vertical (V) Relief in meters**
MaxVRelief	**Maximum (Max) Vertical (V) Relief in meters**
Min_Rug	**Minimum (Min) Rugosity (Rug) Value**
Max_Rug	**Maximum (Max) Rugosity (Rug) Value**
Mean_Rug	**Mean Rugosity (Rug) Value**
Min_BS	**Minimum (Min) Backscatter (BS) Value**
Max_BS	**Maximum (Max) Backscatter (BS) Value**
Mean_BS	**Mean Backscatter (BS) Value**
InitialSlp	**Initial Slope (Slp) in decimal degrees**

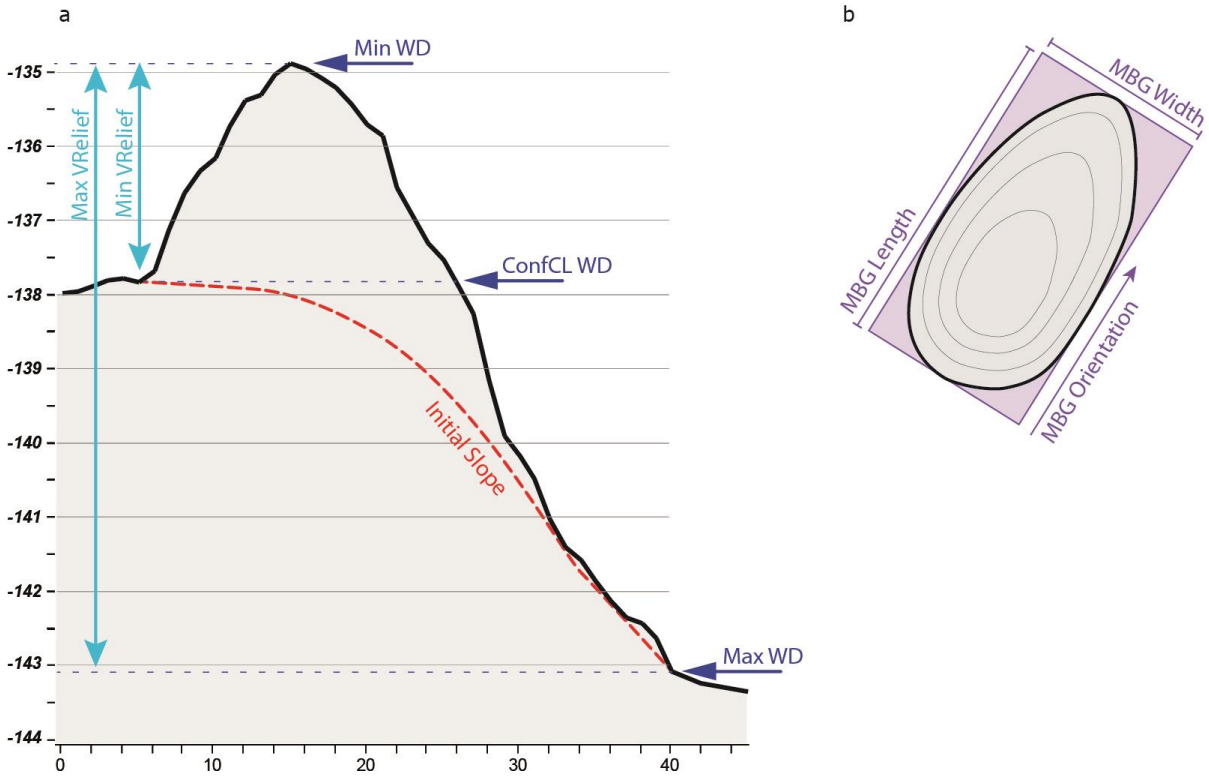

Figure 2.3 (a) A bathymetric profile of a mini-mound at the edge of the Mingulay Reef Complex, showing the position of the vertical relief correspondent to the maximum (MaxVRelief) and minimum vertical relief (MinVRelief), minimum water depth (Min WD), water depth of the deepest confined contour line (ConfCL WD), maximum water depth (Max WD) and Initial Slope. (b) Minimum Bounding Geometry box (MBG) length, width and orientation of a polygon delineating a mini-mound.

The second mapping approach made use of the microbathymetry which showed small circular features and irregularities on the mini-mounds that were identified with high definition (HD) video transects as live coral colonies (1-7 m in diameter) (Figure 2.4). Since the cell-size of the microbathymetry is 0.35 x 0.35 m, coral colonies smaller than 1 m are likely to be undetected. The absence of a live coral colony can therefore not be stated with certainty when it is not visible on the microbathymetry. When dead coral framework were observed in the HD videos, live polyps were always present too. Based on these observations, the assumption were made that all circular structures observed on the microbathymetry were to some degree alive. Their distribution and extent were mapped within ArcGIS (through manual delineation; Figure 2.5a), which allowed calculation of the percentage of live coral cover per mini-mound. Mini-mounds were divided into five different classes based on percentage live coral cover: =0,]0;25], [25;50],]50;75],]75;100]

(Figure 2.5b). The class "=0" indicates that there were no coral colonies present which were larger than 1 m in diameter on the mini-mound.

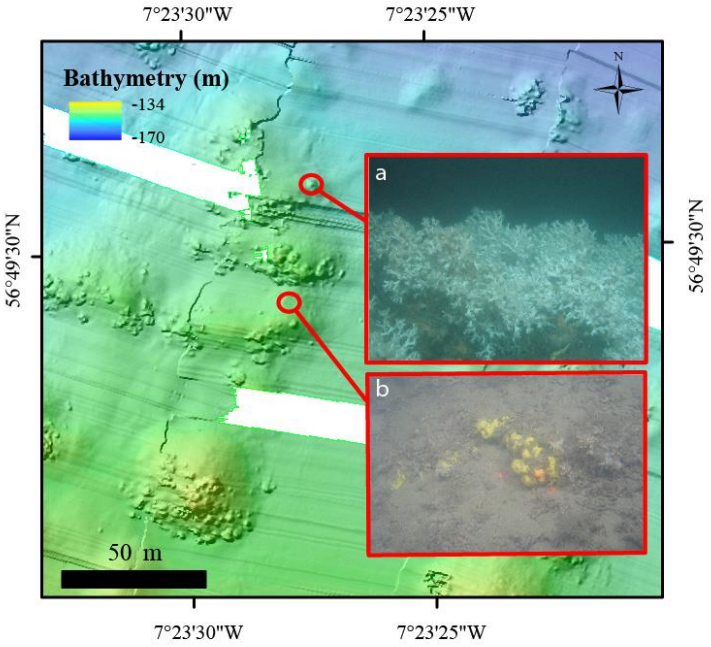

Figure 2.4 Detail of microbathymetry which has only been used for the visual interpretation (section 2.2.1) and here identifies (encircled) a live coral colony **(a)** and the substrate **(b)** which can be found in between mini-mounds (rubble, fine sediment, the yellow sponge *Spongosorites coralliophaga* and the white zoanthid *Parazoanthus anguicomus*)

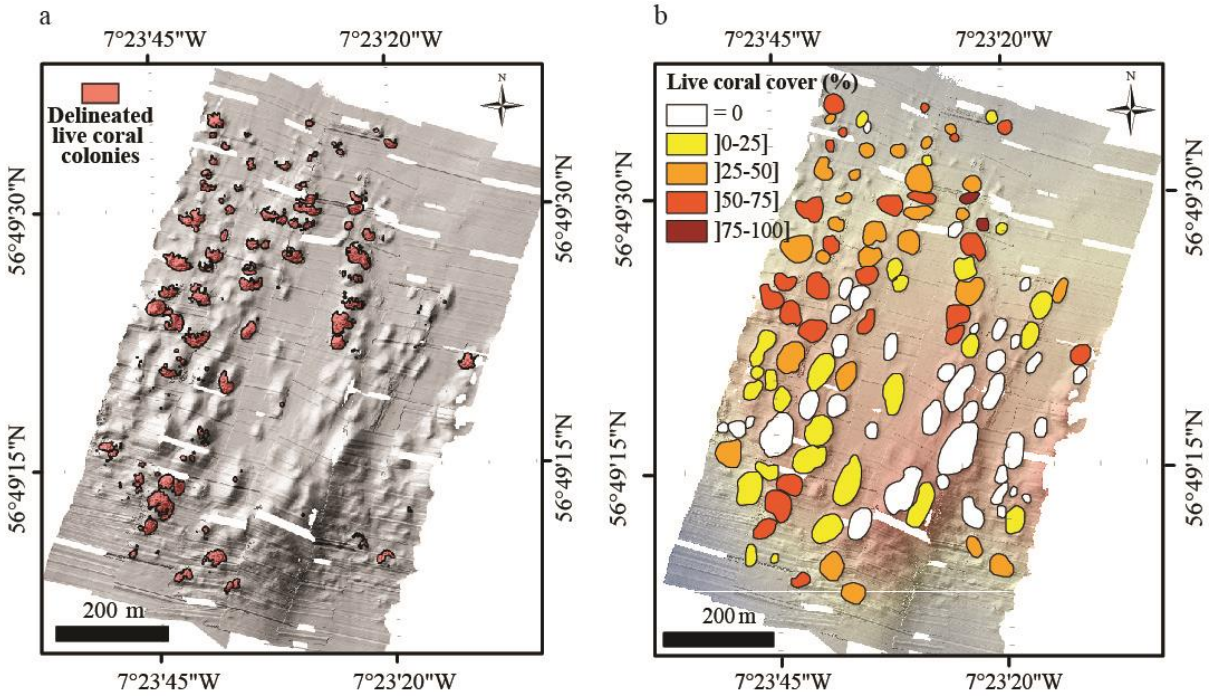

Figure 2.5 (a) The red coloured polygons (manual delineation) on the microbathymetry shows were there are live coral colonies. **(b)** The polygons showed here delineate mini-mounds within the

microbathymetry and were mapped using the BGS Seabed Mapping Toolbox. The percentage live coral cover within the delineated mini-mounds was calculated using the polygon's areas (m^2) of figure 2.5a. The percentage cover of live coral colonies for each mini-mound was represented using five classes: no corals present (=0), or between]0-25],]25-50],]50-75] and]75-100] percent live coral cover present within each mini-mound.

2.2.5 Spatial distribution modelling

Random forest (RF) classification (Breiman 2001) is used here as a modelling technique. A random forest consists of a number of simple decision trees. This group of simple trees vote for the most popular class, which is capable of predicting a response when presented with a set of predictor values. More background information about the application can be found in Cutler et al. (2007) and Rogan et al. (2008). All classifications were carried out in R version 3.2.2 (R Development Core Team 2013) using the random forest package v.1.6-7 (Liaw and Wiener 2002). Here, the mini-mounds as a whole were used as samples, meaning that each mini-mound was a sample and that all mapped mounds were included in the analyses. Three different models were compared. In the first model, the percentage of live coral cover on the mounds were modelled in the five different classes (120 samples). In the second model, the presence/absence of live corals on the mounds within the microbathymetry (120 samples) were modelled. In the third model, the presence of live coral samples from the high definition video analyses were included in the presence/absence model (132 samples). The RF classification models were assessed based on random separation of training and test (validation) data. This was done by leaving one-third of the data out for model training and subsequently using them to test the model. The out-of-bag (OOB) error indicated the prediction error of RF and was calculated for each training sample (Breiman 2001).

The 20 descriptive variables extracted using the feature description tool plus the current value of each delineated mound were considered as predictor variables for the RF models. Initially, the models were estimated by using all the variables. A plot was created with the mean decrease in accuracy for each variable indicating its contribution to the model's performance. Response curves were calculated to show the range of values for each variable for which there is the highest chance of presence.

To evaluate the model, sensitivity and specificity were calculated for both the training and test models. Sensitivity measures the proportion of positives that are correctly identified, whereas specificity measures the proportion of negatives that are correctly identified. The discrimination capacity of the model was assessed using the Area Under the Curve (AUC), an evaluation metric

for binary classification problems. The AUC value for a model can indicate poor (<0.5), random (0.5–0.6) fair (0.7–0.8), good (0.8–0.9) or excellent (0.9–1) discrimination (Fielding and Bell 1997). Higher AUC values for the test models indicate that the training model is good at discriminating between samples or classes.

2.3 Results

2.3.1 Mound delineation and morphometric characteristics

A total of 505 mini-mounds were delineated by the BGS Seabed Mapping Toolbox from the 2 x 2 m bathymetry in the whole MR1 area (Figure 2.6). To examine and characterise the morphology of the mounds, the general morphometric characteristics of the mounds are given in table 2.2.

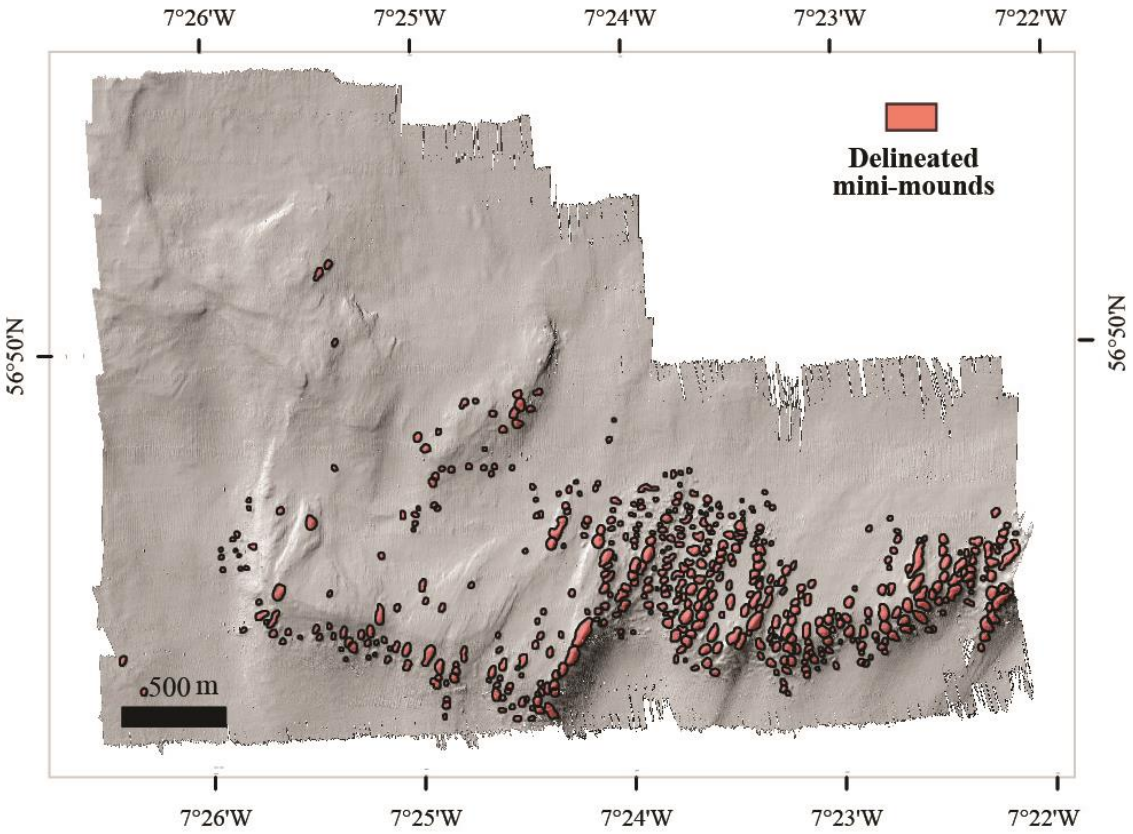

Figure 2.6 Mingulay Reef 01 with mini-mounds delineated in red, obtained with the BPI delineation tool

Table 2.2 Table listing the morphometric characteristics of the mini-mounds

	Range	Average	Standard deviation
Width (MBG)	16 – 30 m	29 m	10 m
Length (MBG)	16 -108 m	42 m	21 m
Polygon area	174-7707 m^2	1075 m^2	897 m^2
Area Ratio	0.52– 0.94	0.78	0.04
Perimeter	48 - 413 m	116 m	51 m
Maximum BPI	2 - 15	6	3
Orientation	0 - 179	70	57
Height	2 – 34 m	8 m	5 m

Two scatterplots are given below. Figure 2.7a shows the relation between the Area Ratio of the mound (shape) and their size (Area). This figure indicates that larger mounds tend to have a lower Area ratio. The second scatterplots examines the relationships between the height of the mounds (minimum versus maximum water depth) and their depth (Figure 2.7b). No pattern is revealed from this figure.

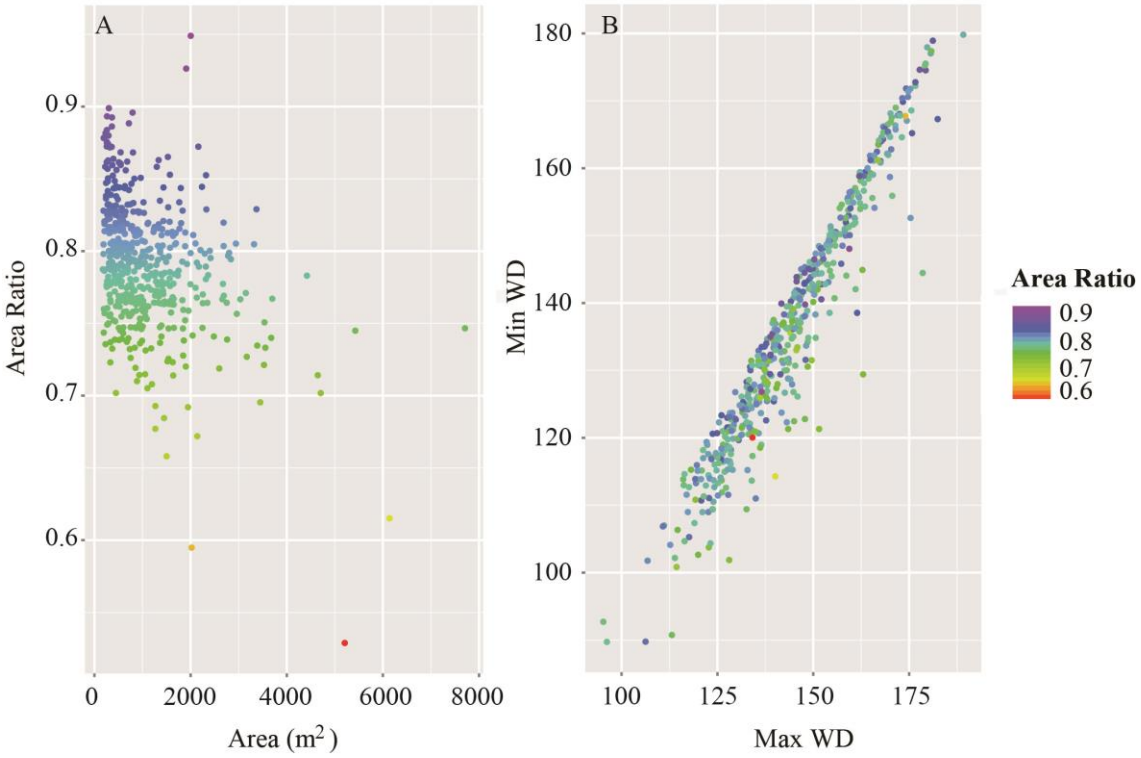

Figure 2.7 Scatterplots are showing the relation between (a) Area Ratio and Area and (b) Minimum water depth (Min WD) and maximum water depth (Max WD). The colours of the dots in both plots represent the value of the Area ratio

2.3.2 Presence of living coral framework

Within the microbathymetry area, 120 mini-mounds were mapped. A total of 82 mini-mounds were covered with circular features 1–7 m in diameter, indicating the presence of live coral framework as confirmed with video recordings (Section 2.2.4, Figure 2.4). The remaining 38 mini-mounds showed no sign of live corals of this size (> 1 m). Only 6% of the microbathymetry area was covered with live coral. The remaining 94% was a mixture of coral rubble covered with the zoanthid *Parazoanthus anguicomus* and sponges, together with fine sediment (Section 2.2.4, Figure 2.4). Visual interpretation showed that the corals colonies were more frequently located on the south-west side of the mini-mounds, facing into the residual current flow to the north-east. Corals seemed to be growing both directly on the mini-mounds and at their base. Corals that were associated with mounds covered between 2 and 1417 m^2. Coral colonies that were not associated with mini-mounds were much smaller and covered surface areas from 0.3 to 23 m^2.

The videos from 2006 and 2012 recorded data from 124 mini-mounds in MR1. On only 29 mini-mounds living coral colonies were identified. Of these 29 mini-mounds, only 12 were outside the microbathymetry area. Seven of mini-mounds with live coral colonies were situated to the east of the microbathymetry area, and five to the west. In the HD video samples, no absence data are included as true absences could not be determined based on a partial survey on the mounds.

2.3.3 Random forest classification

Table 2.3 displays the results of the RF classification for the three different models. The out-of-bag (OOB) error rate for the percentage cover model was the worst, with a value of 42.5% (Table 2.3a). This high error rate is caused by the greater number of categories that can be misclassified. The scenario presence/absence model had an error rate of 21.95% (Table 2.3b). The scenario including the high definition video samples had the lowest error rate of 18.18% (Table 2.3c). These OOB values are given for models after the removal of the correlated environmental variables. The last scenario was further adapted to create a predictive map.

Table 2.3 Random Forest Classification Training model results for **(a)** Percentage live coral cover for each mini-mound within the microbathymetry area with an OOB estimate of error rate of 42.5% **(b)** Presence/Absence of live coral cover within the microbathymetry with an OOB estimate of error rate of 21.95% **(c)** Presence/Absence of live coral cover within the microbathymetry with high definition samples with an OOB estimate of error rate of 18.18% (number of trees = 1500, number of variables per level= 6). When mini-mounds had no live coral colonies present, "=0" or "0" is used here. See section 2.2.5 for more information on the data used in these training models.

(a)	Percentage coral cover					Class.error
	=0	]0;25]	]25;50]	]50;75]	]75;100]	
=0	19	4	1	2	0	0.269
]0;25]	5	10	4	2	0	0.524
]25;50]	0	2	8	5	0	0.466
]50;75]	1	3	4	9	0	0.470
]75;100]	0	1	0	0	0	1.000

(b)	1	0	Class.error
1	49	5	0.070
0	14	12	0.560

(c)	1	0	Class.error
1	58	5	0.079
0	11	14	0.440

Number of trees = 1500, number of variables per level = 6

Since the water depth of the deepest confined contour line and the minimum, mean and maximum water depth were highly correlated (R^2 >0.95), only maximum water depth was included. This variable contributed the most to explaining the variation in the data. The maximum water depth, maximum rugosity, BPI, orientation and maximum current speed were the five most important environmental contributors to the model, as indicated by the mean decrease in accuracy for each variable (Figure 2.8). The response curves (Figure 2.9) illustrate the range of values of the predictor variables and the associated partial probability of live coral presence.

Figure 2.8 Mean Decrease in Accuracy plot indicates what the contribution of each variable is to the model performance. When the Mean Decrease Accuracy value is higher for a certain variable, the removal of this variable from the model will decrease the model's performance. Therefore, the five variables with the highest Mean Decrease Accuracy values (red box) are used in the model as they affect the models performance the most.

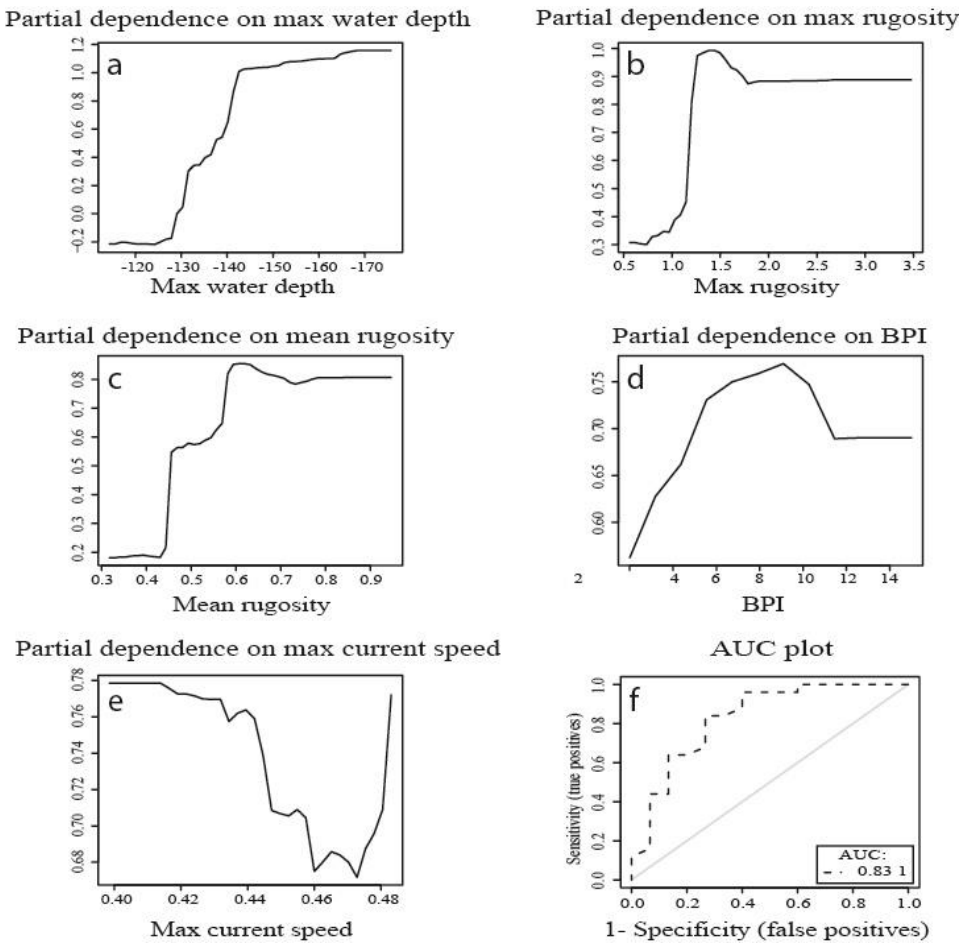

Figure 2.9 (a-e) Response curves for the environmental variables that contribute the most to the performance of the model chosen for prediction. These response curves give the partial probability for live coral presence on the delineated mini-mounds as a function of the individual predictor variables. **(f)** AUC plot for the scenario with the presence/absence of live coral cover + HD videos samples

To validate the model the sensitivity and specificity were calculated. The sensitivity for the training data of the high definition video samples model was 0.92, and the specificity was 0.56. The higher sensitivity indicates that the model was better at predicting presence than absence. The AUC value for the test data was 0.83 (Figure 2.8f), indicating that the model performed very well and was therefore used to predict the probability of the presence of live corals on mini-mounds in the wider MR1 (Figure 2.9).

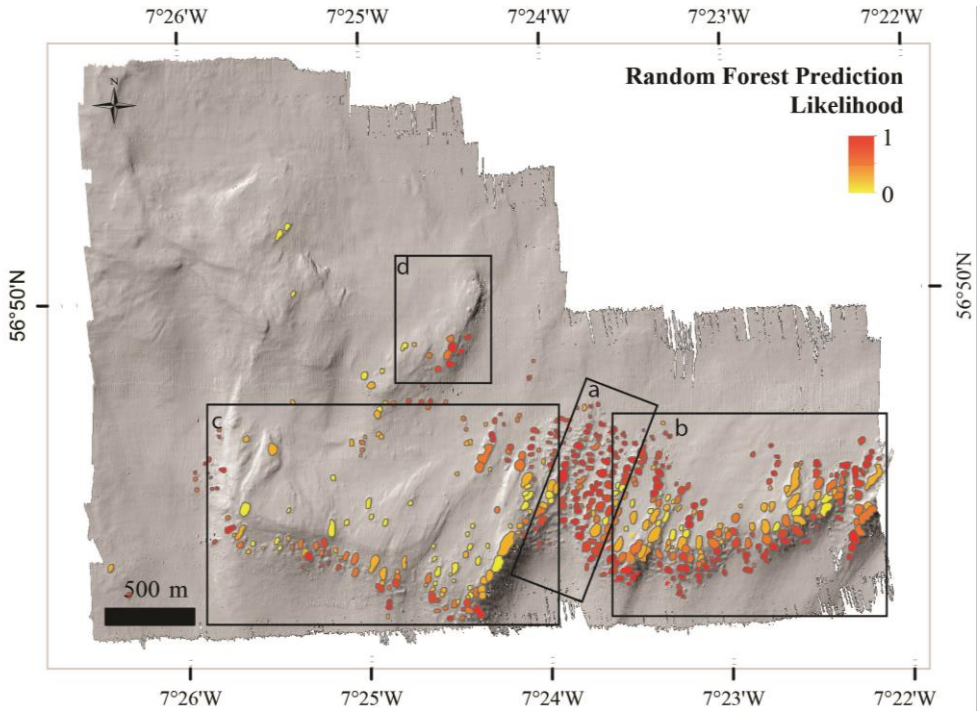

Figure 2.10 Modelled distribution of mini-mounds and their probability for live coral presence. The black box indicates the location of (a) the coll on the reef ridge (b) East Mingulay Reef 1 (c) West Mingulay Reef 1) (d) small ridge feature

The result of the model is a predictive map (Figure 2.10) which illustrates that the highest probability of finding mini-mounds with live coral was at the centre of the reef, near the coll on the reef ridge (Figure 2.10a). The north side of the eastern part of the reef had more mini-mounds compared to the west side of the Mingulay Reef together with a high probability of the presence of live coral (Figure 2.10b). The western part of the reef had lower coverage of mapped mini-mounds, with a low probability of live coral on the north side and higher probability on the south-facing side (Figure 2.10c). A smaller ridge-shaped feature located north of the reef also has a high probability of live coral, especially along the north and eastern sides (Figure 2.10d).

2.4 Discussion

This study is the first to map living cold-water coral colonies acoustically through an ROV-based microbathymetric grid. It is also the first to use the newly developed BGS seabed mapping toolbox. This toolbox allowed us to explore the environmental variables that control coral growth on mini-mounds at MR1 and describe the morphometric characteristics of the mounds. The microbathymetry provided very clear morphological evidence for the presence of live coral colonies and allowed us to calculate the percentage living coral cover on the mini-mounds of MR1. The BGS Seabed Mapping Toolbox was an efficient and reliable tool to identify these mini-mounds rapidly and calculated a variety of environmental factors for each mini-mound. Most of the mini-mounds are round-shaped, while larger mini-mounds are becoming more dendriform-shaped. By integrating the results from the toolbox and the live coral presence dataset, a quick assessment of the morphology of the mini-mounds and the environmental factors that determine which mini-mounds support or do not support live coral was possible. Here, the strongest explanatory model was computed for coral presence/absence with high definition video samples.

2.4.1 Environmental variables

Maximum water depth was the most important contributor to coral presence. The microbathymetry showed that mini-mounds without live coral were more abundant on the upper part of the ridge, while mini-mounds with live corals were more likely to be found at the edges of the ridge of MR1 (Figure 2.5a, 2.5b, 2.10). The proximity of the mini-mounds to the surface could be a factor contributing to coral absence. Mingulay Reef is mainly supplied with food from surface waters through tidal downwelling, which changes environmental conditions experienced by the corals semi-diurnally (Davies et al. 2009, Findlay et al. 2013). The range of environmental changes is not consistent with depth (Findlay et al. 2013), which could contribute to the absence of corals. Maximum current speed, which was least important contributing variable, was slightly lower for mini-mounds with live corals than for mounds without live coral cover. Davies et al. (2009) measured current speeds at the top and foot of MR1 and found a maximum current speed of 26 cm s^{-1} at the foot but maximum current speeds of 81 cm s^{-1} (east) and 67 cm s^{-1} (west) at the top. At greater depths, current speed, temperature and flow velocities will be lower. When the currents are too low, the chances of corals encountering and capturing food will depend on the amount of food passing the polyps (Purser et al. 2010). When the currents are too high, polyp tentacles are bent backwards, reducing their ability to capture food (Sebens and Johnson 1991, Dai and Lin 1993, Purser et al. 2010, Orejas et al. 2016). In slower currents, corals may also be more successful in bringing food to their mouth, as prey could break loose more easily under higher flow conditions

that provide more momentum to escape from the entrapping mucus strands of the tentacles (Patterson 1984, Tsounis et al. 2010). It is important to note that the differences in depth and current speed between mini-mounds with and without live coral cover are small (live coral found between 120-190 m depth). Fine-scale information on current dynamics and food supply for each mini-mound could reveal why these differences were observed.

Rugosity is the second-most important variable related to coral presence. This is a variable that is more related to the morphological properties of the mini-mound and is therefore not an independent characteristic of the mini-mound (Harris et al. 2012). Mini-mounds with high live coral cover are more likely to have greater maximum and mean rugosity than mini-mounds with only dead corals (Alvarez-Filip et al. 2009). When the growth of corals increases, the unevenness of the mound structure increases as the coral polyps grow outwards to obtain better passing food. Mini-mounds composed of rubble without live coral, covered by the zoanthid *Parazoanthus anguicomus* and sediment (Figure 2.4), have lower rugosity as there is less morphological complexity (observation from high definition videos). Erosional processes will also reduce the unevenness of the mound and the reef structure, as when the corals die, the underlying framework may be rapidly bioeroded until it collapses (Roberts et al. 2005, Douarin et al. 2013). Rugosity is easily calculated from bathymetry (section 2.2.4), and can, therefore, be used to identify the potential occurrence of live cold-water corals in other areas.

As anticipated, BPI was higher for mini-mounds with living coral colonies. Corals are typically associated with areas of locally accelerated near-bed currents which are often found on sloping topographies and topographic highs because the encounter rate of food increases with higher current speeds (Genin et al. 1986, Frederiksen et al. 1992 Mortensen 2001, Thiem et al. 2006). Coral colonies can therefore be found on mini-mounds with a higher BPI as these mounds are more exposed to these preferential faster current speeds. At MR1 the formation of mini-mounds is possible as the tidal currents create a highly energetic environment with favourable food and temperature conditions. In deeper offshore settings coral carbonate mounds can be more than 100 m high (Chapter 4) and can, therefore, be picked up by BPI on coarser bathymetric grids (Wilson et al. 2007). This feature also forms the basis for the use of the BGS seabed mapping toolbox. The summits and upper flanks of these coral carbonate mounds are highly diverse and are capped by living cold-water coral and a rich associated community, consisting of sponges, crinoids, and crustaceans (Chapter 4).

2.4.2 Advantage of high definition video records

The model that included the sample data from the microbathymetry area and the high definition (HD) video data performed the best. The model was better at predicting the presence of live coral colonies compared to predicting absence. This was expected, as there was no absence data available from outside the central microbathymetry area. If microbathymetry data covering a wider area of the reef were available, true absence data could be included which would make the model more accurate. The lack of true absence data is a common restriction when modelling species presence/absence (Elith et al. 2006, Phillips et al. 2009). This would result in a more robust model for both presence and absence. Predictive models are sensitive to the number of presence points incorporated into the analyses, but the success differs among approaches (Stockwell and Peterson 2002, Bryan and Metaxas 2007). Adding more presence data on corals from outside the microbathymetry area gave a more equally distributed dataset accounting for the variation in environmental variables across the reef. This study highlights the advantage of using microbathymetry, which allowed us to observe real presence and absence complemented with HD video data to identify live coral colonies. However, a wider coverage of microbathymetry would allow better coverage of both presence and absence of live coral over the range of environmental variables. Combining the centrally located microbathymetry with HD videos gave robust results for presence but less robust results for absence of live coral colonies.

2.4.3 Future implications: climate change

Our understanding of the fine-scale local variation of coral growth at MR1 can be applied to monitor future changes, from anthropogenic impacts (e.g., bottom trawl damage) to the effects of global change including ocean warming and acidification. Corals at the Mingulay Reef Complex are subjected to daily tidal downwelling that delivers warmer and food-rich water (Davies et al. 2009). Since winter-time mixing causes surface-and deep-water conditions to be similar, no added effect of tidal downwelling is expected during this well-mixed season (Findlay et al. 2013). However, during the summer period the surface water increases in temperature (Inall et al. 2009, Findlay et al. 2013). Seasonal changes in bottom waters will only be small compared to the relatively more substantial changes in the surface water's temperature (Artioli et al. 2012, Kitidis et al. 2012). Therefore Findlay et al. (2013) predict that during the summer, corals on the shallower parts of the reef are exposed to a higher daily variability compared to corals located at greater depths. This difference in variability between the seasons could become more extreme because of sea surface temperatures increasing due to climate warming (+0.57°C per decade Inall et al. (2009)). It has been shown that warmer temperatures may increase the metabolism of corals, but can cause them to starve if food supply is not met (Dodds et al. 2007, Davies et al. 2009, Section

1.2). The interplay between current speeds, food supply and temperature are complex but essential to understanding spatial distribution differences in live coral presence at the MRC (Davies et al. 2009).

Ocean acidification is a major concern for many marine ecosystems, particularly calcifiers already growing in water masses close to carbonate under-saturation such as cold-water coral reefs (Guinotte et al. 2006, Roberts et al. 2006, Turley et al. 2006, Aze et al. 2014, Hennige et al. 2014). Ocean acidification impacts not only surface waters but the carbonate chemistry at depth (Caldeira and Wickett 2003). Studies on ocean acidification suggest that the whole ocean will become more acidic with the pH decreasing approximate 0.3–0.4 pH units by the end of the century (Guinotte et al. 2006, Roberts et al. 2006, Turley et al. 2006). This will also influence the depth of the aragonite saturation horizon (ASH), which creates conditions that are less favourable for skeletal growth (Orr et al. 2005, Guinotte et al. 2006, Turley et al. 2007). However, the shallow position of the MRC means that it is unlikely to be affected by the shoaling of the ASH. This makes the reef a possible site of interest as a refuge for cold-water corals in a future ocean where the shoaling ASH exposes deeper-dwelling corals to corrosive bottom waters.

However, for the MRC seasonal surface uptake of food, coastal runoff and increasing seawater temperatures may be of greater importance than the effects of ocean acidification (Findlay et al. 2013). Firstly, sufficient food supply is vital for cold-water coral growth (section 1.4). Duineveld et al. (2012) studied differences in the food supply to the cold-water coral reefs within the Mingulay Reef Complex. Their study showed that the corals here, primarily feed on surface algal matter. Climate change can modify the strength, position and interaction of the North Atlantic subpolar gyre (SPG) with the Subtropical Gyre (STG) (Henry et al. 2014, Victorero et al. 2016, section 5.4). This is likely to affect the oceans temperature, salinity and dissolved oxygen and also the composition and growth of algae in surface waters of locations where cold-water corals occur (Häkkinen and Rhines 2004, Hátún et al. 2005, 2009, 2017, Johnson et al. 2013, section 5.4). How a changing ocean will affect the coral's survival remains speculative. For example, Hennige et al. (2015) showed that *L. pertusa* could adapt to a combination of increasing CO_2 and temperature at the same time. However, this adaptation came with a trade-off for the physical strength of the coral. Coral colonies could, therefore, be more affected by bioerosion and physical damage by 2100 at the Mingulay Reef complex. Further site-specific studies are needed to fully understand the effects of climate change on cold-water coral reefs.

Our detailed map of the current presence of live corals on mini-mounds can function as a baseline and tool for future sampling and monitoring. Even though the bathymetry and video data were collected over several years, the impact on our results would be minimal. Growth rates of *L. pertusa* vary widely, ranging from 5 mm yr^{-1} to 26 up to 33 mm yr^{-1}, and depend on the amount of food-input, depth (closeness to shallow food-rich surface water), temperature and the harmful effects of resuspension (Mortensen and Rapp 1998, Gass and Roberts 2006, 2010, Orejas et al. 2011). If corals grew at the maximum growth rate of 12 mm yr^{-1} (calculated for the Mingulay Reef from downcore U-series by Douarin et al. 2013), from 2003 to 2012, the corals would have grown 120 mm. Thus, this is significantly smaller than the resolution of the bathymetric maps used in this study (35 x 35 cm and 2 x 2 m), and this growth would, therefore, remain unrecorded. After testing the model by ground-truthing, this approach could be used to guide sampling towards mounds with the highest or lowest probability of coral presence to maximize ship time when for example aiming to collect coral samples for fatty acid, isotope analyses, experimental laboratory studies, or to compare mounds in terms of biodiversity, age and sediment composition.

By mapping biogenic reefs, which are habitats (Section 1.2), the nature, distribution, and extent of distinct physical environments is illustrated. But more importantly, as shown here, they can predict the distribution of the associated species and communities (Harris and Baker 2012b). If more microbathymetry maps were to be collected in the areas of the MR1, which weren't covered by the microbathymetry used in this study, these could be used to test the accuracy of our predictive map. Monitoring change in the morphological characteristics of mini-mounds and live coral presence using the BGS Seabed Mapping Toolbox and microbathymetry maps would be useful to study the future development the reefs.

2.5 Conclusion

By using the new BGS Seabed Mapping Toolbox and the high-resolution ROV-mounted microbathymetry, together with the 2 m resolution ship-borne bathymetry and high definition videos, it was possible to predict the presence and absence of *L. pertusa* on mini mounds at the MR1. This improved the understanding of the distribution of live coral colonies at MR1. The uniquely high resolution of the microbathymetry allowed identification of individual live coral colonies in acoustic data (microbathymetry) for the first time. Environmental variables extracted from the 2 m resolution bathymetry provided insight on the local physical conditions of live biogenic reef framework in this area. The Mingulay Reef Complex is a highly energetic environment where coral growth and reef mound formation is regulated mainly by the tidal currents. By providing a detailed map with the current presence and predicted likelihood of presence of live corals on mini-mounds, a tool to guide future sampling and monitoring was provided. This study highlights the need for fine-scale environmental data, as fine-scale processes control live coral presence on the mini-mounds at the MRC and will be important to interpret live coral presence in other sites.

CHAPTER 3-THE EFFECT OF THE LOCAL HYDRODYNAMICS ON THE SPATIAL EXTENT AND MORPHOLOGY OF COLD-WATER CORAL HABITATS AT THE TISLER REEF, NORWAY

Published as peer-reviewed paper: De Clippele LH, Lundälv T, Huvenne VAI, Hennige SJ, Fox A, Orejas C, Roberts JM (2017). Coral Reefs 37(1): 253-266

3.1 Introduction

This chapter focusses on the Tisler Reef which was first discovered in 2002 (Lundälv and Jonsson 2003*).* It lies in the north-eastern part of the Skagerrak in the Hvaler area in Norway (Lavaleye et al. 2009). The reef is located north of the Tisler Island in a 48 km long ocean channel through which Atlantic water flows in the Ytre Hvaler (Guihen et al. 2012) (Figure 3.1).

From the North Sea water flows in the Skagerrak, with a strong haline stratification in the upper layers (Gustafsson 1999). This water mixes with brackish water from the Kattegat as it follows the cyclonic flow around the strait. As mentioned in Chapter 2, the NOA index, and thus the strength and direction of the Westerly winds influence the strength of the Atlantic water and consequently its inflow in the North Sea that results in an increased flow to the Skagerrak (Winther and Johannessen 2006).

The shallow Kattegat (mean depth of 26 m) and the Belt Sea (mean depth of 13m) separate the Skagerrak from the brackish Baltic Sea (Stigebrand 1983). Bottom water is advected from the Skagerrak into the Kattegat and Baltic while surface water flow is in the opposite direction. The Baltic Sea has a net inflow to the Skagerrak (Wither and Johannessen 2006) with an outflowing (towards the Baltic) mean salinity (psu)17.4 and an inflowing mean salinity of 8.7 (Stigebrandt 1983). The Skagerrak Front, between the Skagerrak and the Kattegat, governs inflow and outflow from the Baltic Sea. The Skagerrak Front is geostrophically balanced and typically exists between Jutland, at the northern tip of Denmark, across to the Swedish coast (Stigebrandt, 1983). The front has a dynamic position and may change rapidly due to the barotrophic forcing of sea height differences and sea surface wind forcing (Rodhe, 1996).

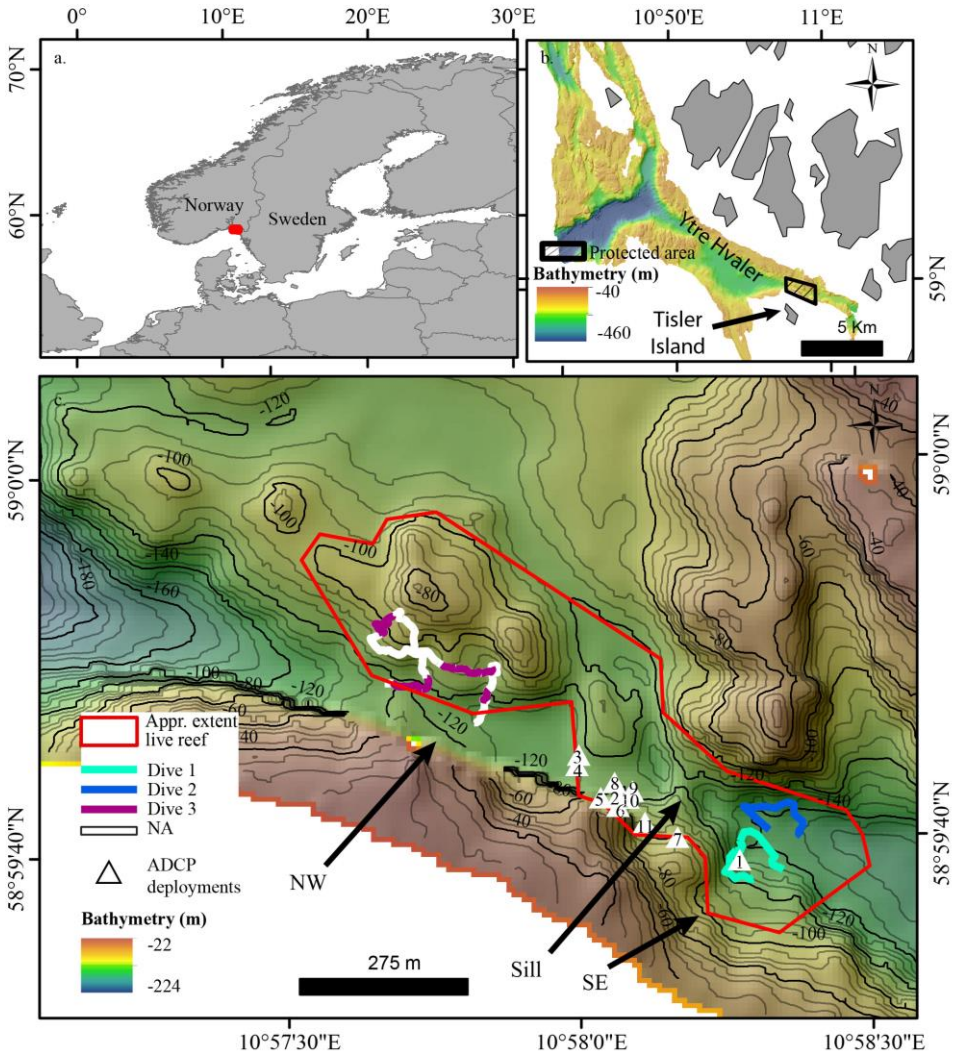

Figure 3.1 (a) Location of Tisler Reef in Norway **(b)** location of protected area surrounding the Tisler Reef (black box) in Kosterfjord **(c)** Dive 1 and 2 are located on the SE part of the Reef, and dive 3 is located in the NW part of the reef. The white part of dive 3 represents data which was not available (NA) for analysis. The white triangles with numbers show locations of the ADCP deployments.

The Tisler Reef is located in the Kosterfjord. The Kosterfjord is a NNE oriented submarine trench that parallels the coastline of SW Sweden to the east and is sheltered by numerous islands to the west but deviates to NW, south of the Sostre Islands where it transists into the deep Norwegian Channel (Wisshak et al. 2005). Freshwater runoff from fjords also plays a large part in the surface salinities in the Skagerrak. A large number of fjords, such as the Gullmar Fjord, Sweden, and the Oslofjord, Norway, empty into the Skagerrak. The Hvaler Deep is connected to the Oslofjord and the Norwegian Trench. The topography and hydrography of fjords cause them to be dynamic environments but sheltered from extreme currents, consequently, a large number of *Lophelia*

pertusa reefs are found in fjords on the Norwegian coastline (Freiwald et al. 2004, Roberts et al. 2006). However, the Kosterfjord is not a fjord as it is open to the sea at both ends (Dahlgren et al. 2006).

At the Tisler Reef, the environmental conditions are similar to the larger Skagerrak. There is a strong baroclinic stratification of the water masses and a wide temperature range (February and March are the coldest months) (Wisshak and Rüggeberg 2005). The water temperature commonly varies around 8 °C (Wagner et al. 2011), and the reef is thought to be between 8,600 and 8,700 years old (Wisshak et al. 2005). The live part of the reef is approximately 70 to 160 m deep, 1.2 km long, 200 m wide and is oriented in a NW-SE direction (Figure 3.1c) (Lavaleye et al. 2009). In December 2003, it was protected against bottom-impacting fishing techniques by Norwegian fishery regulations (Fosså et al. 2010) (Figure 3.1b). Over a period of two years, Wagner et al. (2011) studied the hydrodynamical processes at the Tisler CWC Reef (Hvaler area, Norway) and how these affect the delivery of food to the reef. They found that the Tisler reef has a dynamic environment with average high current speeds of 10- 50 cm s^{-1}, and a peek current speed of 74 cm s^{-1}. The flow direction on the Tisler Reef alternates between north-westward (NW) and south-eastward (SE). The hydrodynamics on the Tisler Reef are similar to those described for the Mingulay Reef Complex, offshore of Scotland, where downwelling occurs downstream of the reef (Duineveld et al. 2012) delivering chlorophyll rich, warmer water (5.6 - 13.9 °C) from the surface to the bottom which can stimulate the growth of CWCs (Davies et al. 2009, Findlay et al. 2013, Moreno-Navas et al. 2014). At Mingulay this downwelling is due to the oscillating tidal currents, dominated by the M_2 component, reversing direction every 6 hours. At Tisler the tides are very weak (5 to 10 cm s^{-1}) and the dominant currents are density and wind-driven (Lavaleye et al. 2009). These reverse direction irregularly, every several days to several weeks (Lavaleye et al. 2009, Wagner et al. 2011). The similarities between the Tisler and Mingulay Reef are that in both cases there is flow over a sill which reverses direction periodically. However, the different timescale possibly makes the downwelling of food and nutrients more varied at Tisler as data from Mingulay suggests pulses of downwelling as the new direction is established. However, since current flow direction reverses and downwelling occurs over downstream sill crests, this vertical flux occurs on both ends of the Tisler Reef where it supplies food to the seabed supporting benthic secondary productivity, including coral growth. Wagner et al. (2011) demonstrated this by analysing near-bed current direction and velocity over a period of two years and by measuring the temperature, chlorophyll *a* concentration, and salinity across the water column using acoustic doppler current profilers (ADCP) and CTD casts on both the SE and NW side of the Tisler Reef (see Figure 2 in Wagner et al. 2011).

Corals, among many other benthic organisms, have different growth forms as they have a high level of phenotypic variation (Foster 1979, Bell and Barnes 2001, Freiwald 2002, Todd 2008, Gori et al. 2013, Vad et al. 2017). Local hydrodynamics, which affect food availability to the corals and their ability to feed over short timescales (Purser et al. 2010, Orejas et al. 2016) and over longer timescales, are an important determinant of coral morphology (Wainwright and Dillon 1969, Mortensen and Buhl-Mortensen 2005, Todd 2008). Branching corals in particular, seem to respond to changes in hydrodynamics, with their shape becoming more compact with high current speeds, and more asymmetrical when these currents are uni-directional. More symmetrical shaped, open frameworks with thin branches form when the current speeds are lower (Kaandorp 1999, Chindapol et al. 2013). The morphology of a coral colony will also affect the availability of food to the polyps by altering small-scale turbulence and slowing current speeds in the immediate proximity of living polyps. Coral colonies that are less compact and have thinner branches are more likely to capture food particles as water will flow through them more easily than in compact colonies. When the current speeds are too high, a more compact morphology with thick branches creates more stability for the colony (Chamberlain and Graus 1975). Aside from the local hydrodynamics, genetic differences and other variables such as the availability of food and sedimentation rates can cause variation in the growth forms of corals (Barnes 1973, Foster 1979, Willis and Ayre 1985, Smith et al. 2007).

The habitat that is created by CWC framework is a place for organisms such as crabs, fish and sharks to feed, shelter and reproduce (Henry et al. 2007, 2016, Baillon et al. 2012, Buhl-Mortensen et al. 2016). The live and dead coral structures provide a substrate for benthic filter feeders such as sponges and crinoids as well as other cnidarians (Orejas and Jiménez 2017). The coral creates an elevated feeding platform, exposing the filter feeders to higher current speeds increasing their chances of capturing food (Roberts et al. 2005, Mortensen and Fosså 2006, Henry and Roberts 2007, Buhl-Mortensen et al. 2016). Sponges can occur in especially large numbers forming a substantial component of CWC reefs biomass (Hogg et al. 2010). They function as nutrient recyclers, substrate stabilisers, bioeroders, as a food source and as a habitat for other organisms (Wulff 2001).

Wagner et al. (2011) provided information on the particulate organic matter (POM) composition in the benthic boundary layer (BBL) across the Tisler Reef and found that this was significantly different between the two sides of the reef. Downstream POM was identified as being fresher in composition compared to upstream samples. With the observation that downwelling occurs on both sides of the Tisler Reef, coral and sponge growth are also expected to be supported on both sides of

the reef. To test this null hypothesis, we examined the percentage cover of important ecosystem engineering species (the coral *L. pertusa* and two dominant sponges *M. lingua* and *Geodia* sp.) in relation to local hydrodynamics and topographical variables. We also assessed the densities of different coral growth morphologies on both sides of the reef.

3.2 Material and methods

3.2.1 Hydrodynamic data

An RDI Workhorse 300 kHz Acoustic Doppler Current Profiler (ADCP) was deployed eleven times to measure current speed and direction every 30 minutes, every month from 2006 to 2010 in different locations of the reef (Table 3.1, Figure 3.1c). The ADCP were all in the vicinity of the reefs sill and not at the NW and SE ends of the Tisler Reef. The data was provided by is part of a larger environmental monitoring project at the Tisler Reef (Lavaleye et al. 2009). Except for the first deployment ADCP1, the instrument was located each time near the centre of the sill (Figure 3.1c). The longest continuous logging occurred during deployment ADCP10, over a period of 8 months and 9 days. ADPC11 only recorded for 3 days and is therefore not included in the analyses. ADCP data were plotted using python and the matplotlib package

Table 3.1 The location, deployment time and depth for the ADCP deployments that were used to record measurements of current speeds and direction

Longitude	*Latitude*	*Data Name*	*Deployed*	*Recovered*	*Depth (m)*	*Days*
10.97126	58.99413	LF ADCP 1	27/03/2006	27/04/2006	138	31
10.96785	58.99511	LF ADCP 2	04/05/2006	02/10/2006	111	181
10.96676	58.99573	LF ADCP 3	05/10/2006	29/04/2007	120	206
10.96670	58.99558	LF ADCP 4	30/04/2007	04/12/2007	121	218
10.96735	58.99510	LF ADCP 5	04/12/2007	15/04/2008	112	133
10.96785	58.99496	LF ADCP 6	15/04/2008	04/08/2008	117	111
10.96951	58.99448	LF ADCP 7	04/08/2008	23/02/2009	109	203
10.96776	58.99531	LF ADCP 8	25/02/2009	05/08/2009	119	161
10.96826	58.99518	LF ADCP 9	06/08/2009	11/11/2009	121	97
10.96813	58.99508	LF ADCP 10	12/11/2009	23/07/2010	113	253
10.96860	58.99471	LF ADCP 11	02/09/2010	05/09/2010	110	3

The flow on the Tisler Reef is channelled over a sill through the sound, which has a NW-SE orientation. The currents can flow in either direction, to the northwest or to the southeast. Using the data provided by ten of the ADCP deployments, the amount of time that the current was in each direction was calculated. The average speed of the flow was calculated per ADCP deployment as an annual average per year was unreliable because the currents vary with the position of the ADPC instrument (Figure 3.1c). The ADCP data were binned at 2 m intervals every 20 minutes. Data

collected very near the bottom experiences higher turbulence caused by friction with the sea floor and the reef itself, therefore, all data used for the calculations were recorded at 86 m depth, at least 20 m above the seafloor for each ADCP deployment and were not affected by higher turbulence.

3.2.2 Multibeam data

Bathymetry data were collected with a shipboard multibeam echosounder of the type SeaBeam 1050 during ALKOR cruise 232 in 2003. Data processing was carried out using the Fledermaus software resulting in a grid with pixel size of 8.22 x 8.22 m. Several topographic variables were derived from the bathymetric grid using ArcGIS 10.1, ESRI Software: slope (percentage), aspect (eastness and northness), rugosity and bathymetric positioning index (BPI). Here, the BPI was calculated within ArcGIS with the Benthic Terrain Model tool (Jenness 2002). The neighbourhood's shape was an annulus, and a size of (inner and outer radius) i3 x o6, i6 x o9, i9 x o12 cells was used. Rugosity was calculated using the Focal Statistics routines available in ArcGIS. The used neighbourhood's shape was a rectangle, and a size of 3 x 3 and 9 x 9 was used to measure terrain roughness (Jenness 2002). Definitions of these variables can be found in section 2.2.4.

3.2.3 BGS Seabed Mapping Toolbox

The semi-automated mapping approach, that was developed and applied to the Mingulay Reef Area in Chapter 2, proved to be a fast and consistent method to delineate and characterise mounds. To explore the application of the BGS Seabed Mapping Toolbox on other reef systems, it was used on the 8.22 x 8.22 m Tisler Reef bathymetry. The results will be used for descriptive purposes only and further applications are discussed in Chapter 5. Detailed information regarding the approach, the BPI feature delineation and description tool can be found in Chapter 2 and Gafeira et al. (2015) (see appendix).

The BPI was calculated from the bathymetry within ArcGIS with the land facet corridor tool (Jenness et al. 2013). Here, the used neighbourhood's shape (annulus) and an inner and outer radius of 6 and 12 cells respectively were chosen. A cut-line BPI value of 6, minimum BPI value of 8, minimum area of 50 m^2 and a minimum width/length ratio of 0.2 were used as the thresholds. A buffer distance of 20 m was chosen based on the morphological characteristics of the mounds and how they are represented in the BPI raster used as data input.

A list of the variables extracted by the tool are given in Table 2.1. As in chapter 2, the area ratio was calculated separately, by dividing the area of the polygon with the area of the MBG box to give an indication of the shape of the mound.

3.2.4 Video data collection

The R/V *Lophelia* from Tjärno Marine Biological Laboratory (TMBL, University of Gothenburg) was used to deploy the remotely operated vehicle (ROV) Sperre SubFighter 7500 DC to record high definition video transects at the Tisler Reef on the 22nd and 23rd of May 2014. Two video transects were collected on the SE end (dive 1 and 2) with a length of 239 m and 203 m, respectively. On the NW end, a single transect was collected (dive 3) (Table 3.2) from which 57 % was not useful due to limited visibility caused by increased sediment resuspension and the high variability in the vehicle's altitude above the seafloor (Figure 3.1). These transects were chosen as they were within the live reef area and closest to the NW and SE stations where Wagner et al. (2011) conducted their first two CTD, chlorophyll and particulate organic matter (POM) measurements.

Table 3.2 HD video transects recorded on the SE and NW sides of Tisler Reef in 2014

Dive	*Side*	*Start Lat*	*Start Lon*	*End Lat*	*End Lon*	*Depth range (m)*	*Av. depth (m)*	*Length (m)*	*Time (min)*
1	SE	58.99397	10.97252	58.99458	10.97224	124–142	135	239	41
2	SE	58.99455	10.97200	58.99487	10.97169	129–147	139	203	28
3	NW	58.99683	10.96219	58.99625	10.96381	77–130	110	622	50

A Sony FCBH11 HD camera with two Sperre 200W HMI lights was used to collect the video footage from an altitude of ~1 m. Video signals were transmitted over an optical fibre and recorded on compact flash cards using a nanoFlash recorder (Convergent Design). The ROV moved at an average speed of 0.7 knots. Two laser beams, spaced by 5 cm, were used as a reference to calculate the transect width as well as to measure the colony size. Navigation data from a Kongsberg Simrad USBL system type HPR 410P, a Simrad dGPS instrument and a Furuno satellite compass were integrated in the software package Olex® to provide ROV navigation and transect position data.

A video frame was extracted every five seconds from the video footage using the software VLC7. This extraction frequency is based on an average speed of 0.7 knots, meaning that a frame is analysed every ~1.8 m along the transect. The average surface area covered per image for each dive was calculated using the calibrating tool in Coral Point Count (see below) (Kohler and Gill 2006). This tool calculated the average maximum width and height for each image. The calculation was based on the 5 cm separation between the two laser points. Each frame covered an approximate area of 1.4 m (width) x 0.80 m (height) with a resolution of 1,280 x 720 pixels. A total of 322 frames were extracted for analyses (158 frames were extracted from dive 1, 68 from dive 2

and 96 from dive 3, see Table 3.3). This approach was based on the method used by Purser et al. (2009), who extracted frames every two seconds, covering an area of 2 x 1.5 m. However, 70% of these frames overlapped. Even though the frequency of frame extraction here was every five seconds rather than every two seconds, still 75% of the frames overlapped or had poor visibility and were not included. This is because the speed of the ROV was on average 0.7 knots but varied depending on the underlying substrate. Extracting a frame every five seconds rather than, for example, every 10 seconds was still preferable as the latter would have resulted in covering unequal amounts of surface area.

3.2.5 Calculation of the spatial extent of the different substrate types, **Lophelia pertusa, Geodia sp.** ***and*** **Mycale lingua**

The percentage cover of the substrate types (coral rubble, soft substrate and hard substrate), the coral colonies (live and dead *L. pertusa*) and sponges (*Geodia* sp., *Mycale lingua*) (Figure 3.2) was calculated with a 50-point quadrat method using the software Coral Point Count with Excel Extensions 4.1 (CPCe) (Kohler and Gill 2006). This CPCe software is freely available, user-friendly, time efficient and provides reliable results for the percentage cover calculations of seabed organisms and substrates. Purser et al. (2009) compared the results and processing time of a 15-point quadrat, a 100-point quadrat and a frame mapping method with those produced by an automated machine-learning algorithm. They concluded that the automated methods gave similar results to all the manual methods. The correlation for the 15-point quadrat approach to the automated one was similar to the 100-point approach (~0.79). However, the processing time differed greatly between the manual methods, for which 3 min per frame were needed for the 15-point approach, while 15 min and 45 min per frame were needed for the respectively 100-point and map approach respectively. Since Purser et al. (2009) pointed out that a low point coverage (15-point) can result in an underestimation of the sponge and coral cover, a 50-point overlay was utilised in the present study. A 50-point approach was still relatively time-efficient and would provide the necessary coverage to produce reliable results. The points were randomly placed over each image, and the species and substrate below each point were noted. In the CpCe software, the percentage cover can be calculated for an individual image or for a group of images.

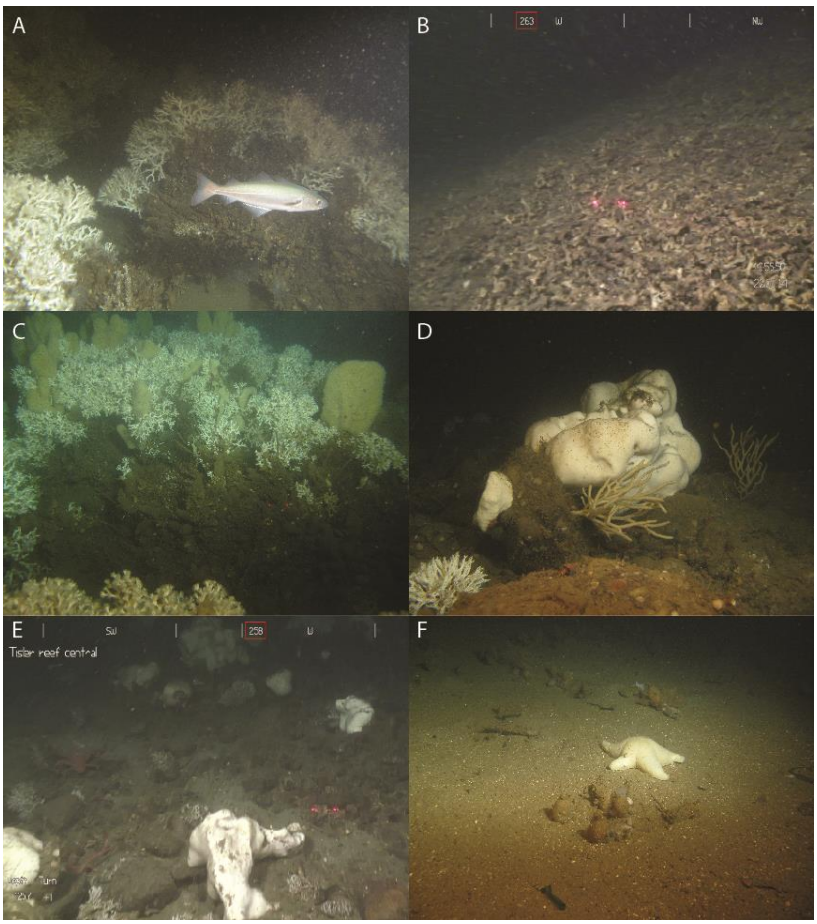

Figure 3.2 Overview of the most representative habitats documented in the video transects conducted in Tisler Reef, **(a)** live *Lophelia pertusa* thickets on top of the dead *L. pertusa* base-layer, **(b)** coral rubble **(c)** *M. lingua* growing within *L. pertusa* branches, **(d)** *Geodia* sp. **(e)** hard substrate colonised by several *Geodia* sp. specimens, **(f)** soft sediment with presence of a starfish.

3.2.6 Lophelia pertusa *morphology*

The morphology of coral colonies at the Tisler Reef was described as a function of their overall shape, branch length and colony size. Past studies have identified two dominant CWC morphology classes. The first is a more compact "cauliflower" shape, which results from live coral branches growing more symmetrically in multiple directions (Freiwald et al. 1999, Rogers 2004, Orejas et al. 2009). The second morphology class has a "bush-like" shape with colonies that grow more unidirectional in a plane (Wilson 1979, Chindapol et al. 2013). Here, these two morphotypes were used as a first category distinguishing the colony's shape as (1) cauliflower *versus* (2) bush- like (Figure 3.3). The colony's overall branch morphology was identified as (1) shorter (< 5 cm) *versus* (2) longer branching patterns (>5-10 cm) (Figure 3.4). The category size included very small (< 5 cm), small (5 – 30 cm), medium (30 – 100 cm) and large (> 100 cm) coral colonies (Figure 3.5). In this study, an individual *L. pertusa* colony refers to a distinctive visual colony. Skeletal fusion in *L.*

pertusa is common (Hennige et al. 2014), and therefore a ‘colony’ as termed here may represent multiple genotypes.

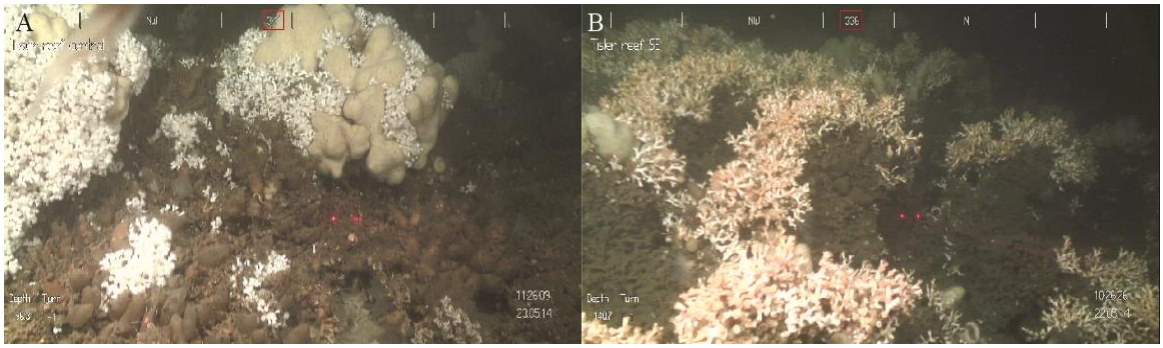

Figure 3.3 (a) *Lophelia pertusa* large “cauliflower” morphotype versus **(b)** medium-sized *L. pertusa* “bush-like” shaped coral colonies. Laser scale: 5 cm

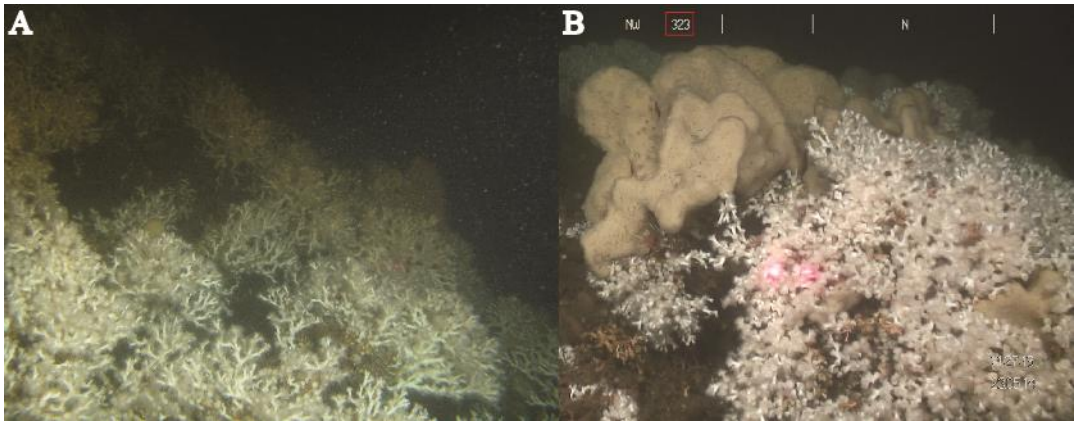

Figure 3.4 (a) *Lophelia pertusa* “long” versus **(b)** *L. pertusa* “short” coral branches. Laser scale: 5 cm

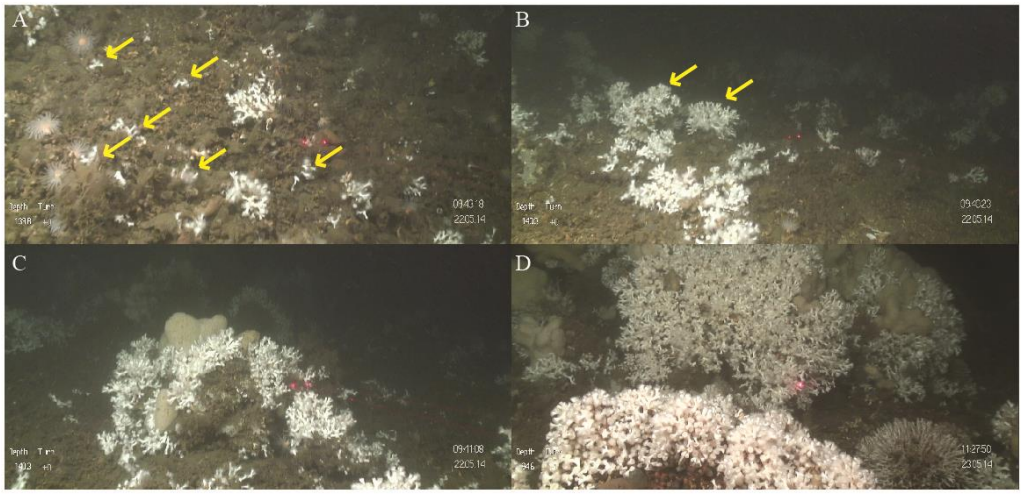

Figure 3.5 The different size classes defined for *Lophelia pertusa* in this study: **(a)** very small *(< 5* cm) **(b)** small (5 -30 cm) **(c)** medium (30 – 100 cm) and **(d)** large (> 100 cm). Laser scale: 5 cm. The yellow arrows indicate what the very small (3.5a) and small (3.5b) coral colonies are in the figure.

3.2.7 Statistical analyses

For the statistical analyses, each dive was divided into 25 m sub-transects. This length was chosen as it gave the best representation of the variability in the data. As mentioned in section 3.2.4, a large proportion of the frames were excluded from the analyses due to overlap or low visibility. The number of frames that were of good quality for analyses varied between the dives (Table 3.3) and caused some of the 25 m sub-transects to contain not enough analysed frames to produce reliable and representable results. Therefore, it was chosen that 25 m sub-transects with a minimum of 9 good frames present were included in the analyses.

A $0.5\ \log_{10}(1+x)$ transformation was applied following the approach of Guinan et al. (2009) who also used CpCe, to the percentage cover data of the substrate classes, *L. pertusa* (live and dead) and the sponges (*Geodia* sp. and *M. lingua*). This transformation decreases the relative importance of high percentage coral cover values and converts the data in a range from 0 to 99, to the range 0 to 1(Aitchison 1986). This transformed dataset was also used to investigate the co-occurrence of the sponges (*Geodia* sp. and *M. lingua*) and *L. pertusa* (live and dead), for which the Pearson Product-Moment correlation coefficient (r), was calculated in R. Since different morphology classes (shape, branch length, size) were attributed to every coral colony, density was used instead of percentage cover. The densities of *L. pertusa*'s morphology classes were calculated by dividing the number of

colonies by the average surface area per sub-transect. It is important to note that this surface area calculation is an approximation, as the precise angle and height from which the ROV was recording the high definition video were unknown.

The software package PRIMER 6 was used to perform the statistical analyses (Clarke and Warwick 2001). The aim was to establish if there was a difference in CWC distribution and morphology between the 25 m samples from the transects according to their location on the reef (SE *versus* the NW side). In PRIMER, a Bray-Curtis resemblance matrix was created from the sample data. From the resemblance matrix, analyses of similarity (ANOSIM) were carried out to determine if there were significant differences between the samples from the SE and NW side of the reef. SIMPER analyses were then carried out to identify how the percentage cover (*L. pertusa*, *M. lingua*, *Geodia* sp. and the different substrates), and *L. pertusa* morphology classes differed between the different locations. The relative contribution of the environmental factors (slope, rugosity, BPI, northness, eastness, depth) to the observed patterns was determined using BIO-ENV analyses in PRIMER.

Table 3.3 Overview of the number of frames extracted and used for statistical analyses.

Dive	*Total # of extracted frames*	*Total # of frames used for analyses*	*Total # of 25 m sub-transect used for statistical analyses*
1	158	148	7
2	68	53	3
3	96	60	6

3.3 Results

3.3.1 Mound delineation and morphometric characteristics

A total of 14 mounds were delineated by the BGS seabed mapping toolbox from the 8.22 x 8.22 m bathymetry in the Tisler Reef Area (Figure 3.6). The morphometric characteristics of the mounds are given in table 3.4

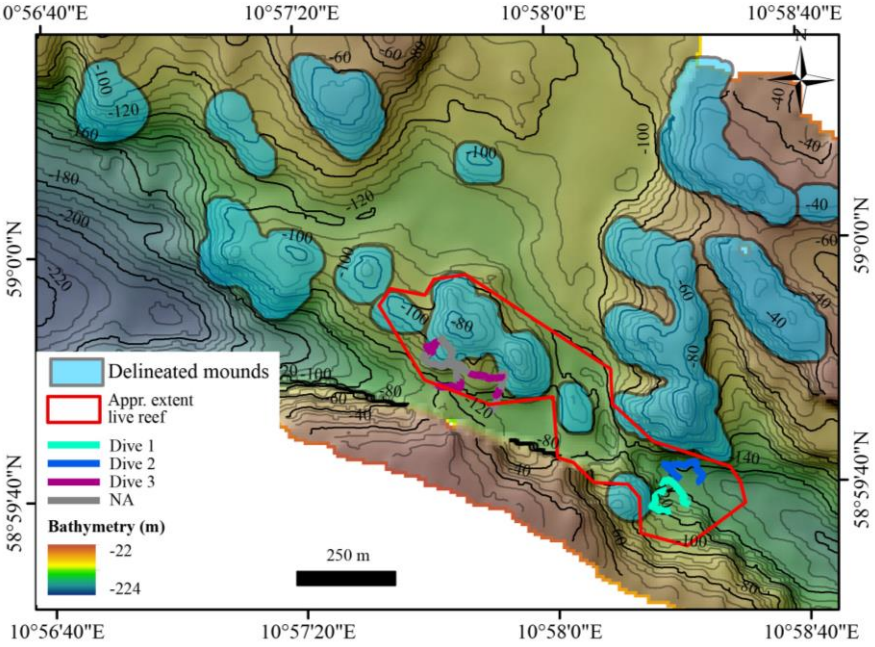

Figure 3.6 Tisler Reef with mounds delineated in red, obtained with the BPI delineation tool

Table 3.4 Table listing the morphometric characteristics of the mounds

	Range	Average	Standard deviation
Width	89-285 m	168 m	68 m
Length	123– 659 m	280 m	53 m
Area	10295-119030 m^2	37990 m^2	32005 m^2
Area Ratio	0.55-0.86	0.73	0.09
Perimeter	378-2216 m	832m	522 m
BPI	8-35	17	8
Orientation	39-177	129	35
Height (m)	11-80	38	24

3.3.2 Hydrodynamic data: current direction and speed

The current direction calculated for the four-year long period was towards the SE for an average of 57 % of the time, and to the NW for 43 % of the time (Figure 3.7 and 3.8). The direction of the flow over the reef typically lasted for several days up to sometimes two weeks, before reversing its direction. The highest current speed recorded in our data set was 99.8 cm s^{-1}, which was measured when the current was flowing in the NW direction. Figure 3.7 shows the speed and direction of the main current axis, for each of the ADCP deployments, at 86 m depth. Our data showed higher current speeds being recorded more frequently when the flow was in the SE-NW direction. From the left to the right, the figure 3.8 shows that current speed recorded varies with the position of the deployments. For example, ADCP3 (at the NW of the group) had stronger currents towards the NW, while ADCP7 (positioned to the SE) recorded stronger southeastward currents (Figure 3.7). This acceleration of near-bed currents downslope, downstream of the sill is characterised of stratified flow over sills (Farmer and Denton 1985).

The ADCP6 plot is N-S while the others are not. There are two possible explanations for this. The first is topographic steering, with the local steep topography re-directing the currents to more N-S than NW-SE. ADCP6 is on the edge of the group, so this is possible. However, the proximity to ADCP5 (which shows the standard directions), and the altered current directions extending to the

surface, is surprising though. A second explanation is that there is something magnetic on the seabed, or on the frame the ADCP is attached to, which has biased the ADCP's onboard compass, which is used in turn to determine the current directions. If this is the case, then from comparison with neighboring ADCP5 we can be confident that the readings have just been biased by < 90 degrees (NW currents showing up as N rather than pushed right round to read N when currents are in fact SE). So, they will still be usable for determining the general direction of flow across the reef.

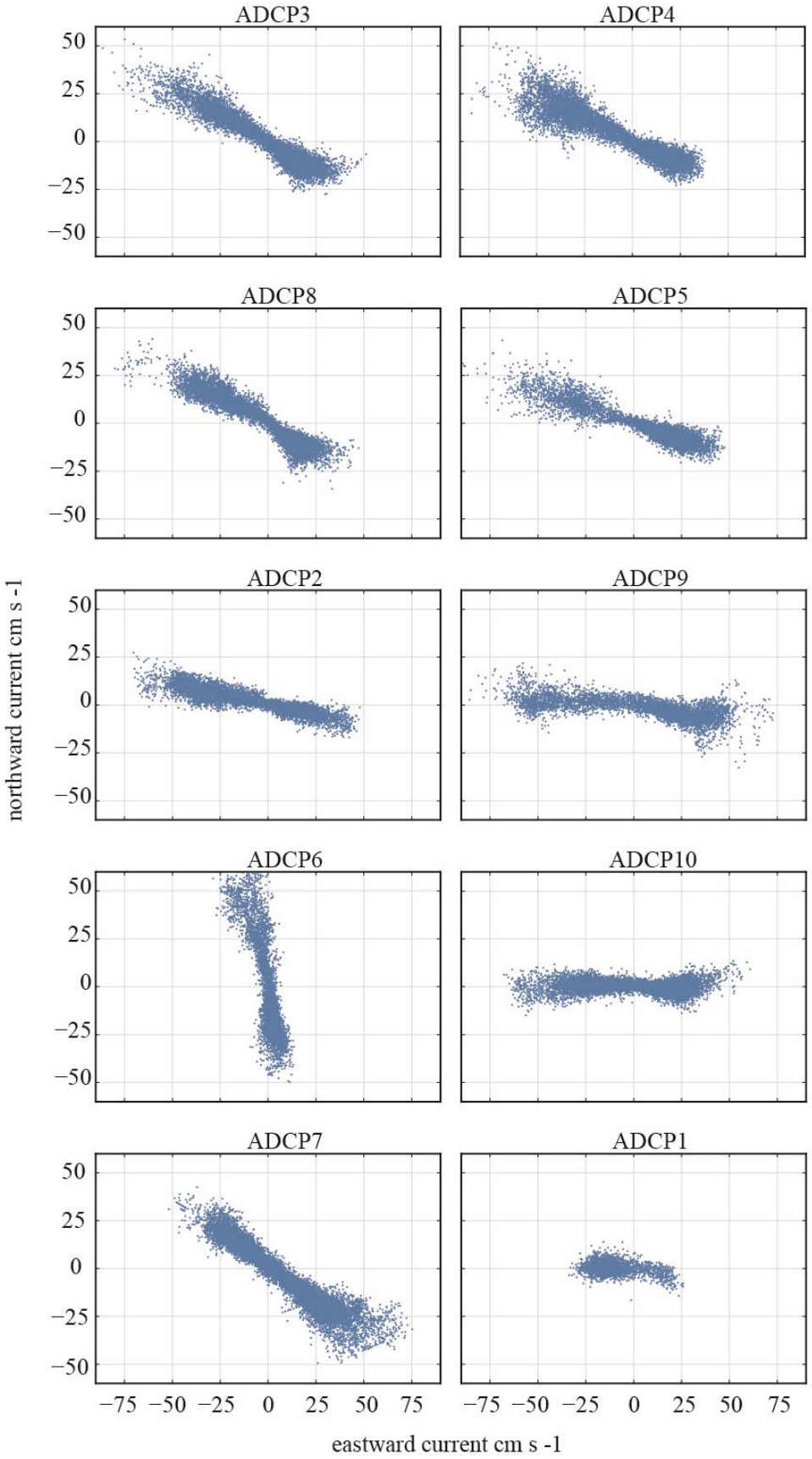

Figure 3.7 The speed (cm s^{-1}) and direction of the main current axis for the ADCP deployments at 86 m depth.

3.3.3 The spatial extent of the different substrate types, the coral **Lophelia pertusa** *and the sponges* **Geodia** *sp. and* **Mycale lingua**

The average percentage of rubble and soft substrates was significantly higher on the NW side, while hard substrates were significantly more prominent on the SE side of Tisler Reef (R: 0.384; $p < 0.01$) (Figure 3.8). The average percentage of both live and dead *L. pertusa* per 25 m sample high on the SE side and also significantly higher compared to the NW (R: 0.57; $p < 0.01$) (Figure 3.8). This was reflected in the ratio of live / dead *L. pertusa*, which is respectively 2.15 on the SE side and 7.17 on the NW side. This indicates that the percentage cover of live and dead *L. pertusa* on the SE is closer to equal, while on the NW side there is a high percentage cover of live but a low percentage cover of dead *L. pertusa*. The percentage cover of the sponge *M. lingua* was significantly higher on the NW side, while, conversely, the sponge *Geodia* sp. had a higher percentage cover on the SE side (Figure 3.8) (R: 0.31; p: 0.02). The environmental variables depth and BPI contributed the most to explain the difference between the two locations (BIO-ENV). However, only depth was significantly different (ANOSIM R: 0.34; p: 0.05). The SE samples are deeper (125 to 145 m depth) compared to the NW samples (98 to 125 m depth).

A weak correlation (of 0.33) for the co-occurrence of live *L. pertusa* with *Geodia* sp. was found. A stronger positive correlation (of 0.67) was found between dead *L. pertusa* and *Geodia* sp. High positive correlations (of respectively 0.69 and 0.70) were calculated for both live and dead *L. pertusa* with *M. lingua.*

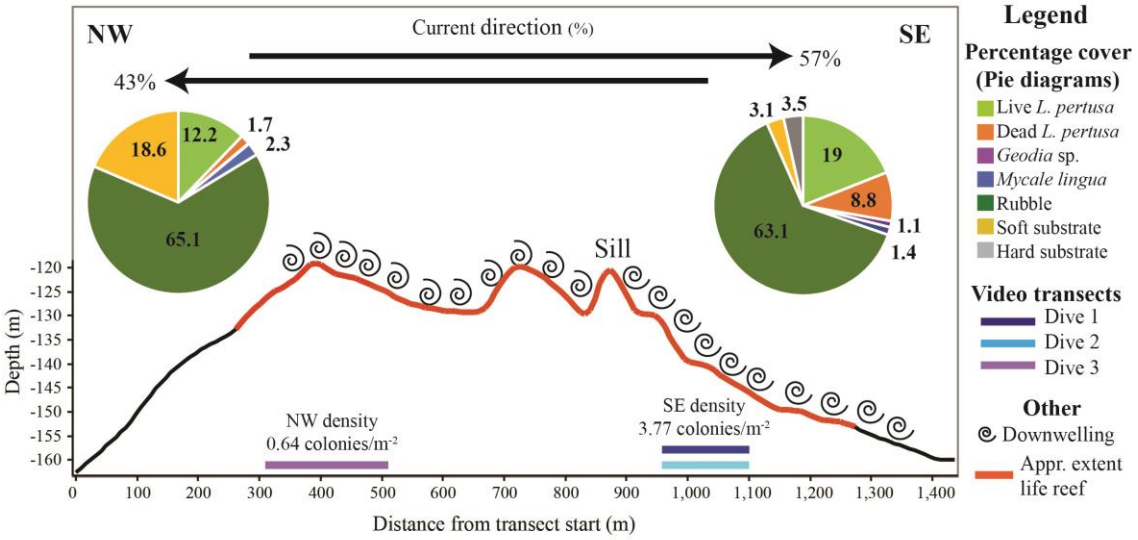

Figure 3.8 Diagram of the Tisler Reef based on Figure 2 in Wagner et al. (2011) with the red line showing the approximate extent of the live reef and the swirls showing where downwelling happens. The orientation of the swirls depends on the direction of the current. When the current is towards the SE, downwelling occurs on the SE side of the sill. Visa versa for the NW side. The values along the x-axis represent the distance from the NW end towards the SE end of the reef. The location of the video transects is indicated by the coloured lines on the bottom of the figure. The black arrows in the top of the figure represent the percentage of the current direction. The pie diagrams contain the average percentage cover of live *Lophelia pertusa*, dead *L. pertusa***,** *Geodia* sp., *Mycale lingua***,** rubble, soft and hard substrate for the NW and SE side. The density of live corals colonies is given for both sides (m^2) just above the location of the video transects.

3.3.4 Lophelia pertusa *morphology*

In total 1,708 coral colonies were counted. The density of corals was significantly lower on the NW side (0.64 corals m^{-2}) than on the SE side (3.77 corals m^{-2}) (Figure 3.8). Very small (n = 544) and small (n = 463) sized colonies had on average between 1-50 branches that were not large enough to visually assign a morphology class. Therefore, only the medium (n = 527) and large (n = 174) sized colonies were described as a function of shape and branch length. ANOSIM analyses in PRIMER showed that there was a significant difference between the NW and SE side of the reef in terms of coral morphology (shapes R: 0.63; $p < 0.01$, branch length R: 0.58; $p < 0.01$, size classes R: 0.54; $p < 0.01$) (Figure 3.9). All morphology classes were more abundant on the SE side of the reef, but the proportion of the different morphologies differed (Figure 3.9). The NW side had a higher proportion of cauliflower-shaped colonies compared with bush-like colonies (SE: 0.02 *vs.* NW: 0.43) (Figure

3.9). The NW side also had a larger proportion of short branches *versus* long branches (SE: 0.12 *vs.* NW: 0.43). The proportion of very small colonies was much higher on the SE side (0.52) compared to the NW (0.14). BIO-ENV analyses revealed that the variables northness and depth contributed most to differences observed in the data. ANOSIM showed that only depth caused a significant difference on the abundance of the shapes, branch length and size of the colonies.

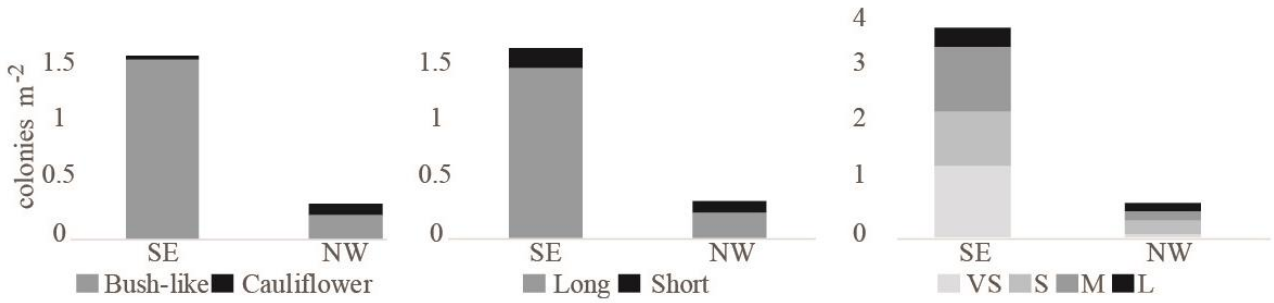

Figure 3.9 Density (colonies m^{-2}) of the colonies with the different shape categories, branch length and the different size classes between the SE and NW side of the reef. **(a)** cauliflower-shaped *vs* bush-like shaped colonies **(b)** short versus long coral colony branches **(c)** Proportion of the different size classes between the SE and NW side of the reef for VS (very small), S (small), M (medium) and L (large)

3.4 Discussion

3.4.1 Percentage cover of Lophelia pertusa

As can be seen from figure 3.1c and 3.6, the live part of the reef extents both on and off the delineated mound structures visible in the reef area. Reefs which have developed after the last glacial are typically smaller in size, have a strong substrate control and owe their overall morphology to the features they colonised (also e.g. Sula Ridge, Mingulay Reef Complex), and are therefore classified by Wheeler et al. 2007 as having an "inherited" morphology. Wagner et al. (2011) stated that on the Tisler Reef, growth and development takes place on both sides of the sill, thanks to downwelling occurring on both sides (Figure 3.1c). However, a significantly lower percentage coverage of coral habitat on the NW side of the reef became apparent in this study, where parts of the transect are located on a delineated mound. Firstly, the higher percentage cover of soft substrates on the NW side is likely to decrease the availability of hard substrates that corals need for settlement (Wilson 1979). Secondly, the four-year-long current direction data indicated that the dominant current flows 57% of the time to the SE and 43% to the NW, which broadly confirmed the pattern observed over a two-year-long period by Wagner et al. (2011). This implies that the SE side of the Tisler Reef is more frequently exposed and for longer periods of time to the downwelling of surface water, where warmer and more chlorophyll-rich water is transported down to the corals, creating more favourable growing conditions for *L. pertusa* and sponges, as already documented in other areas (Duineveld et al. 2007). Together with a higher percentage cover of soft substrates available on the NW side, the difference in the frequency of downwelling could explain why this SE side had a higher percentage of coral habitat.

The Tisler Reef is a highly dynamic environment. Current speeds as high as 99.8 cm s^{-1} were recorded during 2006-2010, higher than previously reported (Wagner et al. 2011). Suspension and filter-feeding organisms, like corals and sponges, thrive in high current speed environments, as it increases their food encounter rates (Best 1988, Hunter 1989, Sebens et al. 1998, Fabricius et al. 1995). Fast currents also help prevent polyps from becoming clogged with sediments (Brooke et al. 2009, Larsson and Purser 2011). Zooplankton capture rates can vary between different coral species and can depend on flow speed, water temperature and prey size (Purser et al. 2010, Gori et al. 2015, Orejas et al. 2016). For *L. pertusa* the zooplankton capture rate is optimal at rather slower speeds of 2.5 cm s^{-1} (Purser et al. 2010). When the current exceeds this speed, the polyps could bend backwards which reduces the feeding surface (e.g. gorgonians: Fabricus et al. 1995, tropical

scleractinians: Sebens and Johnson 1991). At higher current speeds, prey could also escape from the polyps as the higher flow velocities may give them sufficient momentum to break free (Purser et al. 2010). Optimal conditions for coral feeding, and therefore growth, can change constantly in a specific location within a reef as the local current speed and directions also change not only at large time scale but also on a daily basis. For instance, at the Mingulay Reef (Chapter 2), where *L. pertusa* is also the dominant reef-forming coral, current speed varies from ~2 to ~30 cm s^{-1} in a single day (Davies et al. 2009). In coral reefs dense coral thickets are also able to slow down the current speeds, due to friction with their framework (Roberts et al. 2009a). Therefore, in highly dynamic environments, like the Tisler Reef, the optimal conditions for coral feeding will change for different individual coral colonies at different times i.e. many corals will experience 'optimum' conditions over some point during a day. It is likely that depending on the current direction, the SE and NW side are exposed to different current speeds that could affect the CWCs ability to feed and grow. Unfortunately, our data could not be used to compare current speeds between the NW and SE side of the reef. Even though the location of the ADCP deployments are relatively close to each other, differences in the measured current speed were observed. The current speeds measured tend to be stronger for the sites further towards the NW (Figure 3.6). This is as, close to the seabed, flow over a sill will tend to decelerate upstream and accelerate downstream. However, since the direction of the current is more frequently to the SE, this side will experience higher current speeds when reaching deeper depths.

3.4.2 Lophelia pertusa morphology

Corals in a reef are frequently subjected to different flow directions and changes in environmental variables that affect their growth morphology (Wainwright and Dillon 1969, Mortensen and Buhl-Mortensen 2005, Todd et al. 2008, Chindapol et al. 2013). When corals occur in an area with strong uni-directional currents, colonies develop a more bush-like shape with their branches growing in the upstream direction (Chindapol et al. 2013). At the Tisler Reef, the water currents are forced through the sound between the Tisler and Hvaler Islands. As a consequence, the currents are relatively unidirectional resulting in the observed higher density of asymmetrical-shaped bush-like coral colonies. Cauliflower-shaped colonies were less abundant on the Tisler Reef. This symmetrical shape is more likely to develop under low current speeds (Chindapol et al. 2013). Areas, where this shape was observed, could therefore, indicate more sheltered conditions within the reef.

The proportion and abundance of very small colonies was significantly higher on the SE side of the Tisler Reef, which indicates recruitment. Firstly, this could be a consequence of the more optimal

feeding conditions due to more frequent periods of downwelling, allowing coral larvae to survive and grow. Secondly, a positive feedback from the higher percentage cover of live and dead coral structures on the settlement of larvae might be at play. The structure of the live and dead corals increases turbulence (Chamberlain and Grauss 1975, Hennige et al. 2016), which could allow *L. pertusa* larvae to enter the bottom boundary layer more easily towards rubble and other hard substrates for attachment. *Lophelia pertusa*'s planula larvae seems to prefer settling on protruding bodies, like for example in between coral rubble or even on oil rigs (Wilson 1979, Bell and Smith 1999, Gass and Roberts 2006). Live *L. pertusa* is not a suitable settling substrate as its permanent mucus layer (coenosarc) on their skeleton prevents attachment of sessile epibiotic species (Freiwald et al. 2002, Buhl-Mortensen et al. 2010). However diverse microhabitats are provided by dead coral skeletons which facilitate the high biodiversity associated with reef-forming cold-water corals (Mortensen and Fosså 2006, Buhl-Mortensen et al. 2010). The SE side of the reef has large areas of coral rubble, hard substrates and dead *L. pertusa* present which increase both turbulence and provide a great variety of microhabitats for the larvae to settle. The NW side of the reef has coral rubble present, but lacks large amounts of dead *L. pertusa* framework. Together with the higher percentage cover of soft substrates on the NW side, unsufficient settling substrates, turbulence and elevation out of the bottom boundary layer could explain why less small colonies were observed on the NW side of the Tisler Reef (Masson et al. 2003, Strömberg 2016) (Figure 3.2b). Thus, the presence of the structure formed by coral colonies can have a positive effect on the suitability of the area for the larvae.

3.4.3 Percentage cover of sponges

Overall *Geodia* sp. was present in lower percentages compared to *M. lingua*. The low presence of this sponge at the Tisler Reef could be a consequence of interspecific competition between *Geodia* sp. and *L. pertusa* for settling substrate and food. This is also indicated by the positive co-occurrence (r) between the presence of dead *L. pertusa* and the occurrence of *Geodia* sp. Purser et al. (2013) already discussed that competition for substrate can be one of the reasons for the low co-occurrence of *L. pertusa* and *Geodia baretti*. The low percentage cover of *Geodia sp.*, especially on the Tisler Reef, could also be caused by periods where the maximum temperature was 1.5 - 3 °C higher than the normal maxima (~9 °C). These high temperatures recorded at the shallow depths between 90 - 120 m have resulted in mass mortality events (HERMES 2008, Guihen et al. 2012). The depths at which the high temperatures were recorded fall within the depth range at which the transect on the NW side was collected. Interspecific competition, exposure to high temperatures, together with the slow growth rate of *Geodia* sp. could therefore also offer an explanation for the low presence of this sponge at the Tisler Reef.

A positive co-occurrence (r) between the presence of live and dead *L. pertusa* and the occurrence of *M. lingua* was found at the Tisler Reef. This relationship can vary at different reefs; a positive co-occurrence has been documented in the Røst Reef (Norway), whereas a negative co-occurrence was also identified in the investigated reefs by Purser et al. (2013) at the Sotbakken and Traena Reef. In contrast to *Geodia sp.*, *M. lingua* can use living *L. pertusa* itself as a substrate: they can grow within a colony (Lavaleye et al. 2009, Purser et al. 2013) and are therefore not in direct competition for hard substrate for settlement (see Figure 3.2c, 3.3a, 3.4b, 3.5c, d). This could explain why the percentage cover of *M. lingua* is much higher than that of *Geodia* sp. Interestingly, a higher percentage cover of *M. lingua* was found on the NW side of Tisler Reef. This finding seems surprising, as a higher percentage of *L. pertusa* was recorded on the SE side, which *M. lingua* can grow on (Figures 2c, 3a, 4b, 5c, 5d). It is possible that the corals occurring on the NW side were exposed to higher rates of stress, giving *M. lingua* a competitive advantage (Rützler and Muzik 1993). The Tisler Reef is a near-shore reef, and its shallow occurrence makes it more likely to be exposed more frequently to seasonal temperature fluctuations, terrestrial and human-induced influences and more eutrophic conditions caused by river outflow and agricultural activity (van Soest and De Voogd 2015). Studies on intraspecific interactions and environmental stressors could help to gain insight in what drives this difference.

This study highlights that differences in the spatial distribution of live versus dead coral framework and morphology exist within a reef and are mostly related to variations in the substrate and local hydrodynamics. Mortensen et al. (2010) and Wheeler et al. (2007) provided illustrations and acoustic data that gave an indication of the distribution and abundance of live versus dead *L. pertusa* in a CWC reef or on a CWC carbonate mound. De Clippele et al. (2016) showed the presence of live and dead coral framework on small reefs in Mingulay Reef 1 by using microbathymetry (35 x 35 cm cell size). These studies showed that live coral grow into the dominant current to optimize food capture. On Tisler Reef the dominant current direction reverses and therefore Wagner et al. (2010) observed live coral growth on both ends of the reef. Even though live coral was present at both ends, clear differences in the percentage cover of live and dead coral were observed in this study. Wheeler et al. (2007) highlight that environmental controls such as current dynamics, temperature, salinity, pH, food supply and sediment supply affect the growth, and thus the morphology of CWC carbonate mounds. Wheeler et al. (2007) indicated that the morphology of mounds can provide clues to the environment. The difference between CWC mounds and reefs is the shallow nature and relatively young age of reefs, which creates a more dynamic and unpredictable environment compared to CWC mounds. Our study indicates that the local hydrodynamics and food supply affect the reef's growth. Studies describing the morphology,

and fine-scale distribution of the different habitats provided by corals, help to understand how CWC reefs grow. Dead coral framework and coral rubble provide a large variety of microhabitats which can be used by for example crustaceans, crinoids, other corals, fish and microorganisms (Costello et al. 2005, Buhl-Mortensen et al. 2010, Henry and Roberts 2016). This study showed that understanding the variation in the amount of live versus dead coral framework is complex but likely related to differences in fine-scale hydrodynamical processes and food supply. Mapping differences in live versus dead coral framework and rubble can shed light on coral recruitment success within a reef and the distribution of associated organisms.

3.5 Conclusion

This study demonstrates how the percentage cover of *L. pertusa*, *Geodia* sp. and *M. lingua* as well as *L. pertusa*'s morphology is influenced by the local hydrodynamics, depth and the availability of settling substrate. More frequent downwelling on the SE side of the reef creates favourable growing conditions for both *L. pertusa* and the sponges. Differences in the availability of live and dead coral framework can affect the habitat available for organisms such as sponges but also for the corals themselves. Environmental stresses could also affect the presence and distribution of the corals and *M. lingua* which uses *L. pertusa* as a settling substrate. Our results could indicate a greater range of reef habitats on the SE side of the reef compared to the NW side, which could influence the presence of associated reef organisms. By combining existing knowledge of hydrodynamic processes and environmental stresses with observations on the morphology and the spatial extent of corals and sponges, fine-scale differences in their spatial distribution can be revealed and explained. This is key for monitoring purposes and for understanding the current and future development of the reef.

CHAPTER 4 -THE DIVERSITY AND ECOLOGICAL ROLE OF NON-SCLERACTINIAN CORALS ON THE LOGACHEV MOUNDS, ROCKALL BANK

4.1 Introduction

This chapter focuses on collecting information on the ecology, distribution, population structure and functional ecology of non-scleractinian deep-sea corals, as this remains scarce. In contrast, *Lophelia pertusa* and *Madrepora oculata* are the dominant reef-forming scleractinian corals in the deep sea and have been much more widely studied over the last 20 years. However, due to their numerous symbiotic associates, non-scleractinian corals should not be overlooked, as they too play a key role in the structure of cold-water coral reefs (e.g. Etnoyer and Morgan 2005, Tazioli et al. 2007, Wagner et al. 2012, Corbera Pascual 2015, De Clippele et al. 2015).

Collecting information on these non-scleractinian corals at deep depths is challenging and time-consuming (Henry and Roberts 2007, De Clippele et al. 2015). Therefore, to date, most information on deep-sea non-scleractinian corals has been collected through physical removal of specimens and subsequent laboratory analysis (e.g. Mortensen and Buhl-Mortensen 2004, Williams et al. 2006, Wagner et al. 2012). This results in a limited number of samples and makes it especially challenging to study the corals in situ and to understand their associated mobile fauna. However, the recent development and use of remotely operated vehicles (ROVs) with underwater video equipment has allowed us to gain access to greater depths and study scleractinian and non-scleractinian coral communities and their associated fauna in situ (e.g. De Mol et al. 2012b, Guinan et al. 2012). To increase knowledge of non-scleractinian cold-water corals, the genera belonging to the Order Antipatharia (Milne-Edwards and Haime 1857), also known as black corals, as well as the Order Alcyonacea (Lamouroux 1816) which include the bamboo corals and gorgonians, are studied here using high definition video recordings from ROVs.

Black corals (Cnidaria: Anthozoa: Hexacorallia) encompass seven families (Opresko 2001, 2002, 2003, 2004, 2005a, 2005b, 2006, Mcfadden and Collins 2007, Opresko and de Laila Loiola 2008) with 75% (c. 180 species) found below 50 m depth (Cairns 2007). The majority of black corals are azooxanthellate, but microalgal symbionts (*Symbiodinium*) have been discovered in low densities in the gastrodermal tissue of ten species (eight genera and four families) living at depths between 11-396 m (Wagner et al. 2011). The black coral's lifespan is greater than most other deep-sea coral species (Andrews et al. 2001, Andrews et al. 2009, Roark et al. 2009). A *Leiopathes* colony in

Hawaii (USA) was estimated to be 4,265 years old with radial growth rates between 0.005-0.022 mm yr^{-1} (Sherwood et al. 2009, Roark et al. 2009).

Soft corals, bamboo corals and gorgonians (Cnidaria: Anthozoa: Octocorallia) belong to the Order Alcyonacea, which includes 30 families (Mcfadden and Collins 2007, Bayer 1981). Bamboo corals can be found at intermediate to deep water depths of 400 to 3000 m in most ocean basins and can live over a hundred years (Hill et al. 2011, Watling et al. 2011). Octocorals grow faster and have lower lifespans than black coral species, with radial growth rates between 0.05 and 0.44 mm yr^{-1} (Andrews et al. 2001, Watling et al. 2011).

This study focussed on the non-scleractinian corals that grow on cold-water coral carbonate mounds in the Logachev area. The Logachev mounds are located on the south-east slope of the Rockall Bank in the northeast Atlantic (Kenyon et al. 2003) (Figure 4.1). Within Rockall Trough there is a mixture of North Atlantic Current Water and Eastern North Atlantic Water (ENAW) occupying the upper layers down to 1,200-1,500 m (Inall et al. 2009). The latter contains influences of the Mediterranean Water and also Sub-Arctic Intermediate Water (Ellet et al. 1986, Holliday 2003). It is variation in the location of the subpolar front (east-west) which causes changes in the inflowing water masses (Holliday 2003, Chapter 5). The deepest water originates from the Labrador Sea (Inall et al. 2009). The prevailing current direction in Rockall trough is northward, while off the mound the currents flow towards the north-west (Hutnance 1989, Mienis et al. 2007, White et al. 2007).

The Logachev mounds consist of a cluster of mounds that are built up from accumulated fine sediments baffled by coral reef framework, dead coral fragments and live coral on the summit. The base of the mounds is covered by bio-and siliciclastic sands with various amounts of pebbles, cobbles and boulders (de Haas et al. 2009). The flanks of the mounds are covered with patches of coral rubble, dead coral branches and living corals, while the summits of the mounds are characterised by a dense cold-water coral cover (Kenyon et al. 2003, Van Weering et al. 2003, de Haas et al. 2009). They are between 5 and 360 m high, up to a few kilometres long and located between 600-1000 m depth which is within the boundaries of the (ENAW) (Kenyon et al. 2003, Mienis et al. 2007, 2009, de Haas et al. 2009). The Logachev carbonate mounds are predominantly built up by the scleractinian cold-water coral *L. pertusa* (Kenyon et al. 2003). Cold-water coral mounds engineer the availability of resources directly or indirectly for the corals themselves and other species. They do this by causing changes in the physical state and biological environment and

by creating important habitats for invertebrates and fish (Jones et al. 1997, Roberts et al. 2009a, van Oevelen et al. 2009, Buhl-Mortensen et al. 2010, Soetaert et al. 2016, Chapter 1).

The formation of mounds is controlled by temperature, current strength, the presence of hard substratum for initial settlement and food availability (Frederiksen et al. 1992, Freiwald et al. 2002, Kenyon et al. 2003, White et al. 2005). The presence of the coral framework will slow down the currents, baffle sediments, which then can accumulate between the coral branches ensuring further growth of the mounds (Dorschel et al. 2007, de Haas et al. 2009, Mienis et al. 2009, Roberts et al. 2009a). The interaction of tidal currents with the prominent topographies of the cold-water coral mounds on the seafloor induces downwelling of surface water due to the formation of internal waves or hydraulic jumps (Davies et al. 2009, Kenyon et al. 2003, Wagner et al. 2011, Findlay et al. 2013, Cyr et al. 2016). The interaction of internal waves and tidal currents with seabed sediments also causes nepheloid layers which contain increased amounts of suspended seabed sediment that can supply the corals with food at deeper depths (Kenyon et al. 2003, Mienis et al. 2007). They occur in areas on the slope of the mound where the angle is critical to the resonance of internal waves (White et al. 2003). Intermediate Nepheloid Layers (INL) have been identified as turbidity clouds between 450 and 900 m depth and varied in depth and shape coinciding with the diurnal cycle. The largest turbidity cloud can be found between 200-500 m depth, just above the carbonate mounds. A second smaller turbidity cloud can be found 25 km from Rockall Bank between 500-700 m depth (White et al. 2003, Mienis et al. 2006, 2007). The near-bed currents (800 m depth) between the carbonate mounds are shaped and directed by the morphology of the mounds but are in general flowing to the south-west (Kenyon et al. 2003, Mienis et al. 2007, White et al. 2007).

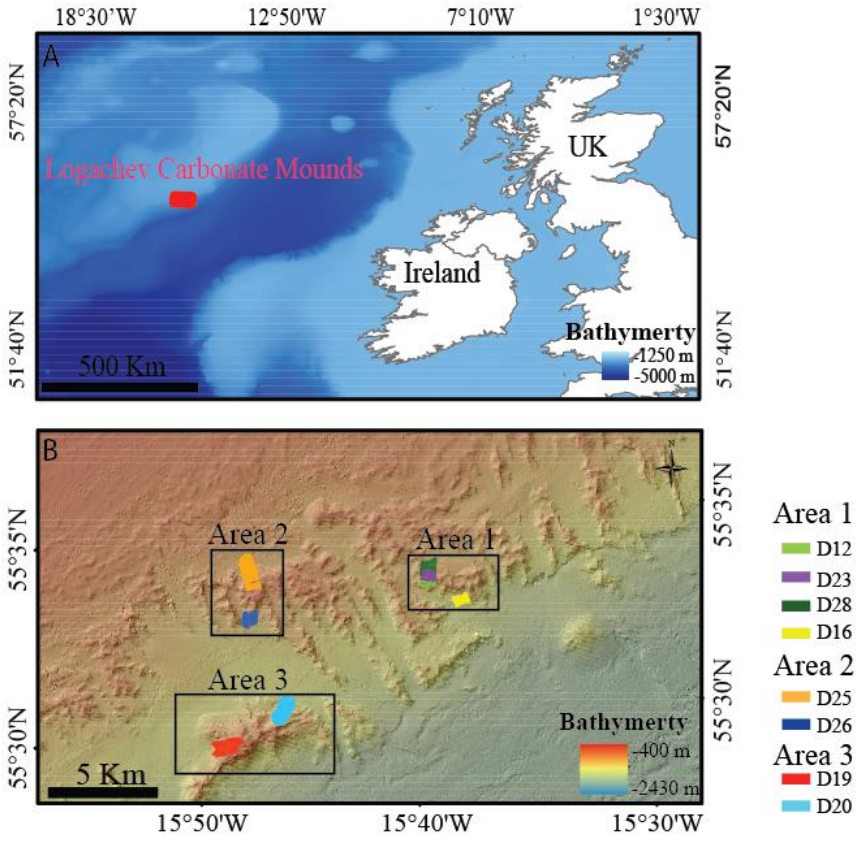

Figure 4.1 (a) Location of the Logachev Mounds **(b)** Location of the three study areas and dives in the Logachev Mounds area on the south-east side of Rockall Bank.

Disturbance and removal trough bottom fishing (Althaus et al. 2009) and exploitation for commercial therapeutic and art use (Grigg 2001) are current threats to these long-lived deep-sea corals. Therefore, deep-water black corals and octocorals are covered under the term 'Vulnerable Marine Ecosystem' (VME) (Fuller et al. 2008). The United Nations General Assembly Resolutions 61/105 and 64/72 ensured that nations must develop plans to safeguard these VMEs when fishing on the high seas (Rogers and Gianni 2010).

In the Rockall area the presence of black corals, gorgonians and bamboo corals have been mentioned in previous studies (Duineveld et al. 2007, Roberts et al. 2008, Henry et al. 2014) but their community, ecology and role have not been studied. Therefore, we (1) documented the diversity of these non-scleractinian corals in the Logachev area, (2) determined what drives differences in their abundance and diversity and (3) studied their role acting as hosts for other species. The goal of this study is to provide more information on these non-scleractinian corals to ensure that management can be better informed to protect these long-lived organisms.

4.2 Methodology

4.2.1 High-definition videos

High-definition (HD) video data were collected in the Logachev Mound area in 2012 (RRS *James Cook* Cruise 073, 18 May-15 June 2012) using the remotely operated vehicle (ROV) *Holland-1*. The data were recorded with a combination of cameras mounted on the ROV: an HD Insite mini-Zeus video camera with a direct HDSDI fibre output, a Kongsberg 14-208 digital still camera, a Kongsberg 14-366 pan and tilt camera and an Insite Pegasus-plus fixed zoom camera. Four lights were used: two 400-W deep-sea power and light SeaArc2 HMI lights and two 25,000 lumen Cathx ocean APHOS LED lights. Two deep-sea power lasers spaced 10 cm were also mounted on the HD camera. The position and depth of the ROV were determined by USBL (Sonardyne) underwater positioning system and recorded using the OFOP (Ocean Floor Observation Protocol) software.

In total eight video transects with a total length of ~3.4 km were analysed in three different areas within the Logachev Mound area. These three different areas contained clustered cold-water coral carbonate mounds (Figure 4.1). These mounds have an elongated shape, perpendicular to the regional depth contours (Kenyon et al. 2003, Van Weering et al. 2003, Mienis et al. 2006). These clustered mounds which will be referred to as area 1, 2 and 3 are located at different distances from the shallowest point of Rockall Bank and occur at different depth ranges. Area 1 (560-700 m depth) is located ~ 23 km from the bank, area 2 (530-700 m depth) ~19 km and area 3 (530 -850 m depth) ~25 km. The video transects in each area were collected from alternate sides on the mounds (Figure 4.1, Table 4.1). Each dive transect was divided into 40 m long sub-transects for statistical analyses, as this length gave the best representation of the substrate and species variability.

Table 4.1 High definition dive information. Lat and Lon stand for respectively latitude and longitude. Average aspect represents the side of the area/ clustered mound at which the video transects were collected (North (N), East (E), South (S), West (W)).

Dive (area)	*Start Lon*	*Start Lat*	*End Lon*	*End Lat*	*Aspect*	*Depth*	*Length (m)*
12 (1)	-15.65523	55.55799	-15.65557	55.55567	NE	[640;722]	200
16 (1)	-15.63350	55.55119	-15.63142	55.547439	S	[758;872]	240
23 (1)	-15.65630	55.55847	-15.65571	55.55965	NE	[563;584]	40
28 (1)	-15.65585	55.56014	-15.65389	55.56674	S	[575;701]	240
25 (2)	-15.78718	55.57206	-15.78421	55.56013	NW	[547;705]	1040
26 (2)	-15.78795	55.55020	-15.78918	55.54672	SW	[702;768]	360
19 (3)	-15.82089	55.49419	-15.80442	55.49478	NE	[559;801]	880
20 (3)	-15.76447	55.51220	-15.77232	55.50529	NW	[610;873]	360

4.2.2 Substrate Classification

First the substrate types were identified from the high definition videos, which included; *L. pertusa* thicket, dead exposed coral framework with scarce live *L. pertusa* colonies, coral rubble, lithified hardground, fine sediment with pebbles, cobbles and boulders (<100 cm diameter), mixed sediment with large boulders (>100 cm) and fine sediment (Figure 4.2). The dominant substrate type for each navigation point was recorded from the high definition videos and noted in Excel. Then for each 40 m sample, the percentage contribution of the seven different substrate types was calculated. The total contribution for each 40 m sample sums up to 100%.

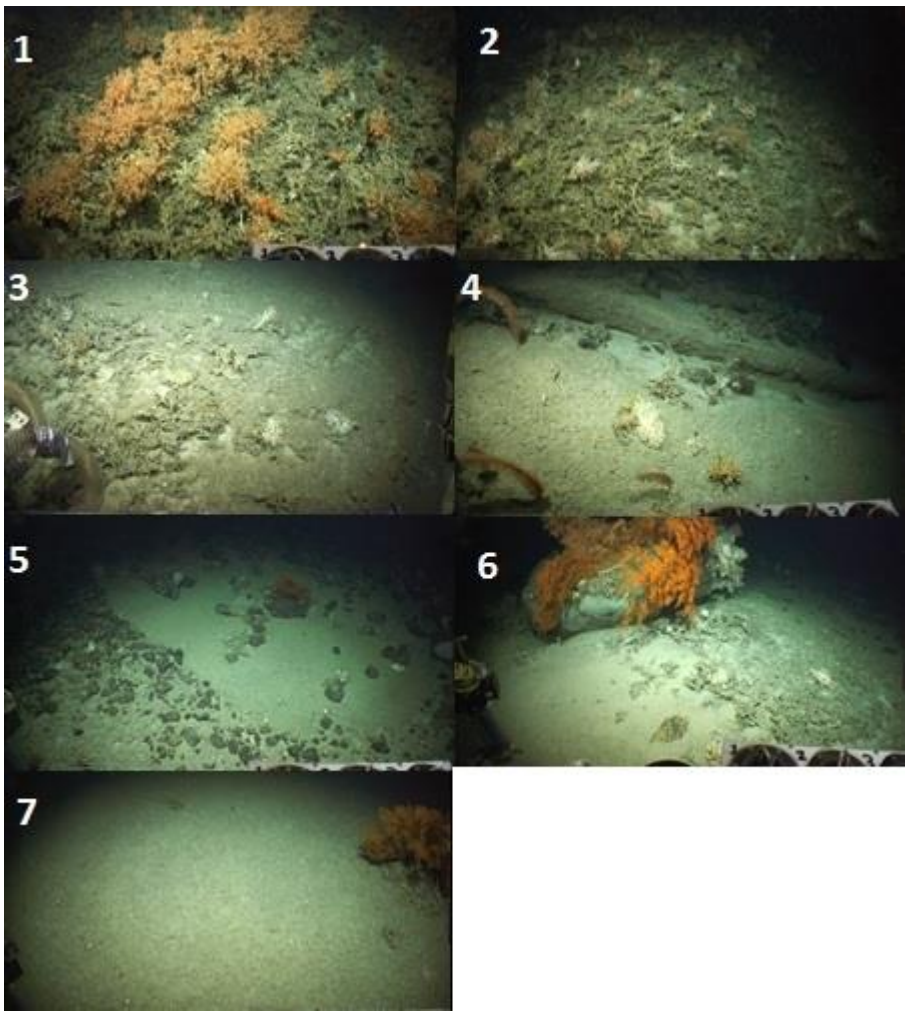

Figure 4.2 Substrates identified in the Logachev Mound area: **1.** *Lophelia pertusa* thicket (LpT), **2.** Dead exposed coral framework with scares live *L. pertusa* colonies (DEC), **3.** Coral rubble (CR), **4.** lithified substrate (LiH), **5.** Fine sediment with pebbles, cobbles and boulders (FS/P/C/B), **6.** Mixed substrate with large boulders (MS/LB), **7.** Fine sediment (FS)

4.2.3 Coral identification and associated fauna

The non-scleractinian coral species were identified with the help of the expert Dr Tina Molodtsova, and counted from the high definition videos. The recorded presences were noted in an Excel spreadsheet. Preliminary evaluation of the high definition videos indicated a large number of occurrences of different size classes of the black coral species *Leiopathes* sp. which was therefore classified as small (< 30 cm), medium (30-100 cm) and large (>100 cm).

The associated mobile megafauna was identified, and their location on the coral colony specified as central branch versus outer branch and on the base, middle or top part of the colony.

4.2.4 Bathymetry

The bathymetry dataset were provided by the Irish National Seabed Survey programme (INSS) and has a 20 x 20 m resolution (www.gsiseabed.ie). Several topographic variables were derived from the bathymetric grid using the ArcGIS 10.1, ESRI Software and the Benthic Terrain Modeler (Wright et al. 2012): slope, aspect (eastness and northness), rugosity (rectangle, height and width of resp. 3x3 and 9x9) and bathymetric positioning index (BPI) (inner and outer radius of 3x6 and 6x9 cells). More information on these variables can be found in Chapter 2 and in for example Wilson et al. (2007), Guinan et al. (2009) and Henry et al. (2010).

4.2.5 BGS Seabed Mapping Toolbox

After the BGS Seabed Mapping Toolbox semi-automated mapping approach was applied to the Mingulay Reef Area (Chapter 2) and the Tisler Reef (Chapter 3), it is here applied to the Logachev Mound area. The results were used for descriptive purposes only and further applications are discussed in Chapter 5. Information regarding the BPI feature delineation and description tool and the results of the sensitivity to the BPI input and threshold values can be found in Chapter 2 and Gafeira et al. (2015) (Appendix).

The BPI was calculated within ArcGIS with the land facet corridor tool (Jenness et al. 2013). Here, the used neighbourhood's shape (annulus) and an inner and outer radius of 6 and 9 cells respectively were chosen. A cut-line BPI value of 2, minimum BPI value of 6, minimum area of 80 m^2 and a minimum width/length ratio of 0.1 were used as the thresholds. A buffer distance of 40 m was chosen based on the morphological characteristics of the mounds.

A list of the variables extracted by the tool are given in Table 2.1. As in chapter 2, the area ratio was calculated separately, by dividing the area of the polygon with the area of the MBG box to indicate the shape of the mound. To examine the difference in the height of the mounds, the maximum water depth was retracted from the minimum water depth. Scatterplots are created in the software package R 3.2.2 (R Development Core Team 2013) to examine the relation between the Area Ratio, the size and the height of the mounds. Some degree of manual editing was required when artefacts were delineated or when adjacent mini-mounds were inaccurately delineated as a single feature (Chapter 2).

4.2.6 Statistical analyses

Since here no categorical variable were used, such as in chapter 2, Generalized Linear Regression Modelling was used instead of a Regression Tree Model (e.g. Random Forest). Linear regression describes how a continuous response variable changes in relation to one or more predictor variables (McCullagh and Nelder 1989). Here, the change in the abundance of certain species (continuous response variable) was studied in relation to the variables which were extracted from the bathymetry (section 4.3.4). Because our response variables didn't follow a normal Gaussian distribution, the more flexible generalized linear model (GLM) was used. For GLMs the probability distributions all belong to the exponential family. Here our data belongs to the quasi-poisson family (McCullagh and Nedler 1989, Dobson and Barnett 2008). The statistical software package R was used to perform generalised linear modelling (GLM) (R Development Core team 2010). Linear regression cannot include missing values, and since here changes in the abundance of a certain species was studied, samples that had no abundances of the analysed species present were excluded (McCullagh and Nedler 1989, Dobson and Barnett, 2008). Backwards stepwise regression decided which environmental variables (% occurrence of the seven substrate types and the variables derived from the bathymetry) contributed the most to the performance of the model. The best model was chosen based on the Akaike Information Criterium (AIC) which is a function of the log-likelihood function adjusted for the number of covariance parameters (Cnaan et al. 1997). Once the variables were selected, a GLM was performed. By taking the exponent of the coefficient values, the percentage change in the abundance of the coral per change in one unit of each variable was calculated. Species that had less than 50 individuals present were excluded from the statistical analyses due to the effect on the reliability of the calculated result of the small number of 40 m samples (section 4.2.1) with these particular species present.

4.2.7 Diversity, evenness and density

The species diversity, density and evenness of all non-scleractinian corals were calculated in the PRIMER software (Clarke and Warwick 2001) for each 40 m transect, for each alternate side of the areas and for the whole area. The Shannon diversity index (H') method was used to calculate the diversity of the non-scleractinian corals in the study area per sample. The Pielou's evenness value can range from 0 to 1, and gives an indication of dominant species being present in a sample (~0) or if there is an equal abundance of all species (~1). Density was calculated by dividing the total number of individuals per linear meter of transect.

4.3 Results

4.3.1 Mound delineation and morphometric characteristics

A total of 123 mounds were delineated by the BGS Seabed Mapping Toolbox from the 19.30 x 19.30 m bathymetry in the Logachev area (Figure 4.3). The morphometric characteristics of the mounds are given in table 4.2.

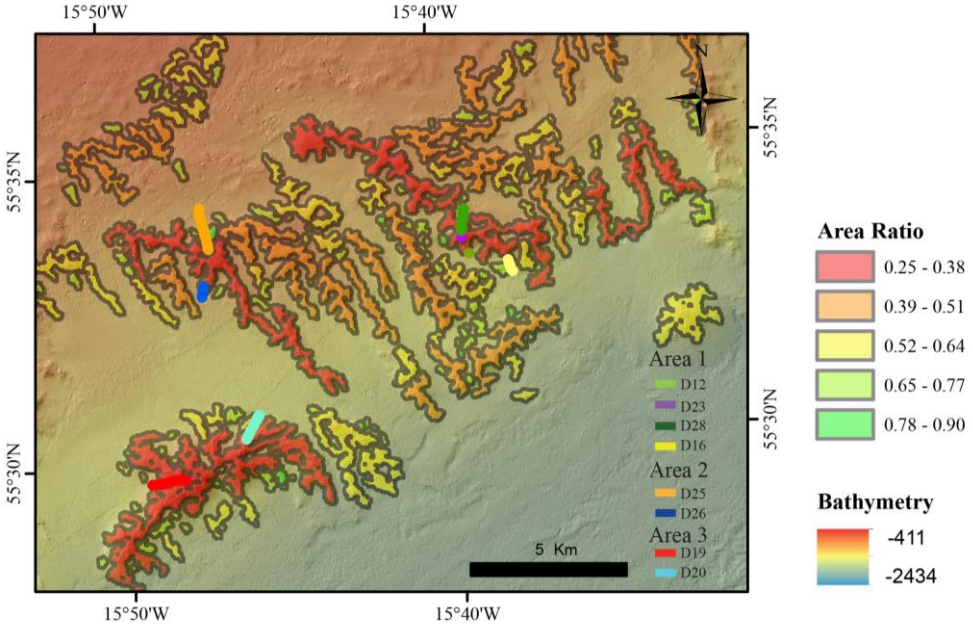

Figure 4.3 Logachev Area with delineated mounds delineated. The colours within the mounds reflect the Area Ratio, showing the diversity in shapes across the area. delineation tool.

Table 4.2 Table listing the morphometric characteristics of the mounds

	Range	Average	Standard deviation
Width (MBG box)	160 – 4902 m	553 m	558 m
Length (MBG box)	203 – 1209 m	1018 m	1209 m
Polygon area	0.02 – 11 km2	0.5 km2	1 km2
Area Ratio	0.25 – 0.89	0.65	0.13
Perimeter	578 – 77947 m	4245	7899
Maximum BPI	6-67	23	15
Orientation	0-179	107	55
Height	8- 502 m	96 m	78 m

Two scatterplots are given below. Figure 4.4A shows the relation between the Area Ratio of the mound (shape) and their size (Area). This figure indicates a clear relationship with the size of the mounds and the Area ratio. Larger mounds have a lower Area Ratio and are therefore more dendriform-shaped. The second scatterplot examines the relationships between the height of the mounds (minimum versus maximum water depth) and their depth (Figure 4.4B). Mounds which are heigher in size have their maximum water depth at greater depths.

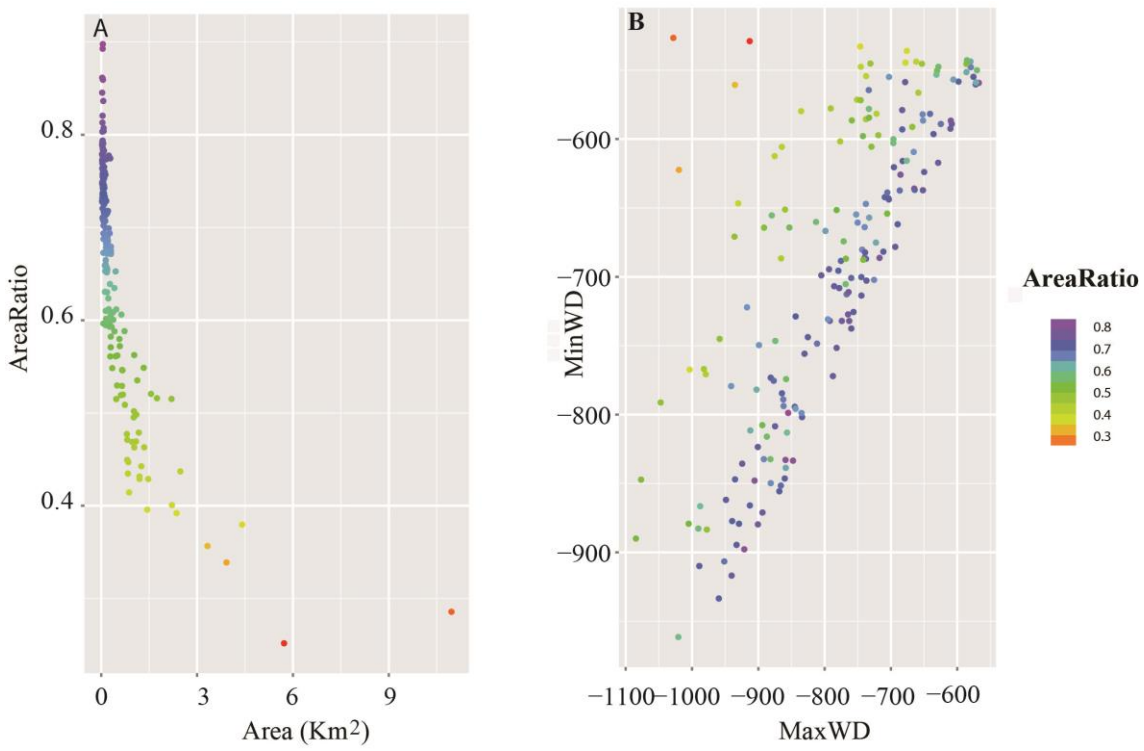

Figure 4.4 Scatter plots showing the relation between the difference in height of the mound (MaxWD versus MinWD) and the area versus the Area Ratio. The colours of the dots in both plots represent the value of the Ratio Area

4.3.2 Substrate types

Coral rubble (33.4%), dead exposed coral framework (25.7%) and fine sediment with pebbles, cobbles and boulders (23.2%), were the most abundant substrate types recorded in the entire studied area. *Lophelia pertusa* thickets covered 10.8 %, Lithified hardground covered 4.2%, fine sediment covered 2.3% and mixed substrate with large boulders cover 0.4%. Dead exposed coral framework and coral rubble were present in high percentages in all the areas (Table 4.2). *Lophelia pertusa* thickets were found predominantly in area 1 on the NE flank of the mound. A total of ~39% in area 2 and 3 were covered with the hard substrates; pebbles, cobbles, boulders, large boulders and lithified hardgrounds, all on the NW flank of their mounds. Area 1 had only 4% of these hard substrates present.

Lophelia pertusa thickets were found at shallower survey depths between 560 and 610 m. Dead exposed coral framework was found from 560 to 800 m depth, coral rubble between 560 and 840 m depth and fine sediments were found between 570 and 700 m depth. Fine sediment with pebbles, cobbles and boulders was found between 690 and 870 m depth. Mixed sediments with large

boulders were observed between 680 and 870 m depth and lithified sediment between 580 and 860 m depth.

Table 4.3 Percentage contribution of the different substrates per mound: *Lophelia pertusa* thicket (LpT), Dead exposed coral framework with scarce live *L. pertusa* colonies (DEC) Coral rubble (CR), lithified hardground (LiH), Fine sediment with pebbles, cobbles and boulders (FS/P/C/B), Mixed substrate with large boulders (MX/LB), Fine sediment (FS)

Area	LpT	DEC	CR	LiH	FS/B/P/C	MX/LB	FS
1	**31.92**	**38.72**	**20.16**	**1.59**	**1.66**	**0.24**	**5.71**
1 NE	24.93	19.84	1.40	0	0	0	0
1 S	6.99	18.88	18.76	1.59	1.66	0.24	5.71
2 (total)	**0.16**	**13.49**	**41.79**	**7.64**	**27.91**	**3.14**	**5.88**
2 NW	0.16	7.58	11.41	4.15	20.52	2.43	1.31
2 SW	0	5.92	30.37	3.49	7.39	0.71	4.56
3 (total)	**1.72**	**20.84**	**38.82**	**5.11**	**33.22**	**0.12**	**0.17**
3 NE	0.01	3.13	3.30	0	0	0.01	0.06
3 NW	1.71	17.70	35.52	5.11	33.22	0.11	0.12

4.3.3 Non-scleractinian species

A total of 1,707 non-scleractinian coral specimens were counted across the three mound areas. Black corals were the most abundant non-scleractinian corals overall, with 1,695 individual black corals recorded. In total eight different black coral species were identified: three species belonging to the family Schizopathidae (*Bathypathes* sp., *Parantipathes* sp. 1, *Parantipathes* sp. 2), one species belonging to the families Leiopathidae (*Leiopathes* sp.), Cladopathidae (*Trissopathes* sp.) and Antipathidae (*Stichopathes cf. gravieri*) and two unidentified species which we refer to as *Antipatharia* sp. 1, *Antipatharia* sp. 2. Only two species belonging to the Order Alcyonacea were identified: one bamboo coral belonging to the Isididae family (*Acanella* sp.) and one gorgonian belonging to the Plexauridae family (*Paramuricea* sp.). The different species are shown in Figure 4.5.

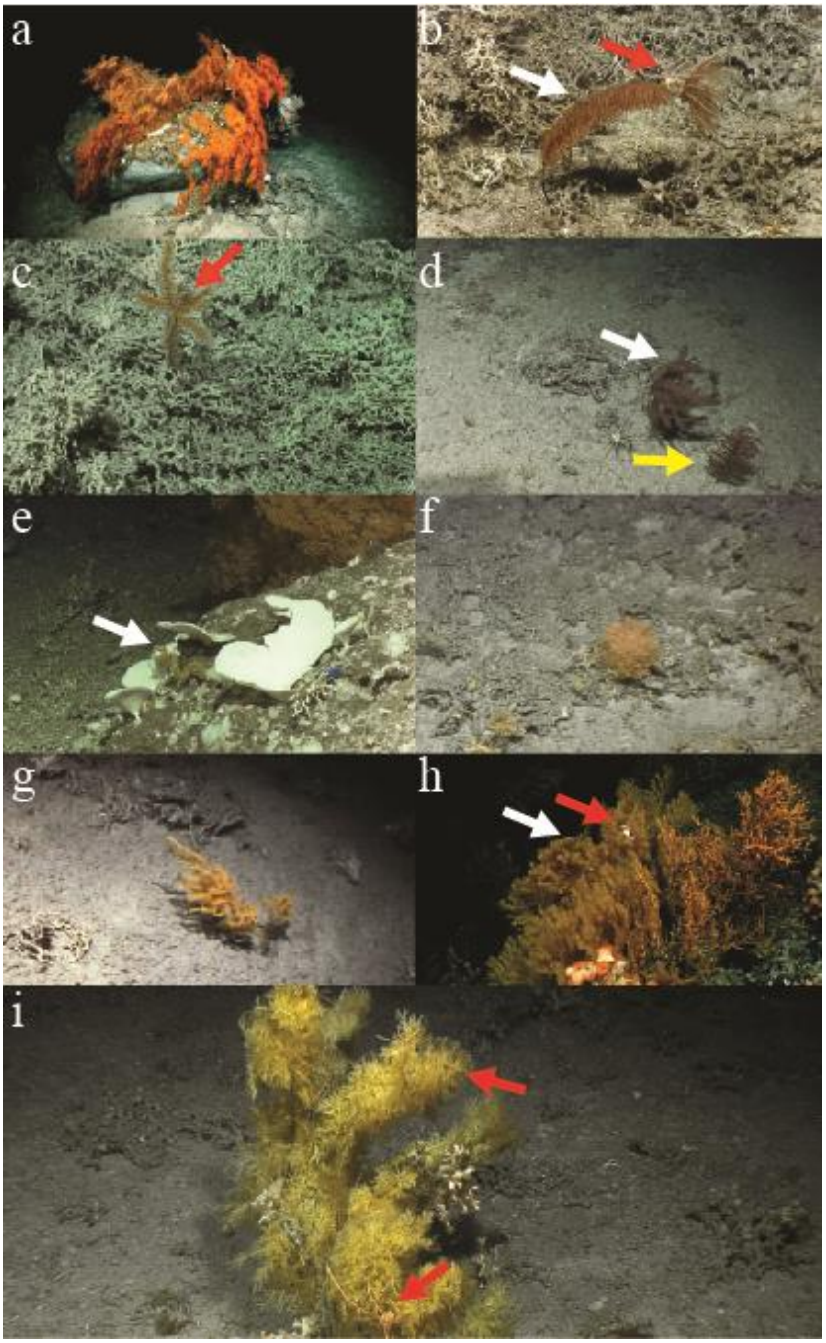

Figure 4.5 (a) *Leiopathes* sp. **(b)** *Parantipathes* sp. 1 (white arrow) with two crinoids sp attached to the top (red arrow) **(c)** *Parantipathes* sp. 2 **(d)** *Trissopathes* sp. 1 (white arrow) *Bathypathes* sp. (yellow arrow) **(e)** *Stichopathes cf. gravieri* **(f)** *Acanella* sp. **(g)** *Antipathes* sp.2 **(h)** *Paramuricea* sp. (white arrow) with *Gorgonocephalus* sp. (red arrow) **(i)** *Parantipathes* sp. 1 with Crinoids (top red arrow) and *Gastropyctus* sp. (bottom red arrow)

The black coral *Leiopathes* sp. was the most abundant black coral present with a total of 1,583 individuals. The second most abundant coral was also a black coral species, *Parantipathes* sp. 1, with a total of 60 individuals. The other non-scleractinian species were rarer ranging between 1-11 counts (Table 4.4) and their abundance varied with depth (Table 4.4 and Figure 4.6)

Table 4.4 Observed number of individuals and their recorded depth range.

Species	***Min depth (m)***	***Max depth (m)***	***Depth range (m)***	***No. ind.***
***Acanella* sp.**	772	860	88	2
***Antipathes* sp. 1**	*860*	860	0	4
***Antipathes* sp. 2**	628	628	0	1
***Bathypathes* sp.**	678	859	181	13
***Leiopathes* sp. (all)**	547	874	327	1,583
***Leiopathes* sp. (large)**	571	780	209	58
***Leiopathes* sp. (medium)**	571	780	209	20
***Leiopathes* sp. (small)**	547	874	327	1,505
***Paramuricea* sp.**	546	796	250	10
***Parantipathes* sp. 1**	565	691	126	60
***Parantipathes* sp. 2**	565	699	134	11
Stichopathes cf. gravieri	663	696	33	20
***Trissopathes* sp.**	629	860	231	3

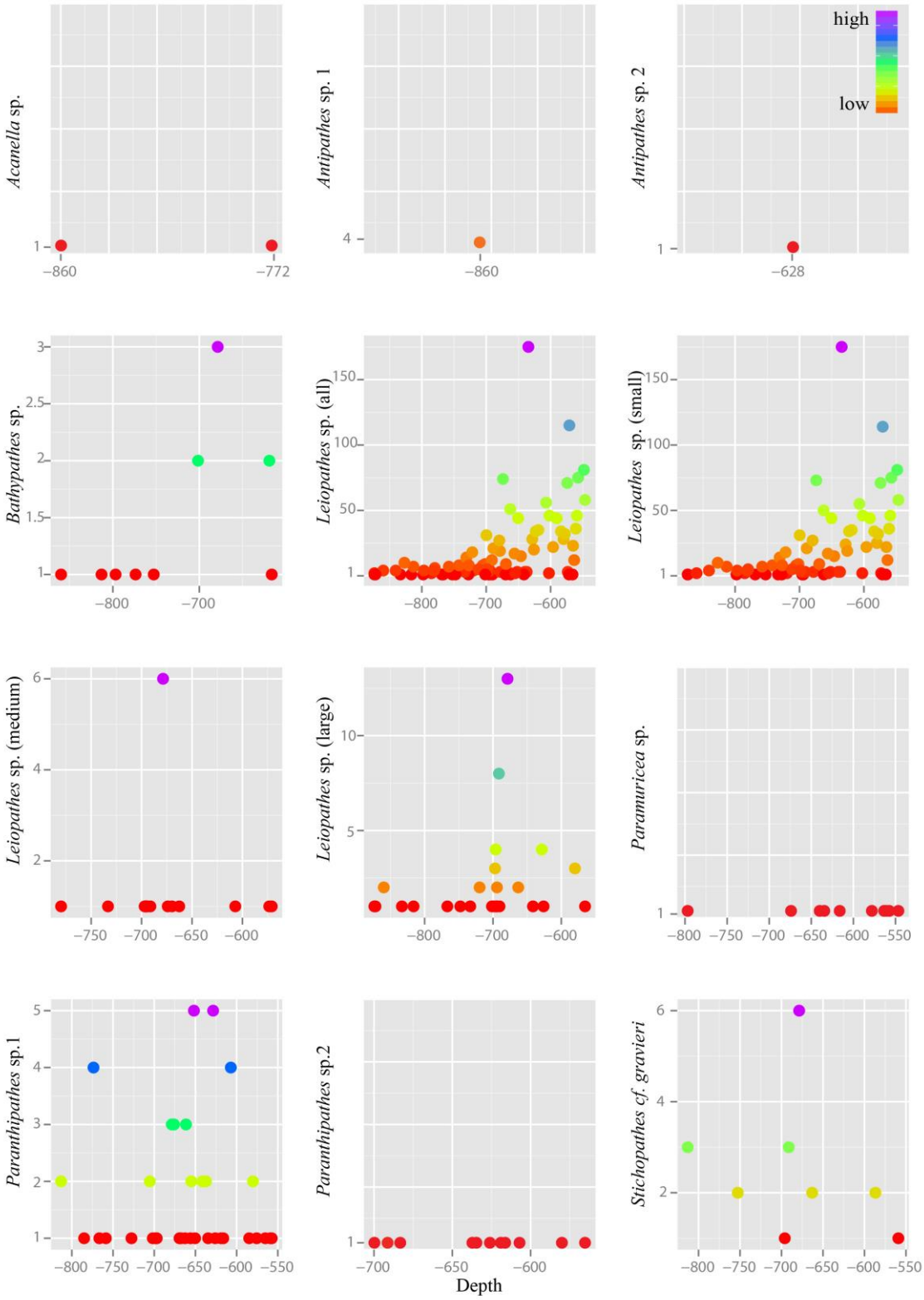

Figure 4.6 These figures provides a visual overview of which species were more abundant compared to others and how their abundance varies with depth.

A total of 45% of the 40 m transects which had dead exposed coral framework and coral rubble present were occupied with non-scleractinian corals. A slightly lower percentage of the 40 m transects which contained large boulders (39%), fine sediment (37%), *L. pertusa* thickets (37%) and pebbles, cobbles, boulders (35%) had non-scleractinian corals present. Only 22% of the transects that had lithified hardgrounds had corals present.

An overview of the percentage substrates occupied by each species is listed in Table 4.5 and described here:

Leiopathes sp. occurred in all three study areas and on all substrates except *L. pertusa* thicket. The larger sized *Leiopathes* sp. colonies occurred mostly in areas with large boulders (78%) while, the smaller sized colonies preferred dead exposed coral framework (96%). Medium sized colonies occurred both ~50% on dead exposed coral framework and big boulders. This species has the largest depth range in the Logachev area, it was the shallowest (547 m), and deepest (847 m) recorded species.

Like *Leiopathes* sp., *Parantipathes* sp. 1 was found in all three study areas, on all substrates, except from one, fine sediment. This species occurred 78% on dead exposed coral framework. 6% and 8% respectively were found on large boulders and fine sediment with pebbles, cobbles, boulders. This species had a much narrower depth range of 565 m to 691 m depth.

Parantipathes sp 2 had a similar depth range and substrate preference to *Parantipathes* sp. 1 and also occurred in all the study areas. The only difference was that this species was also found in fine sediments.

Stichopathes cf. gravieri was found in all the studied areas, on three substrates; large boulders (52%), dead exposed coral framework (39%) and *L. pertusa* thicket (9%). This species had the narrowest depth range and was only found between 663 m and 696 m.

Bathypathes sp. occurred mostly in areas with dead exposed coral framework (61%), large boulders (17%) and fine sediment with pebbles, cobbles and boulders (11%). This species occurs at deeper depths between 678 m and 859 m. This species was only found in area 1 and 2.

All four individuals of *Antipathes* sp 1 together with one *Antipathes* sp 2 individual were found in one particular location in area 1 with coral rubble as a substrate at 860 m depth.

All three *Trissopathes* sp. individuals were found in areas with dead exposed coral framework, at a wide depth range of 860 m to 629 m, in area 1 and 2.

Only two recordings of *Acanella* sp. were made, one was located in an area with dead exposed coral framework, the other in coral rubble. This species was only found at deeper depths of 772 m (area 2) and 860 m (area 1).

Seven of the *Paramuricea* sp. colonies were observed in dead exposed coral framework, while three were observed in *L. pertusa* thickets and one in coral rubble. This species was found at depths of 546 m to 797 m. This species was recorded in all the study areas.

Table 4.5 Overview of the percentage substrate occupied per species. *Lophelia pertusa* thicket (LpT), Dead exposed coral framework with scarce live *L. pertusa* colonies (DEC) Coral rubble (CR), lithified hardground (LiH), Fine sediment with pebbles, cobbles and boulders (FS/P/C/B), Mixed substrate with large boulders (MX/LB), Fine sediment (FS)

Species	**LpT**	**DEC**	**CR**	**LiH**	**FS/B/P/C**	**MX/LB**	**FS**
***Acanella* sp. (2 ind.)**	0	50	50	0	0	0	0
***Antipathes* sp. 1 (4 ind.)**	0	0	100	0	0	0	0
***Antipathes* sp. 2 (1 ind.)**	0	0	100	0	0	0	0
***Bathypathes* sp. (13 ind.)**	0	61	6	0	11	17	6
***Leiopathes* sp. (all) (1583 ind.)**	0	93	2	0	1	3	1
***Leiopathes* sp. (large) (58 ind.)**	0	13	3	0	2	78	5
***Leiopathes* sp. (medium) (20 ind.)**	0	48	0	4	4	44	0
***Leiopathes* sp. (small) (1505 ind.)**	0	96	2	0	1	0	0
***Paramuricea* sp. (10 ind.)**	20	70	10	0	0	0	0
***Parantipathes* sp. 1 (60 ind.)**	5	77	3	2	8	6	0
***Parantipathes* sp. 2 (11 ind.)**	0	76	0	0	6	6	12
***Stichopathes cf. gravieri* (20 ind.)**	9	39	0	0	0	52	0
***Trissopathes* sp. (3 ind.)**	0	100	0	0	0	0	0

4.3.4 Non-scleractinian species: diversity, evenness and density

The highest diversity was recorded in area 2, with an H' of 0.40 and a total of eight different species recorded. The SE flank had a higher diversity of species compared to the transects on the NW flank. In area 1, a total of nine species were recorded, but the overall H' was slightly lower 0.33, with the S side of this area being higher in diversity. The lowest number of species and diversity was found in area 3, with respectively six species and an H' of 0.11. Here, the highest diversity was found on the NW flank. An H' of 1.389 and 1.386 were recorded in area 1 at respectively 616 and 860 m depth. In area 2, the highest H' of 1.175 and 1.039 were found at respectively 679 and 753 m depth.

The distribution of the most abundant and therefore dominant species, *Leiopathes* sp., also differed and affected the evenness on the different mounds. Area 3 had the lowest evenness with a value of 0.06, followed by area 1 with 0.15 and area 2 with 0.19. In area 1 an evenness of 1 was found at

616 and 655 m depth. Area 2 had an evenness of 1 at 663 and 728 m depth. The evenness in the different areas was always greater on the flanks which also had the greatest diversity of species.

Area 2 had the highest average density of 0.518 ind. m^{-1}. Even though the diversity is low in area 3, it had the highest average densities of non-scleractinian corals (0.669 ind. m^{-1}) present, which was predominantly caused by the presence of high abundances of *Leiopathes* sp. Area 1 had the lowest average density of corals present of only 0.208 ind. m^{-1} (Table 4.6). The density of non-scleractinian corals was highest on the flank of the areas which had a lower diversity and evenness.

As mentioned earlier, the black coral *Leiopathes* sp. is the most abundant non-scleractinian coral found in the Logachev area (Table 4.7). Small sized colonies were the most abundant size class, which occur at a wide depth range between 874 m and 547 m but with the highest densities of 1.78 - 4.50 ind. m^{-1} found at shallower depths between 548 and 674 m. Medium sized colonies were the least represented and had a density of 0.025 ind. m^{-1} and are observed between 571 and 780 m depth. One peak in their density was observed in area 2 at 678 m depth of 0.15 ind. m^{-1}. Large sized colonies were recorded at depths between 874 and 565 m. The large colonies had its highest densities of 0.20 and 0.33 ind. m^{-1} in area 2 at 679 and 691 m depth.

Table 4.6 The diversity, number of species, evenness and average density per area

Area	*Diversity (H')*	*Nr. species*	*Evenness*	*Density (ind. m^{-1})*
1	**0.33**	**9**	**0.15**	**0.208**
1 NE	0.29	3	0.26	0.236
1 S	1.48	9	0.67	0.164
2	**0.40**	**8**	**0.19**	**0.518**
2 NW	0.38	8	0.18	0.663
2 SE	0.67	4	0.48	0.100
3	**0.11**	**6**	**0.06**	**0.669**
3 NE	0.14	6	0.07	0.895
3 NW	0.49	4	0.35	0.116

Table 4.7 Density (per linear meter) of the different non-scleractinian corals for the three different areas and for the different sides in each area

Species	1	1 NE	1 S	2	2 NW	2 SE	3	3 NE	3 NW
***Acanella* sp.**	**0.00**	0.00	0.00	**0.00**	0.00	0.00	**0.00**	0.00	0.00
***Antipathes* sp. 1**	**0.01**	0.01	0.00	**0.00**	0.00	0.00	**0.00**	0.00	0.00
***Antipathes* sp. 2**	**0.00**	0.00	0.00	**0.00**	0.00	0.00	**0.00**	0.00	0.00
***Bathypathes* sp.**	**0.01**	0.01	0.01	**0.00**	0.00	0.00	**0.00**	0.00	0.00
***Leiopathes* sp. (all)**	**0.13**	0.18	0.06	**0.48**	0.61	0.08	**0.66**	0.89	0.11
***Leiopathes* sp. (large)**	**0.01**	0.01	0.01	**0.04**	0.04	0.01	**0.00**	0.00	0.01
***Leiopathes* sp. (medium)**	**0.00**	0.00	0.00	**0.01**	0.01	0.00	**0.00**	0.00	0.00
***Leiopathes* sp. (small)**	**0.12**	0.18	0.05	**0.43**	0.56	0.06	**0.65**	0.88	0.10
***Paramuricea* sp.**	**0.00**	0.00	0.01	**0.00**	0.00	0.00	**0.00**	0.00	0.01
***Parantipathes* sp. 1**	**0.04**	0.02	0.07	**0.02**	0.02	0.01	**0.00**	0.00	0.00
***Parantipathes* sp. 2**	**0.00**	0.00	0.01	**0.00**	0.01	0.00	**0.00**	0.00	0.00
Stichopathes cf. gravieri	**0.01**	0.01	0.01	**0.01**	0.01	0.01	**0.00**	0.00	0.00
***Trissopathes* sp.**	**0.00**	0.00	0.00	**0.00**	0.00	0.00	**0.00**	0.00	0.00

The diversity and density on versus off the delineated mounds differed. On the mound the diversity was 1.45 (SD 1.18) and density was 0.74 (SD 1.33). Off the mounds the diversity was 0.86 (SD 1.03) and density was 0.45 (1.3).

4.3.5 Statistical analyses

Statistical analyses to identify the environmental variables which cause differences in the abundance of the species were limited to the two most abundant species; *Leiopathes* sp. and *Parantipathes* sp 1. The analyses for *Leiopathes* sp. were performed for its most abundant size classes small and large. Due to the small sample size of the remaining species, no significant results were found.

Leiopathes sp.*:* Dead exposed coral framework, depth and eastness ($p < 0.0001$) significantly affected the abundance of small-sized *Leiopathes* sp. When these variables increase with one unit, the abundance of the colonies increased with respectively 2% and 0.8% and decreased by 48%. The number of large boulders contributed significantly to changes in the abundance of large *Leiopathes* sp. Individuals ($p < 0.001$). The abundance of large corals increases by 27% when large boulders increase a unit which is also supported by the video observations.

Parantipathes sp 1*:* Lithified hardground contributed significantly to changes in the abundance of *Parantipathes* sp 1 ($p < 0.01$). Its abundance increases 6% when the percentage cover of lithified hardground increases a unit.

4.3.6 Associated fauna

Depending on the speed and height of the ROV, associated species were not always visible. Therefore, no quantitative data is presented here. Instead, a qualitative overview is given of which non-scleractinian coral species had associated organisms present, with their location on the coral colonies observed.

On both small and large sized *Leiopathes* sp. colonies the anomuran crab *Gastropyctus* sp. was found on the middle and top outer branches (Figure 4.7a and b). Small sized colonies would always host one specimen, while larger sized colonies hosted up to 3 specimens at the same time. In one occasion a *Munida* sp. was found sheltering under a small *Leiopathes* sp. colony (Figure 4.7h). Ophiuroids and crinoids were only observed on larger sized colonies.

A close-up of a *Parantipathes* sp. 2 showed a small shrimp in between the branches (Figure 4.6c-2). But also *Gastropyctus* sp. (Figure 4.7c-1) and crinoids were found hosted on this species (Figure 4.7d). In one occasion a case of a skate egg was found attached to the top middle branch of a *Parantipathes* sp. 2. individual (Figure 4.7c).

One *Parantipathes* sp. 1 coral had two crinoids attached to the top central branch (Figure 4.5b). *Parantipathes* sp. 1 was found carried by three *Paromola cuvieri* crabs (Figure 4.6f-2). Two crabs were found carrying the gorgonian coral *Paramuricea* sp. (Figure 4.6e) ten crabs carried a sponge (Figure 4.7f-1), nine carried nothing, and on six occasions it was unclear whether or not they were carrying something.

Antipathes sp. 1 was only found in one location, where it was covered by large amounts (~10) of crinoids and also one *Gastropyctus* sp. specimen (Figure 4.6i).

Finally, *Gastropyctus* sp. was also found on the top central branch of three *Bathypathes sp.* individuals (Figure 4.7g).

One large *Paramuricea* sp. was observed with a *Gorgonocephalus* crinoid attached to it in the central top branches (Figure 4.7h)

No large megafauna was visible on the corals *Acanella* sp., *Antipathes* sp. 2, *Stichopathes cf. gravieri* and *Trissopathes* sp.

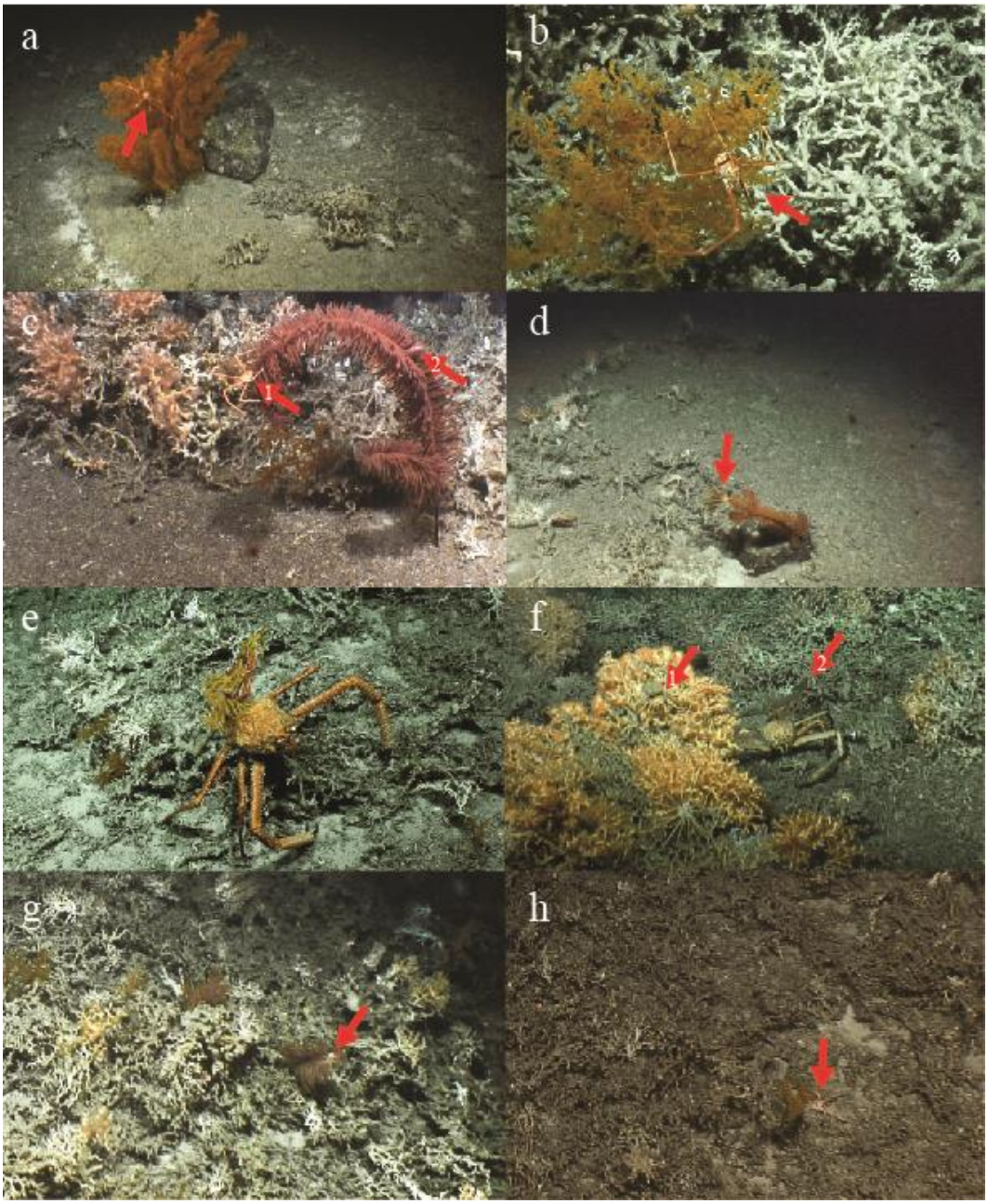

Figure 4.7 (a and b) large and small-sized *Leiopathes* sp. colonies with *Gastropyctus* sp. **(c)** *Parantipathes* sp. 2 with *Gastropyctus* sp. **(c-1)** and a small shrimp **(c-2). (d)** *Parantipathes* sp. 2 with a crinoid. **(e)** *Paramuricea* sp. carried by *Paromola cuvieri* **(f)** Sponge **(f-1)** and *Parantipathes* sp. 1 **(f-2)** carried by *Paromola cuvieri* **(g)** *Gastropyctus* sp. on the top central branch of *Bathypathes* sp. **(h)** *Munida* sp. sheltering under a small *Leiopathes* sp. colony.

4.4 Discussion

A total of nine different non-scleractinian coral species were identified in the Logachev area, from which eight belonged to the Order Antipatharia (Black corals) and two to the Order Alcyonacea. It is accepted that like scleractinian corals, non-scleractinian corals are confined to areas where high current speeds enhance food availability and where hard substrate is available for settlement (Thiem et al. 2006, Davies et al. 2009, Roberts et al. 2009a). Cold-water coral carbonate mounds are habitats where such conditions exist (Mienis et al. 2007). However, when the fine-scale spatial distribution patterns are investigated for different cold-water coral species, this food- and substrate availability relationship becomes more complex.

The first peak in non-scleractinian diversity is observed at 616 m depth on the north flank of area 1, right below the *L. pertusa* thickets. High concentrations of suspended organic matter (mixture of e.g. dissolved organic matter, bacteria, marine snow and small zooplankton) which are produced in the photic zone above Rockall bank, can be observed above the Logachev mounds, while off-reef seafloor areas at comparable depths are depleted in suspended organic matter (Duineveld 2007, Soetaert et al. 2016). When scleractinian cold-water corals, like *L. pertusa* and *M. oculata*, form mounds of a certain size they can engineer the environment by altering the local hydrodynamics to their benefit. The Logachev mounds have reached this size, and therefore induce tidal up- and downwelling, internal waves, and as a consequence also large INL, which supply the corals together with other filter feeders in their community with food (Mienis et al. 2007, Soetaert et al. 2016). This increased concentration of organic matter is reflected through healthy dense live *L. pertusa* thickets on the summits of the clustered mounds in our study area at a relatively shallow depth (between 560 and 610 m depth). Dead exposed coral framework and coral rubble become more abundant with increasing depth as the concentration of fresh organic matter decreases, and food becomes scarce towards deeper waters (Kenyon et al. 2003).

4.4.1 Diversity, evenness and density patterns of non-scleractinian corals

There are different possible explanations to explain why high densities or diversity of non-scleractinian corals are not found on the summit of the mounds where organic matter concentrations are the highest (Soetaert et al. 2016). First, studies have shown that rather than the presence of live coral, it is the diverse microhabitats provided by dead coral skeletons which facilitate the high biodiversity associated with reef-forming cold-water corals (Mortensen and Fosså 2006, Buhl-Mortensen et al. 2010). This is because a permanent mucus layer (coenosarc) on the skeleton of live scleractinian corals prevents attachment of sessile epibiotic species (Freiwald et al. 2002, Buhl-Mortensen et al. 2010). As a consequence, the dense live scleractinian skeletons are not a suitable substrate for the non-scleractinian corals. Secondly, in our study area, *L. pertusa* might outcompete

other filter and suspension feeders for food on mound summits. The efficiency of food capture for different species can be strongly dependent on current velocity, seawater temperature and polyp size. High flow velocities can deform coral polyps reducing the exposed feeding surface area (Dai and Lin 1993, Purser et al. 2010, Wijgerde et al. 2012, Gori et al. 2015). Higher flow speeds may also make the polyps less efficient at holding prey (Sebens et al. 1998, Orejas et al. 2011). Colder temperatures may cause the polyps to contract or affect nematocyst function (Gori et al. 2015). Warmer temperatures may increase the metabolism of corals, but can cause them to starve if food supply is not met (Dodds et al. 2007, Davies et al. 2009). Some coral species which have larger polyps can remove particles from their environment more efficiently than those with smaller polyps (Porter 1976, Palardy et al. 2005, Wang et al. 2012). The effect of flow velocity, temperature and polyp size have not been studied for the non-scleractinian corals described in this study. Since food supply is essential to maintain the basic physiological processes of cold-water corals (Naumann et al. 2011), information on the factors that affect coral efficiency in capturing food may help to explain the distribution pattern of the non-scleractinian corals in the Logachev area.

Peaks of non-scleractinian diversity are recorded at greater depths of 680 m (NE flank), 750 m (S flank) and 860 m (S flank) depth in area 1 and 2. A difference between the alternate sides of the areas was also observed. Area 1 and 3 had a higher diversity of species on the respectively S and SE flanks, while area 2 had a higher diversity on its NW flank. A more diverse range of substrates was found in these locations and is, therefore, a possible explanation for our peaks in diversity on these flanks of the areas. The Logachev area is exposed to SW-NE directed currents (White et al. 2007) which could be responsible for sweeping sediments away from the hard substrates and creating a more diverse range of substrates for the corals to settle on. As mentioned earlier, *L. pertusa* isn't a suitable substrate for non-scleractinian corals to settle on. This explains why the diversity and density of non-scleractinian corals is lower in areas where there are *L. pertusa* thickets (e.g., area 1). Instead, our data showed that a range of substrates including coral rubble, dead coral framework and hard substrates (lithified hardgrounds, pebbles, cobbles, boulders) were used as settlement substrates. A significant correlation was found between lithified hardgrounds and the abundance of *Parantipathes* sp. Only a small percentage (22%) of the substrates in the study area consisted of these hardgrounds, but they are an important aspect of overall mound growth and development as they provide stability to the steep slopes of the mounds and can be used as substratum for mound-building invertebrates (Noé et al. 2006). Hardgrounds on the coral carbonate mounds in the Rockall area have been identified in the past (van Weering et al. 2003). These hardgrounds can be completely exposed, showing signs of current erosion and sponge borings or can have different degrees of sediment cover with live and dead coral colonies (Wheeler 2005,

2007). The exposure of these hardgrounds is associated with strong bottom currents (Noé et al. 2006). Therefore, the presence of hardgrounds not only provides a stable settlement substrate, but their lack of sediment cover also indicates high SW-NW diurnal tidal current speeds (White et al. 2007) which could mean an increase in the food-encounter rate for cold-water corals that settle there.

The density of non-scleractinian corals differed between the three areas and was generally higher where the diversity of species was lower. This difference could be related to substrate availability, the distance of the studied areas to the shallow part of the Rockall Bank but also to the southwest direction of the bottom residual current (Soetaert et al. 2016). Area 1 has a high diversity but a low density of non-scleractinian corals. Firstly, this low density can be explained by the fact that this area has the highest percentage cover of *L. pertusa* thickets. As mentioned above, the skeleton is not a suitable substrate for non-scleractinian corals to settle on. In all the areas, the density of non-scleractinian corals was higher on the sides which had an overall lower diversity in substrates. Secondly, there might be a difference in the concentration of food between the areas which has been indicated shown by the models in Soeataert et al. (2016). The suspended organic matter that feeds the corals originates from the productive surface water above the bank and is delivered to the corals trough downwelling (White et al. 2005, Mienis et al. 2007, Soetaert et al. 2016).

Non-scleractinian corals were recorded both on and off the mounds that were mapped with the BGS Seabed Mapping Toolbox. This is expected, as suitable settling substrates are observed on and off the delineated mounds. When examining the changes in substrate, dead exposed coral framework and *L. pertusa* thicket were found to be more abundant on the mounds. The diversity and density were both higher on the delineated mound compared to off. This difference is likely related to a higher percentage presence of dead exposed framework on the mounds, which indicates a diversity of microhabitats for the non-scleractinian corals to settle.

As shown by Soetaert et al. (2016), mounds that are located closer to Rockal Bank access more optimal food and current conditions which is suggested by the model output of vertical current velocities and organic matter concentration in the water column in the Logachev area. Therefore, the distance of the studied areas from the shallow bank to the deeper located mounds could impact the concentration of the organic matter reaching the corals on the mounds. The food that originates from the productive surface waters above Rockall Bank can also be delivered to the deeper located corals by the resuspension of seabed particles in intermediate nepheloid layers (Kenyon et al. 2003, Mienis et al. 2007). On the south-east slope of Rockall Bank, intermediate nepheloid layers are

found between 200 and 500 m depth and between 500 and 700 m depth (White et al. 2003, Mienis et al. 2007). The second intermediate nepheloid layer, which is located deeper, is smaller than shallower intermediate nepheloid layers and starts approximately ~ 25 km from the bank (Mienis et al. 2007). This is approximately where area 3 is located and might explain why it is possible to maintain high densities of corals further away from the bank. Area 1 is closer to the bank than area 3, making it possible that sufficient food supply reaches the corals from the shallower and deeper intermediate nepheloid layers. Area 2 is located the closest to Rockall Bank. The highest diversity and density was calculated for area 2 and could be a result of the corals benefitting from receiving the highest concentrations of suspended organic matter as this area is located closest to the shallow bank in combination with a diverse range of substrates for settlement. The direction of the residual current might also cause the density pattern observed in our data. The flanks of the areas with higher densities of corals were located perpendicular to the SW orientated residual current, likely exposing this side to higher concentrations of organic matter.

The most abundant and therefore dominant non-scleractinian coral in our study areas is *Leiopathes* sp. Our data showed that *Leiopathes* sp. occupied all available substrates. Therefore, this species is more likely to thrive in areas with a lower diversity of substrates, especially of the food input is still high enough. *Leiopathes* sp. has a slow radial growth rate of 0.005-0.022 mm yr^{-1} and is one of the longest living species on earth (Roark et al. 2009). The slower radial growth rates and their longevity might be of advantage in areas where food supply is scarcer. More information on the suspended organic matter concentrations for each particular area, supplied by tidal downwelling, intermediate nepheloid layers and the residual currents, and information on the physiological demands of the different coral species in our study area would offer more robust explanations for the observed difference.

4.4.2 Leiopathes sp. size classes

An interesting difference in the abundance of the various size classes of *Leiopathes* sp. was observed. The vast majority (95%) of the colonies in our area were small sized (> 30 cm), while 1% was medium (30 – 100 cm) and 4% were large (> 100 cm). A high abundance of small-sized colonies could indicate a successful dispersal event with a high survival rate after settlement. However, substrate stability might be another factor influencing the distribution of the different size classes. Small sized colonies were found in areas with dead exposed coral framework (95%), while the large sized colonies were mainly found in areas with large boulders (78%). Medium sized colonies were found in similar abundances on both substrates. This difference in survival is likely to be related to the stability large boulders provide to a large colony. Colonies growing on dead

exposed coral framework are inclined to fall when exposed to high current speeds. Towards the summit of the cold-water coral mounds, these large boulders become rare as they are covered with live and dead *L. pertusa* and therefore making them unavailable as a stable substrate for large-sized *Leiopathes* sp. colonies. Therefore, the higher percentage cover of dead exposed framework versus large boulders also explains why a difference in the abundances of the different size classes is observed.

4.4.3 Role of non-scleractinian corals as a habitat

Non-scleractinian corals are known to be an important habitat for a diverse range of organisms (Buhl-Mortensen and Mortensen 2004, Wagner et al. 2012, De Clippele et al. 2015). However, their mobile associated fauna has been poorly documented, although this has become easier thanks to the development of ROVs. In past studies as well as here, shrimps, crabs, crinoids and ophiuroids were found to be using non-scleractinian coral species as a feeding platform and a place to shelter. No associates were observed visually on the bamboo coral *Acanella* sp. and *Paramuricea* sp. However, *Paramuricea* species have been found occupied by megafauna elsewhere (Rosenberg et al. 2005, De Clippele et al. 2015). The number of crabs occupying a black coral colony increased with increasing colony size. This is expected as smaller sized colonies are unable to have more than one crab attached due to competition for perch sites. These associated organisms were mainly located on the top outer parts of the colonies, which increases their food encounter rate as their elevated position is further away from the slower current in the near-bottom boundary (Fujita and Ohta 1988). On one occasion, the crab *Munida* sp. was found sheltering under a small *Leiopathes* sp. colony. This behaviour was also observed under the sea pen *Kopholobelemnon stelliferum* (De Clippele et al. 2015). The corals' size, the number of branches and the availability of sufficient food will impact the presence of associates on colonies. My data illustrate the importance of black corals in the Logachev area for these particular filter and suspension feeding organisms. However, only 1% of the non-scleractinian corals had associated fauna present. This low percentage is likely to be caused by the lack of detailed surveying and area covered in our study, a high flexibility of the coral branches, and the low availability of large-sized colonies. The non-scleractinian corals in our study have a more flexible skeleton compared to e.g. the gorgonian *Paragorgia arborea* which commonly has associated fauna present (Buhl-Mortensen and Mortensen 2004, Buhl-Mortensen and Mortensen 2005, De Clippele et al. 2015). The skeleton of black corals is more flexible and chitinous, which is an adaptation for living in areas with very strong currents. To withstand strong currents, *P. arborea* grows much thicker branches compared to other corals (Mortensen and Buhl-Mortensen 2005) which provide the associated organisms with a more robust and larger surface area to inhabit. A negative relationship between the presence of

associated fauna and the flexibility and size of the colonies and branches has been shown and therefore explains our lower presence of these associates (Buhl-Mortensen and Mortensen 2004, Santavy et al. 2013).

4.4.4 Association of non-scleractinian corals with Paromola cuvieri

In total, 30 carrier crabs (*P. cuvieri*) were found in this study, of which most were carrying a sponge, but also the black coral species, *Parantipathes* sp. 1 and the gorgonian *Paramuricea* sp. Antipatharians and gorgonians have previously been reported to be carried by *P. cuvieri* between the dactyls and propodi of the fifth pereiopods (Wicksten 1985, Guinot et al. 1995, Weaver et al. 2009, Braga-Henriques 2012). For example, Braga-Henriques et al. (2012) studied the behaviour of 16 carrier crabs (*P. cuvieri*) in the Azores. This study observed that damage of the fifth pereiopods could be a reason for when there was no object being carried. In the study presented here, no damage was observed, but this could be related to the distance between the ROV and seabed limiting the resolution of the video.

The species that is carried varies depending what species are available in the surrounding habitat. However, it will not necessarily be the most common invertebrates in that habitat (Braga-Henriques et al. 2012). The selection process of which species is carried is still unclear but is possibly related to weight, size and palatability (Braga-Henriques et al. 2012). In the Azores study, and in this study, camouflage-type behaviour was observed, as in some occasions the crab would lift the object above their carapace when disturbed by the ROV and its lights. However, Capezutto et al. 2012 only observed such behaviour as an adaptation to an anti-predator defence. At present, there are no indications of *P. cuvieri* using the carried species to attract other crabs or species. The sponges and cnidarians can distract predators, but also have the ability to protect them with spicules and secondary metabolites against predators (Coll et al. 1982, Hill and Hill 2002, Barsby and Kubanek 2005, Hill et al. 2005).

4.5 Conclusion

A diverse range of non-scleractinian cold-water corals, especially black corals, were found on the Logachev mounds. Between the clusters of cold-water coral carbonate mounds, differences in the diversity and density of these corals were observed. This is likely to be related to the availability of a diverse range of substrates, food supply, distance of the mounds to the shallow Rockall Bank and the presence of *L. pertusa* thickets. Substrate availability and stability is an important contributor to the differences observed in diversity, density but also for the size class distribution of *Leiopathes* sp. The studied areas that were located further away from the bank had a lower diversity of non-scleractinian corals which might be related to the availability of food reaching the areas trough intermediate nepheloid layers and tidal downwelling. It is likely that the scleractinian coral *L. pertusa* outcompetes other cold-water corals for food and substrate in the areas with high suspended organic matter. The explanations that are given here for the differences in the fine-scale spatial distribution of non-scleractinian corals remain speculative, as information on their ecophysiology and detailed hydrodynamic data are unavailable to date. These non-scleractinian corals are however present in high densities on the studied cold-water coral carbonate mounds and function as a key habitat for other organisms. Further research is needed to ensure that these vulnerable, long-lived species are understood and protected worldwide.

CHAPTER 5- DISCUSSION

5.1 Summary of the results

Thanks to recent developments in technology, an increasing amount of information on deep-sea seabed structures has become available (e.g. Huvenne et al. 2011, Tong et al. 2013, Moreno-Navas et al. 2014, Buhl-Mortensen et al. 2015). In this thesis, I showed how the integration of ecological, geophysical and hydrodynamical data leads to a better understanding of what causes fine-scale differences in the distribution of live and dead cold-water coral colonies within a reef complex.

In Chapter 2, novel acoustic and visual mapping tools were addressed. A new ArcGIS-based seabed mapping toolbox developed by the British Geological Survey was used to semi-automatically map and characterise small *Lophelia* "mini-reefs" within the Mingulay Reef Complex. A microbathymetric grid (35x35 cm pixel size) from the central area within Mingulay reef area 01 was used together with high-definition video data, to identify which of these small reefs had live coral colonies present. The microbathymetry allowed me to delineate and measure individual coral colonies and visualise the distribution of mini-mounds in five classes of percentage live coral cover. This ArcGIS-based seabed mapping toolbox was used to examine how environmental variables differ between live and dead biogenic reefs. Water depth, rugosity, bathymetric positioning index and current speeds were found to be the main drivers of the observed differences in the distribution of live reefs. This information was then used to create a predictive map of live biogenic reefs in the wider Mingulay Reef Complex. The predictive map showed higher concentrations along the channel in the centre of the reef and on the south side of the ridge. These observations are most likely related to the higher current speeds found in these areas. Both the microbathymtery and the predictive map can function as a baseline and tool for future sampling and monitoring.

In Chapter 3, differences in the direction of the current at the Tisler Reef were shown to have significant fine-scale effects on the morphology and growth of the reef. The ArcGIS-based seabed mapping toolbox was used to delineate and characterise the cold-water coral mound features within the Tisler Reef. The percentage of live and dead coral cover were calculated, and the morphology of the coral colonies was quantified for the north-west and south-east side of the reef. The south-east of the reef had a higher percentage of both dead and live *L. pertusa* colonies, and had higher densities of very small coral colonies. This was caused by a higher percentage cover of hard settling substrates and a higher frequency of downwelling on this side of the reef, providing the

corals with higher concentrations of food and/or warmer water from the surface. The presence of dense living and dead coral structures also increases local turbulence, which might enhance coral larval settlement. This local hydrodynamics and intra-specific interactions are essential for the future development of the reef on the south-east side. Interspecific interactions between the corals and the two dominant sponges were also observed in this area. The abundance of the sponge *M. lingua* is positively correlated to the abundance of *L. pertusa*, which is expected as this sponge can use live *L. pertusa* as a substrate. This is beneficial for the sponge as it can grow further from the bottom boundary layer into higher current speeds. Sponges are filter feeding organisms and need high current speeds to increase their food uptake. A weaker correlation was found between the abundance of the sponge *Geodia* sp. and *L. pertusa*, as they compete for similar settlement substrates and food.

In Chapter 4, differences in the distribution, diversity and density of non-scleractinian corals were shown to be related to the local hydrodynamics, substrate availability, interspecific competition with *L. pertusa* and possibly the distance of the studied areas to the shallow Rockall Bank. First high-definition video data of the Logachev mounds were used to identify the various types of substrates allowing me to determine where different species of non-scleractinian corals occur. The ArcGIS-based seabed mapping toolbox was also used to delineate and characterise the cold-water coral mound features within the Logachev Area. The availability, diversity and stability of the substrate are likely to be a major contributor to the differences in the fine-scale spatial distribution patterns observed in the studied areas. This has been particularly clear for differences in the distribution of large versus small *Leiopathes sp.* colonies. Large boulders are necessary to provide stability to larger colonies in strong current environments. The ecophysiology of different species might also be important to explain their distribution. Understanding how the supply of organic matter varies between the studied clustered carbonate mounds would provide information to unravel the differences in the distribution, density and diversity observed. High-definition video analyses were also useful to study the role of non-scleractinian corals for the mobile megafauna. A variety of organisms were found to be associated with non-scleractinian corals, mostly using them as a feeding platform to reach higher current speeds, but also as a structure to shelter from predators. However, most of these non-scleractinian corals were small and had a flexible skeleton which is not an optimal substrate for these organisms. Therefore, the percentage of corals with associates present was low.

Throughout this thesis, a fine-scale approach was used for specific sites. By considering specific sites, a broader understanding of what drives spatial differences of cold-water coral reefs is possible

and can contribute considerably to the development of monitoring tools. This thesis contributed to a user-friendly tool which mapped mini-reefs semi-automatically in the Mingulay area and can be used for future management and monitoring (Chapter 2). This tool is adaptable and has been used for other seabed structures such as pockmarks (Gafeira et al. 2012). Using acoustic data and high-definition video analyses for the calculation of the percentage cover and quantification of the morphology of coral colonies (Chapter 3, Chapter 4) and reefs (Chapter 2, Chapter 3) provides a second approach to monitoring the status and future development of these habitats.

5.2 Using the BGS Seabed Mapping Toolbox to classify cold-water coral mounds within cold-water coral reefs

Initially, the BGS Seabed Mapping Toolbox was developed to map seabed pockmarks (Gafeira et al. 2012). Then the tool was adjusted to map cold-water coral mounds in the Mingulay area and the extracted morphometric information was used to create a predictive map of the likelihood of presence of live biogenic reefs (De Clippele et al. 2016, Chapter 2). This illustrated that this tool was not only able to describe the morphometric characteristics of reefs, but that this information can also be used to study their ecology. This is as mapped seafloor geomorphology is a very useful physical attribute (Harris 2012).

To explore possible further applications of the tool, it was used to describe the morphometric characteristics of the mounds on the Tisler Reef and at the Logachev area.

Firstly, without using the toolbox, it was clear that the reefs gross morphologies were very different. Due to the shallow location close to the coast, both the Mingulay Area 1 (live reef:120 - 190 m deep) (Chapter 2) and the Tisler Reef (live reef: 70 - 160 m deep) have only developed since the last Glacial (Chapter 1). Therefore, the gross morphology of the reef resembles that of the colonised structure (Inherited morphology) (Wheeler et al. 2007, Chapter 1). The structure that is colonised at the Mingulay Reef is believed to be a northward dipping sill intruded with Lower Jurassic sedimentary mudstone rocks (Stewart and Gatliff 2008). Information on the bedrock that the corals would have colonised at the Tisler Reef is currently unavailable (Geological Survey of Norway). As can be seen from figure 3.1c, the live part of the reef extends both on and off the mound structures visible in the reef area. ROV-examinations by Lundälv T. (HD-video) indicated that the outcrops inside and outside the live reef are made up of both live and dead coral. To know with certainty if the mounds structures at the Tisler Reef inherited the morphology of the bedrock, seismic data is needed. The Logachev cold-water coral carbonate mounds (live reef: 500-1000 m deep) have developed over glacial-interglacial time periods and its morphology reflects that of the dominant

hydrodynamic controls (Developed morphology) (Kenyon et al. 2003, van Weering et al. 2003, Mienis et al. 2007, Wheeler et al. 2007). Rockall Bank is part of the deeply eroded Rockall Igneous Centre that was formed as part of the North Atlantic Igneous Province (55 million years ago) (Sutherland 1982, Ritchie et al. 2011). These broad scale structures will affect both the distribution of sediment types and biological communities within the reef and in the immediate surrounding area of the reef (Buhl-Mortensen et al. 2012).

Secondly, fine-scale differences in the morphology of the reefs within the gross area became apparent when the tool was applied. There were large differences in the number of mounds mapped within each area. This is because the mapped areas differed in size. Mingulay Reef 1 covered an area of 11 km^2, on which 505 small round-shaped biogenic reefs were mapped. The Tisler Reef had the smallest area of 0.23 km^2, on which only 14 round-shaped mounds were mapped. These were on average slightly larger than the mounds mapped at the Mingulay Reef. The Logachev area was the largest covering 424 km^2, on which 123 mounds were mapped.

The shape, size and variety of shapes within a reef were different for the different reefs. Firstly, two distinct morphologies were observed: round-shaped and dendriform-shaped mounds. All the areas had reefs which were round-shaped (Figure 2.6, 3.6, 4.3, 5.1a). This was indicated by the value of the Area Ratio (Figure 5.1a). When this value is closer to 1, the shape of the mound is more roundish. When this value is closer to 0, the shape of the mound is more dendriform. The highest Area Ratio value was found for the mounds at the Mingulay Reef. The average value was slightly lower for the Tisler Reef, indicating that their shape slightly more irregular. The lowest average value was found for the Logachev Mounds. This area is particularly interesting as this area consisted of a significant number of round-shape mounds, but also of very large dendriform-shaped mounds. These comparisons are visualised in figure 5.1.

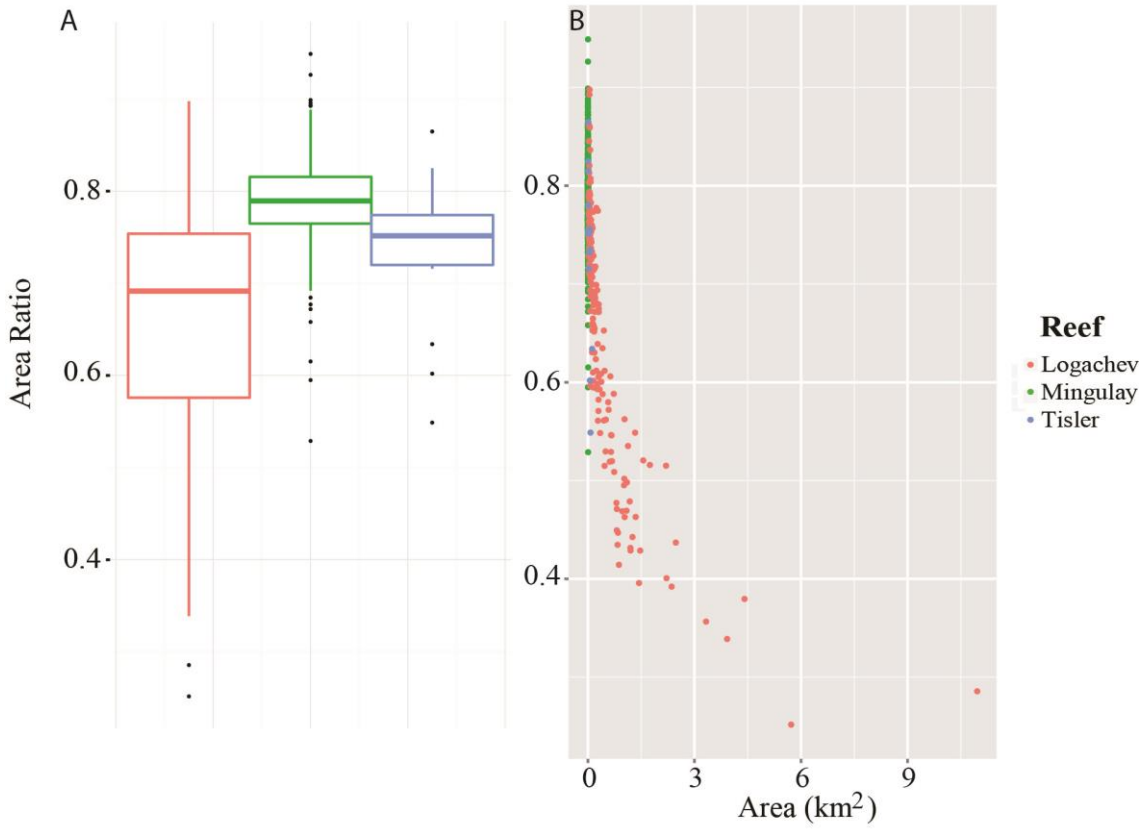

Figure 5.1 (a) Boxlplot of the Area Ratio for the different study areas. A value closer to 1 means that the mound has a roundish shape. A value closer to 0 means that the shape of the mound is more dendriform. **(b)** Scatterplot of the Area Ratio over the Area (Km^2) for the different reefs.

The dendriform shapes which were observed when applying the BGS Seabed Mapping Toolbox have been described as clustered mounds (de Haas et al. 2009, Chapter 4). The cold-water coral mounds on the SE Rockall Bank have been described to be several kilometres in diameter, up to 380 m high and mostly occurring as elongated clusters of various sizes that appear to form ridges (van Weering et al. 2003, Mienis et al. 2007, de Haas et al. 2009). This observation is here confirmed. However, the maximum height observed here was 504 m (Table 4.2). These clusters can be up to 10 km in length and are oriented perpendicular to the general bathymetric contours (de Haas et al. 2009). The areas in between the mounds are filled up with both carbonate debris and glacial sediments (van Weering et al. 2003).

Figure 5.2A shows that mounds that are larger in area and higher, have a lower Area Ratio and are therefore more dendriform- shaped. This is especially clear for the the mounds in the Logachev Area (Chapter 4). Figure 5.3B shows the difference in minimum and maximum water depth and indicates that larger mounds have a deeper maximum water depth. Soetaert et al. (2016) showed that there is a positive feedback between the growth of the mounds and the supply of food from the

surface. As a result, when coral mound formation is induced at deeper depth, they will form higher mounds as seen in our data. The initiation and formation of mounds happen under favourable environmental regimes as explained in chapter 1 (Freiwald et al. 1997, Kenyon et al. 2003, de Haas et al. 2009). The largest mound structures in the Logachev area have developed over glacial-interglacial time periods (Kenyon et al. 2003, van Weering et al. 2003, Mienis et al. 2007) and joined, forming clustered dendriform-shaped mounds.

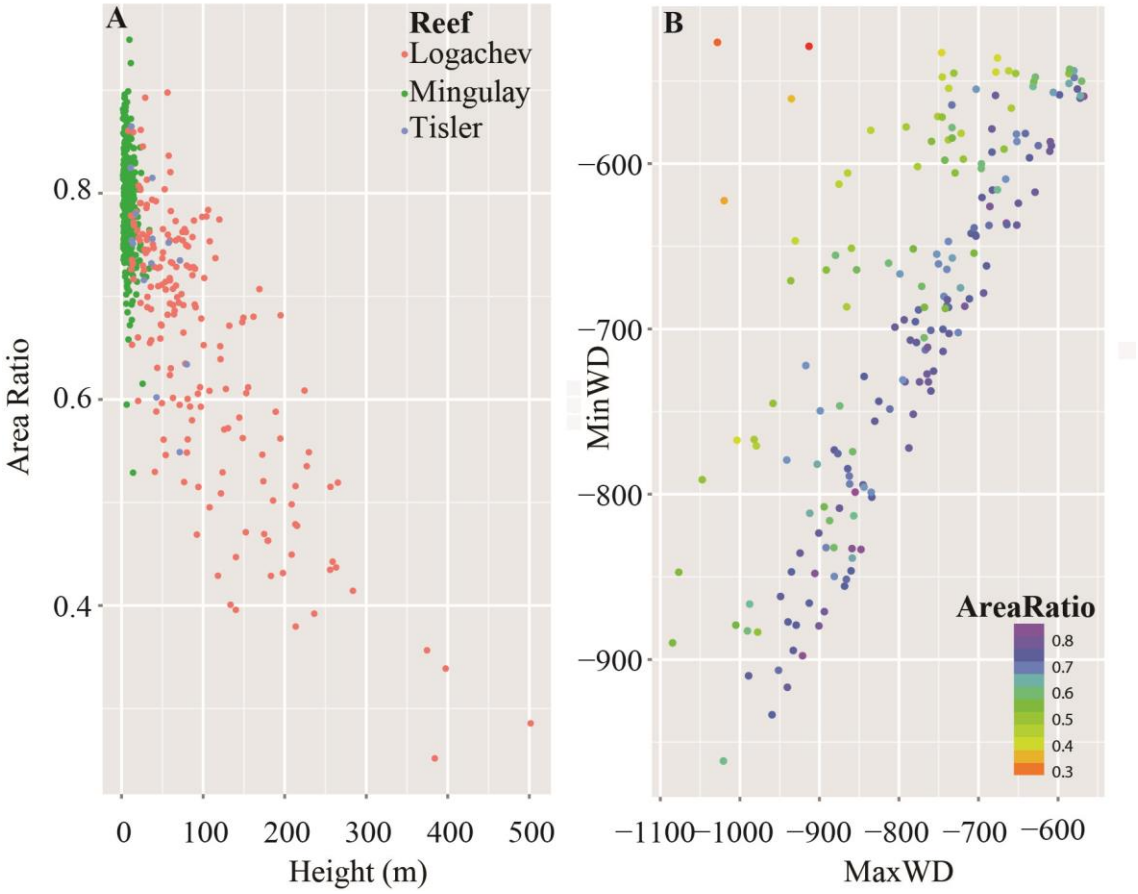

Figure 5.2 (a) Scatterplot of the Area Ratio over height of the of the mounds for the different reefs. **(b)** Scatterplot of minimum water depth (MinWD) and maximum water depth (MaxWD) indicating the depth of the base of the mounds and their height.

It is important to note that the accuracy of the characteristics calculated by the BGS Seabed Mapping toolbox can be affected by the resolution of the bathymetry versus the size of the analysed features. If the number of bathymetry cells within a delineated feature are too small, the calculation of the variables orientation, slope, and difference between the minimum and maximum water depth are not reliable. Fortunately, the number of cells within the delineated features in all our locations always exceeded 8 (MGB width) and 15 (MGB length), and therefore result in the accurate calculation of all the variables.

The delineated mounds in the areas studied here varied in size, shape and height. The BGS Seabed Mapping Toolbox extracted the morphometric characteristics efficiently and can be a useful tool to examine other reef mounds in the future. By studying the shape of the colonised structure, the age of the mounds and the oceanographic conditions, a better understanding of the present and future morphology of the mounds can be obtained. Here, a first description of the morphology of three different reefs is provided. Further studies are needed to investigate the exact relationships between the environmental variables and the morphology of the mounds (Sayago-Gil et al. 2012).

5.3 Importance of studying fine-scale spatial patterns

To understand the spatial relationships between the occurrence of organisms and their preferred habitats information should be collected on both (Harris and Baker 2012a). Information on how cold-water coral reefs grow and can change in the future, knowledge on what drives differences in the fine-scale spatial distribution of scleractinian and non-scleractinian coral species is needed. This thesis has highlighted how local hydrodynamics can have a particularly significant impact on the morphology, distribution, density and diversity of cold-water coral species within a reef. Previous work in these study areas has shown the importance of locally enhanced bottom currents, internal waves, nepheloid layers, tidal currents, resuspension of bottom currents in relation to the presence of cold-water coral reefs (Dorschel et al. 2007, Mienis et al. 2007, Wagner et al. 2011, Duineveld et al. 2012, Findlay et al. 2013, Soetaert et al. 2015, Chapter 2, Chapter 3, Chapter 4) as they transport nutrient-rich water to the corals (Duineveld et al. 2007, Davies et al. 2009, Wagner et al. 2011, Soetaert et al. 2016).

At the Mingulay Reef Complex (Chapter 2), the acoustic data allowed me to study the distinct "mini-reefs" which are distributed along the reef. In this chapter, I showed how the growth and shape of these mini-reefs are likely to be affected by the direction of the dominant current, the current speed and the locations of optimal organic matter concentrations. My findings also showed that the mini-reefs at the summit of the ridge, where the highest current speeds were recorded, were composed of dead coral framework.

When studying the Tisler reef (Chapter 3), differences in the percentage cover and morphology between the southeast and northwest side were observed. Since the direction of the dominant current changes frequently, downwelling is expected on both sides of the reef where it provides the corals with organic matter from the surface waters and therefore stimulates coral reef formation and growth. However, here differences in coral growth were observed between the two sides of the reef. This was suggested to be related to the frequency of downwelling on either side of the reef.

This chapter revealed that these fine-scale differences in hydrodynamics could have profound effects on coral growth, coral- larvae settlement, coral feeding and the abundance of associated reef organisms such as sponges.

In the Logachev Mounds (Chapter 4) the non-scleractinian corals were found at deeper depths and in locations where higher current speeds are expected compared to where scleractinian corals were found. At the summit of these mounds, the framework of the *L. pertusa* thickets slow down the currents due to frictional drag (Roberts et al. 2009a). The skeleton of the non-scleractinian corals is more flexible and chitinous than that of the scleractinian ones, and can, therefore, withstand higher current speeds (Bo et al. 2009). Another explanation for finding non-scleractinian corals at deeper depths is a lower amount of competition for food and settlement substrate. However, it became apparent that to understand the fine-scale spatial differences in the diversity and density of non-scleractinian corals, more information on their physiological demands is needed as it would offer insight in why and how they could thrive under different flow and food conditions.

There are four further general purposes for mapping fine-scale spatial patterns: (1) it supports government spatial marine planning, management, and decision making (2) it supports and underpins the design of marine-protected areas (MPAs) (3) it conducts scientific research programs which aim at generating knowledge of benthic ecosystems and seafloor geology (4) it conducts both living and non-living seabed resource assessments for economic and management purposes (Harris and Baker 2012a).

5.4 Importance of studying cold-water coral habitats in relation to climate change

Radiocarbon dating of *L. pertusa's* aragonite skeleton can be used for studying past reef growth and its distribution across geological timescales (Douarin et al. 2014, Henry et al. 2014). These records have indicated that changes to the ocean currents, which in turn influence deep-sea temperatures, oxygen, pH and food supply, have affected the distribution and growth of deep-sea reefs (Thomas and Gooday 1996, Yasuhara and Cronin 2008, Yasuahara et al. 2008, 2016, Douarin et al. 2014). For example, during the last glacial, *L. pertusa* was restricted to the temperate zone as surface productivity was low and the waters were cooler (Frank et al. 2011). These past changes were caused by the natural ocean-atmospheric changes and variability in the total solar irradiance (Stuiver and Braziumas 1993, Bond et al. 2001, Helama et al. 2010). At present, rising atmospheric greenhouse gasses (pre-industrial: 280 ppm, present: 407 ppm) are adding to the effects of the natural climate cycles (Dodds et al. 2007, Thiagarajan et al. 2013, Douarin et al. 2014, Henry et al. 2014, Glecker et al. 2016, Sweetman et al. 2017). Increasing amounts of greenhouse gasses

trap outgoing infrared radiation emitted by the Earth's surface and warm the atmosphere. Most of this excess heat is absorbed by the oceans. As a consequence, deep-sea temperatures are rising (Purkey and Johnson 2010), oxygen minimum zones are expanding (Stramma et al. 2008, 2010, 2012, Keeling et al. 2010, Helm et al. 2011), the pH is decreasing (Byrne et al. 2010) and the particulate organic matter flux to the seafloor has been changing (Ruhl and Smith 2004, Smith et al. 2013, Sweetman et al. 2017). These changes affect cold-water corals in varied ways.

Firstly, variation in the strength, position and interaction of the North Atlantic subpolar gyre (SPG) with the Subtropical Gyre (STG) affect the growth of cold-water corals in Atlantic Ocean (Henry et al. 2014, Victorero et al. 2016). The North Atlantic subpolar gyre (SPG) and the Nordic Seas are the main regions in the North Atlantic Ocean where deep water is formed and creates a southward flow of deeper cooler and fresher water (Hall and Bryden 1982, Hansen and Østerhus 2000, Read 2001) which is part of the Atlantic Meridional Overturning Circulation (AMOC), a global circulation system which has a large impact on Earth's climate (Hátún et al. 2005). When the SPG is strong and displaced eastward, deep water mixing, and convection is promoted. When the SPG circulation is weak, the influence of the STG increases, causing mixing to reduce in the North Atlantic (Colin et al. 2010, Sgubin et al. 2017). Due to changes in the climate, the intensity of the SPG has weakened over the last 25 years, causing the cold-water coral communities in the North Atlantic to become exposed to warmer, saltier and more nutrient-poor water, which negatively affect cold-water corals and other organisms (Häkkinen and Rhines 2004, Hátún et al. 2005, 2009, 2017, Johnson et al. 2013)

Secondly, the majority of *L. pertusa* records are found where the dissolved oxygen is between 3 and 5 mL L^{-1} (Rogers 1999). In warmer water, it becomes more difficult for O_2 to dissolve, and together with increased thermal stratification, it is likely that the ocean becomes less oxygenated especially between 100-1000 m depth (Stramma et al. 2012, Bopp et al. 2013). This is exactly where most cold-water coral reefs occur (200 - 1000 m depth). The studies in this thesis took place in the Atlantic Ocean. At present the dissolved oxygen concentrations range in the Atlantic Ocean is from 1.48 to 7.54 mL L^{-1} but are predicted to decrease from -0.03 to 0.02 mL L^{-1} by 2100 (Sweetman et al. 2017). When the concentrations are below 0.5 mL L^{-1} mass mortality of cold-water corals and other benthic organisms will occur (Diaz and Rosenberg 1995).

Thirdly, cold-water corals need areas where there is enough food supplied trough the mixing of productive surface water to deeper depths and trough the resuspension of bottom sediments (see section 1.3). However, global warming will cause a higher input of freshwater (by glaciers melting

and river runoff) and reduce ocean mixing caused by stratification. Warming can also cause changes in the phytoplankton community with a shift from large fast sinking diatoms to slow sinking picoplankton (Bopp et al. 2005) causing a reduction of the food flux to the seafloor. Sea surface productivity and transfer to the deep sea will change in differently in different areas of the world. However, an overall decrease in particulate organic matter is predicted for 2100 (Sweetman et al. 2017).

Fourthly, calcifying organism, such as the coral *L. pertusa*, can grow when they are located above the depth of the Aragonite Saturation Horizon (ASH) where the sea water is saturated with respect to aragonite (Orr et al. 2005, Chapter 1). Near the ASH, the pH gradually reduces causing the aragonite skeleton of calcifying organisms (Orr et al. 2005) and, thus also of *L. pertusa* (Guinotte et al. 2006), to dissolve and become more brittle (Hennige et al. 2015), making them more susceptible to predation and loss of habitat (Sweetman et al 2017). The rising atmospheric CO_2 concentrations, increase ocean acidity causing the ASH to shallow and therefore reduce the depth at which calcifying organisms can grow (Gehlen et al. 2014).

Finally, the degree of connectivity between cold-water coral reefs has an impact on the genetic diversity of species. Climate change could affect the distribution of marine species as the transportation of propagules, the larval physiology and ecology can be affected by changes in the strength and pathway of ocean currents, water temperatures, food supply and mortality rates (Cowen and Sponaugle 2009, Fox et al. 2016). Higher sea temperatures would decrease the connectivity and dispersal ability of *L. pertusa* as its pelagic larval duration shortens when the temperature increases (Strömberg 2016).

This thesis has emphasised that knowing where the optimal hydrodynamical conditions for coral growth and feeding are within a reef, how this changes over time and space, and what the ecophysiological demands of different species are, are crucial to understand both broad- and fine-scale spatial differences in cold-water coral species distribution now and in the future but also for the fauna that is associated with the habitats they form.

5.5 Recommendations

Even though technological advances have allowed us to expand our knowledge of the deep sea, the fine-scale hydrodynamic, acoustic and taxonomic data needed for robust analyses are often unavailable.

Firstly, site-specific fine-scale spatial and long-term temporal three-dimensional modelled data of the local currents, which can be used for statistical analyses, of our study areas were not available. This is not uncommon for deep sea habitats. Other studies commonly use terrain variables, together with no (e.g Røst Reef Norwegian margin: Tong et al. 2013, Hatton Bank and George Bligh Bank: Howell et al. 2011, Rockall Bank: Robert et al. 2016) or broad-scale information on the local hydrodynamics (e.g. Pacific and Atlantic Continental Margins of North America: Bryan and Metaxas 2007, Irish continental margin: Rengstorf et al. 2012, 2013) to predict the distribution of cold-water coral habitats. At the Mingulay Reef, a hydrodynamic model of a scale of 100 x 100 m was used (Moreno-Navas et al. 2014). It is important to note, that this makes the Mingulay Reef Complex having more hydrographic information available compared to most cold-water coral habitats globally. However, the size of the mini-reefs in this area are smaller than the scale of the hydrodynamic data (Chapter 2). Therefore, a more detailed analysis on how the currents shape the mini-reefs and how they affect the distribution of live versus dead coral framework was impossible. At the Tisler Reef (Chapter 3), only the direction of the dominant current speeds could be used with confidence, since the strength of the currents changed depending on the location of the Acoustic Doppler Current Profiler (ADCP). Having three-dimensional modelled data available with the exact locations of downwelling each year, would provide a better insight into the fine-scale differences in the distribution of the live colonies, and would be useful to make more accurate predictions on the future development of the reef. Hydrodynamic data relating to the exact locations that were sampled in our study on the Logachev mounds (Chapter 4) could have provided a better understanding of the difference of the ecology of the different coral species. Many studies have investigated the hydrodynamics in the wider area, (White et al. 2003, Mienis et al. 2007, Wagner et al. 2011, Duineveld et al. 2012, Moreno-Navas et al. 2014, Soetaert et al. 2016) which were useful to understand the observed patterns in density and diversity in our study. However, to confirm our conclusions, fine-scale hydrodynamic data should be processed and integrated into the statistical analyses to explain the spatial differences in the distribution of the non-scleractinian cold-water corals. Numerical models such as MOHID (Modelo Hidodinamico), BOM (The Bergen Ocean Model) (Berntsen 2000) and SPEM (3-D S-coordinate Primitive Equation Model (Mohn and Beckmann 2002) can be used to create such a model, by using and/or integrating bathymetry data,

Conductivity Temperature and Depth (CTD) data, Chlorophyll concentrations, wind stress data, baroclinic and barotropic pressure gradients (e.g. Hannah et al. 2001, White et al. 2005, Moreno-Navas et al. 2014, http://wiki.mohid.com).

Secondly, during data processing of the acoustic data image artefacts can occur, as was shown for the microbathymetry in chapter 2. This increases the number of errors in the data and complicates the application of image and spatial analysis techniques with, for example, geographic information systems (GIS). Therefore, the use of the microbathymetry in chapter 2 was restricted to visual interpretation. This approach is valuable when modelling the presence and absence of coral colonies on the mini-reefs. However, environmental variables such as e.g. aspect, bathymetric positioning index and rugosity derived from this microbathymetry would allow a more detailed and finer scale analyses.

Finally, it is important to highlight that differences in video sampling technique (drop frame or ROV), water visibility (e.g. less/more light, low/high turbidity), ROV speed and height above the seafloor complicate the ability to compare video data within and between reefs. As a consequence, lower level taxonomic identification from video data can be limited. Since no physical samples were used in our studies, it was only possible to study the larger megafauna (>10 cm). Studies using grab, box core and trawl samples (Troffe et al. 2005, Mortensen and Fosså 2006, Mortensen et al. 2008, Henry et al. 2010) allow a finer taxonomic identification of organisms but only cover small surface areas, are destructive, expensive, time-consuming and cannot provide reliable data on the mobile fauna. Therefore, using high definition videos is preferred as a non-destructive tool allowing the assessment of the associated megafaunal diversity over larger surface areas (Schlacher et al. 2010, Buhl-Mortensen et al. 2015, De Clippele et al. 2015).

5.6 Outlook for future research

There is a need for a next generation of studies to integrate information from broad- and fine-scale studies and inter- and intra-specific interactions with a changing environment. These complex interactions between biodiversity, the abiotic environment and ecosystem properties will become easier with the use and development of new techniques.

The importance of fine-scale hydrodynamics has been highlighted throughout this thesis. Developing nested hydrodynamic models with a fine-scale grid around the study site and a broad-scale grid of the wider area is needed as the deep sea epifauna depends on sufficient water flow to provide them with food, oxygen and to disperse their larvae (see section 5.4). Developing these

models will also increase our understanding of the cold-water coral reefs ecosystem functioning, especially in relation to organic carbon cycling. Climate change causes sea-surface temperatures to rise which can reduce water column mixing and intensify the recycling of organic matter in the surface waters of the ocean. If this happens, the export flux of organic carbon would be reduced to the deep sea (Bopp et al. 2001, Sweetman et al. 2017). Developing hydrodynamical models is needed to gain a better understanding on how climate-induced changes in flow and food supply will affect the ecosystem functioning of cold-water coral communities.

In Chapter 2, using a semi-automated toolbox to map and characterise cold-water coral reefs was shown to be a promising time- and cost-effective technique. On the other hand, automated image analyses can be used to calculate the percentage coral cover, health and species composition in both shallow tropical water and cold-water coral reefs (Purser et al. 2009, Stokes and Deane 2009, Beijbom et al. 2012, Shihavuddin et al. 2013, Elawady 2015). ROVs and AUVs are collecting increasing amounts of videos and images from the seabed in the deep sea. However, because analysing these data is time-consuming (e.g. -17 hours to annotate 22 frames with the map method by Purser et al. 2009) only ~ 0.0001% has been subjected to scientific investigation (van den Hove and Moreau 2007). Therefore, developing accurate automated image analyses tools would lead to a faster and broader understanding of deep-sea habitats.

In chapter 3, the sponge *M. lingua* was mainly located on the top exposed parts of the *L. pertusa* coral colonies. We are unsure how this inter-species relationship affects the health of a *L. pertusa* colony. Studies have shown that aside from abiotic controls (e.g. water temperature, nutrient availability, current speed, sedimentation), biotic controls can be important, determining the size of a coral reef. Many tropical coral reef studies have shown the effects of harmful species-species interactions such as competition, predation by corallivory and disease (Aronson and Precht 2001, Cole et al. 2008, Rotjan and Lewis 2008, Lenihan et al. 2011). In cold-water coral reefs, several Asteroidea have been identified to be corallivores (Mah et al. 2010). However, bioeroding species seem to be more common than corallivores in the deep sea. Bioeroders have been identified to be bacteria, fungi (Beuck and Freiwald 2005), foraminifers (Cedhagen 1994, Freiwald and Schönfeld 1996), sabellid worms (Freiwald et al. 1997, Freiwald 1998), sponges (Freiwald and Schönfeld 1996, Boerboom et al. 1998, Freiwald and Wilson 1998), bivalves (Wisshak et al. 2005) and urchins (Stevenson and Rocha 2013). Bioerosion decreases the topographic complexity and cause dead coral skeletons to weaken or collapse due to the chemical and mechanical activities of a diverse range of biotic agents. Dead corals are often exposed to higher rates of bioerosion compared to live coral (Glynn and Manzello 2015). Compared to corralivory the loss of structure by

bioerosion isn't immediate, as bioerosion takes time. Understanding these inter-species interactions and mapping them, could be a useful tool for indicating what the ecological status is of deep-water corals.

5.7 Conclusions

This PhD illustrated that both within and between cold-water coral reefs, a great diversity of the morphological characteristics of cold-water coral mounds is present and that this can affect the distribution of live scleractinian corals, non-scleractinian corals and sponges. Key findings of this thesis were:

1) The successful development and application of the BGS Seabed Mapping toolbox (Chapter 2 ,3, 4).
2) The morphological characterisation and classification of cold-water coral mounds (Chapter 2, 3, 4, 5).
3) Gaining understanding on the impact of the local hydrodynamics on the spatial extent and morphology of corals at the Tisler Reef, and their relation to associated organisms such as sponges (Chapter 3).
4) Gaining understanding on the role, ecology and distribution of non-scleractinian corals in the Logachev area (Chapter 4).

Integrating acoustic, video and oceanographic data allowed a deeper understanding of what drives the development of cold-water coral reefs and the distribution of key reef inhabitants such as sponges and non-scleractinian corals. By studying the morphological characteristics of the cold-water coral mounds at the different reefs and the distribution of live corals within the reefs, the importance of local hydrodynamics, substrate and food supply became clearer. The age of the reef and the local environmental conditions will influence the diversity, abundance, distribution and complexity of the ecosystem. Food supply at both the Logachev Mounds and the Mingulay Reef are influenced by tidal currents and the interaction with the reef structure itself (Kenyon et al. 2003, Davies et al. 2009, Findlay et al. 2013). However, the Mingulay reef is located close to the shore, at a relatively shallow depth and its gross morphology follows that of the underlying bedrock (Roberts et al. 2005, Stewart and Gatliff 2008). The Logachev Mounds are located on Rockall Bank, far away from coastal influences and at much deeper depths (Kenyon et al. 2003, Mienis et al. 2007, 2009, de Haas et al. 2009). The Tisler reef, like the Mingulay reef, is a shallow young reef located close to the shore (Lavaleye et al. 2009). At the Tisler Reef tidal influence is small, with flow direction alternating due to density and wind-driven changes in the broader area (Lavaleye et al. 2009). Even though the environmental conditions in all of the studied locations allow reef

development, a great diversity in the morphology and complexity of the reef has been shown throughout this thesis. This thesis increased the understanding of the broad and fine- scale differences in the environmental conditions, ecology and morphology within and between cold-water coral reefs.

APPENDIX A

The attached CD-ROM contains the following data sets which were used for analyses:

Chapter 2 Mingulay reef:

- GIS: Backscatter, Bathymetry, Microbathymetry, Prediction raster
- Excel: BGS Toolbox data, live coral from microbathymetry, live coral from video data

Chapter 3 Tisler Reef:

- GIS: Bathymetry, Shapefile dive 1-3, Shapefile outline live reef, Shapefile protected area
- Excel: ADCP location data, BGS Toolbox data, Dive 1-3 location data, Percentage cover data, Density data
- ADCP raw data

Chapter 4 Logachev Mounds

- GIS: Bathymetry, Shapefile locations data with coral presence
- Excel: Substrate data, coral data, BGS Toolbox data

APPENDIX B

Gafeira J, Diaz-Doce D, Long D (2015) Semi-automated mapping and characterisation of coral reef mounds: Mingulay Reef proof of concept. British Geological Survey, Marine Geosciences Programme: Internal report IR/15/042

British Geological Survey
NATURAL ENVIRONMENT RESEARCH COUNCIL

Semi-automated Mapping and Characterisation of Coral Reef Mounds: Mingulay Reef Proof of Concept

Marine Geosciences Programme

Internal Report IR/15/042

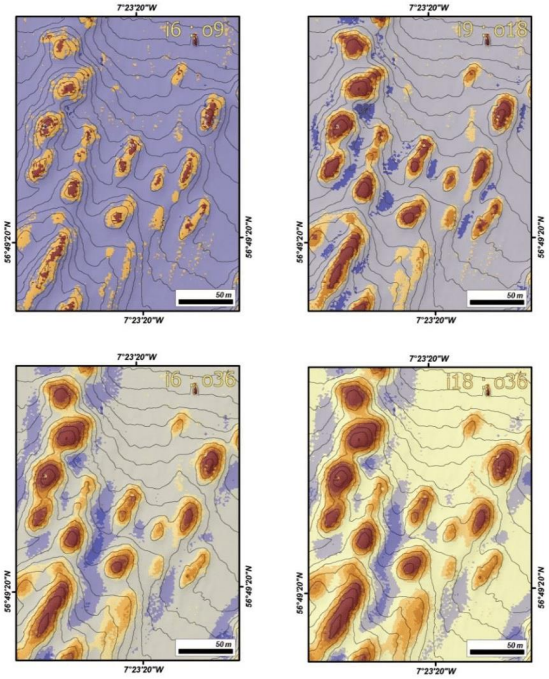

BRITISH GEOLOGICAL SURVEY

MARINE GEOSCIENCES PROGRAMME

INTERNAL REPORT IR/15/042

Semi-automated Mapping and Characterisation of Coral Reef Mounds: Mingulay Reef Proof of Concept

J Gafeira, D Diaz-Doce, D Long

Contributor

L De Clippele

Keywords

Automated mapping, Coral Reef Mounds, Seabed mapping, Mingulay Reef Complex.

Front cover

Four different BPI maps of an area of the Mingulay Reef Complex, created using different analysis neighbourhood.

Bibliographical reference

GAFEIRA, J, DIAZ-DOCE, D, LONG, D. 2015. Semi-automated Mapping and Characterisation of Coral Reef Mounds: Mingulay Reef Proof of Concept. *British Geological Survey Internal Report,* IR/15/042. 21pp.

Edinburgh, British Geological Survey 2015

BRITISH GEOLOGICAL SURVEY

The full range of our publications is available from BGS shops at Nottingham, Edinburgh, London and Cardiff (Welsh publications only) see contact details below or shop online at www.geologyshop.com

The London Information Office also maintains a reference collection of BGS publications, including maps, for consultation.

We publish an annual catalogue of our maps and other publications; this catalogue is available online or from any of the BGS shops.

The British Geological Survey carries out the geological survey of Great Britain and Northern Ireland (the latter as an agency service for the government of Northern Ireland), and of the surrounding continental shelf, as well as basic research projects. It also undertakes programmes of technical aid in geology in developing countries.

The British Geological Survey is a component body of the Natural Environment Research Council.

British Geological Survey offices

BGS Central Enquiries Desk

Tel 0115 936 3143 Fax 0115 936 3276

email enquiries@bgs.ac.uk

Environmental Science Centre, Keyworth, Nottingham NG12 5GG

Tel 0115 936 3241 Fax 0115 936 3488

email sales@bgs.ac.uk

Murchison House, West Mains Road, Edinburgh EH9 3LA

Tel 0131 667 1000 Fax 0131 668 2683

email scotsales@bgs.ac.uk

Natural History Museum, Cromwell Road, London SW7 5BD

Tel 020 7589 4090 Fax 020 7584 8270

Tel 020 7942 5344/45 email bgslondon@bgs.ac.uk

Columbus House, Greenmeadow Springs, Tongwynlais, Cardiff CF15 7NE

Tel 029 2052 1962 Fax 029 2052 1963

Maclean Building, Crowmarsh Gifford, Wallingford OX10 8BB

Tel 01491 838800 Fax 01491 692345

Geological Survey of Northern Ireland, Colby House, Stranmillis Court, Belfast BT9 5BF

Tel 028 9038 8462 Fax 028 9038 8461

www.bgs.ac.uk/gsni/

Parent Body

Natural Environment Research Council, Polaris House, North Star Avenue, Swindon SN2 1EU

Tel 01793 411500 Fax 01793 411501

www.nerc.ac.uk

Website www.bgs.ac.uk

Shop online at www.geologyshop.com

Foreword

Over the last decades, we have been observing an exponential increase of the areas of seabed being surveyed with multibeam echosounder, providing the marine scientific community with vast volumes of data. However, our understanding of the seabed nature and processes will only follow this exponential growth if we are capable of study and distribute the information revealed by this datasets. That can require as much if not more resources than what needed to acquire the data since even the base mapping can be extremely time-consuming. Developing semi-automated mapping methods provide ways to reduce the effort invested to on production of maps. Additionally, interpretation of bathymetric data is implicitly subjective and any analysis of such data is vulnerable to errors by the interpreter, also minimise by the use of semi-automated methods.

After successfully develop a semi-automatic workflow and script to map pockmark (Gafeira *et al.,* 2012), it was decided to attempt to adapt that method or develop similar automated methods for other seabed bathymetric features. This report describes a new mapping approach developed to semi-automatically map coral reef mounds and to extract their attributes from multibeam datasets without interpreter bias.

Acknowledgements

This work has been carried out as part of the BGS Marine Geosciences Programme. We thank Laurence De Clippele and Prof Roberts Murray from the School of Life Sciences at Heriot-Watts University for providing the perspective of an end-user of a tool for semi-automated mapping of cold-water coral reefs.

Contents

FIGURES

Summary

This report describes a new approach to map coral reef mounds. The study area used for this mapping exercise is located approximately 13 km east of the island of Mingulay (56°50′N, 7°30′W) and is known as the Mingulay Reef Complex. The approach adopted consists on the combination of the *Bathymetric Position Index* tool for habitat mapping and the semi-automated mapping method developed initially to map pockmarks at seabed. During this exercise, 354 coral reefs were successfully mapped. The results of this test-of-concept supported the creation of a customised tool for semi-automated mapping of cold-water coral reefs, to derive coral mound attributes from multibeam datasets without interpreter bias.

1 Introduction

Datasets such as sidescan sonar or multibeam echosounder give an indication of size and density of coral mounds at seabed. However, manual mapping of these features can be extremely time-consuming and it is implicitly subjective and any analysis of such data is vulnerable to interpretation errors. As such datasets have been acquired digitally over the last decade this provides an opportunity for the development of automated mapping methods to minimise interpretation errors.

After successfully developing a semi-automatic workflow and script to map pockmark (Gafeira *et al*., 2012), it was decided to attempt to adapt that method or develop similar automated methods for other seabed features. Cold-water coral reefs can develop mound-like structures that can have comparable geometry to pockmarks but as a topographic high rather than a depression. Therefore, it was expected that would be possible to develop an approach to automatically map and describe the cold-water coral reefs. The Mingulay Reef was chosen as test site for this attempt, due to *1)* the high resolution of the dataset available and *2)* the possibility to collaborate with potential end-users.

2 Mingulay Reef Complex

The Mingulay Reef Complex is located in the Sea of the Hebrides, approximately 13 km east of the island of Mingulay (Figure 1). It comprises several cold-water coral reef areas constructed by the azooxanthellate *Lophelia pertusa* that provides 3D habit for many different species.

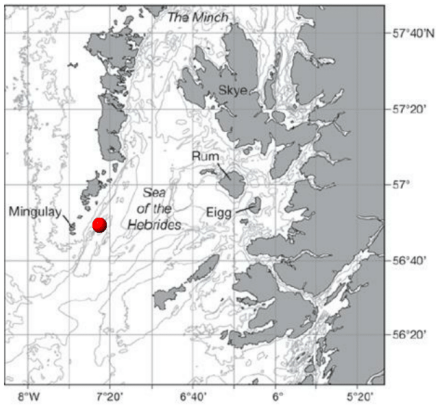

Figure 1 – Location of Mingulay Reef Complex, (adapted from Roberts *et al*., 2009).

The area of the Mingulay Reef Complex includes E-W orientated bedrock ridges that rise to less than 100 m water depth, within an area where water depths locally reach 260 m, causing disruption to the oceanographic currents flowing north-north-eastwards into the Minch (Figure 2). Upon the ridge, prominent mound-like structures are observed predominately in Mingulay Reef 1, Mingulay Reef 5 (North and South) and on the Banana Reef (Davies *et al.*, 2009). Those near-circular features are up to 5 m high and have a general diameter of 15 m (Long and Wilson, 2003).

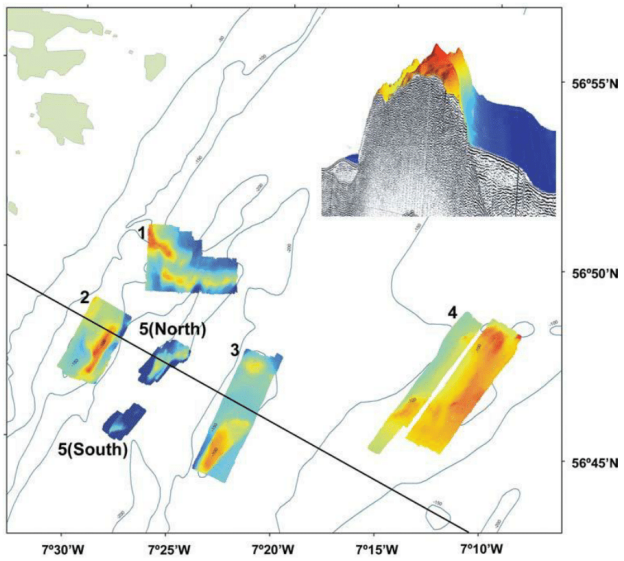

Figure 2 – Map extracted from (Roberts *et al.*, 2005).

Some of these reefs have been dated to over 4,000 years old, however, they are likely to be much older as the samples collected were from surficial sediments. Growth rates reached up to 12 mm a^{-1} which is the highest growth rate so far found in any cold-water coral reef (Douarin *et al.*, 2013). These figures have been derived from more than 50 dates (U/Th and ^{14}C) acquired from the Mingulay Reef, however, Douarin *et al.* (2013) did not find evidence of coral growth from 1.4 ka to modern times despite video and samples revealing live coral on the reef. She identified several collapses in the coral ecosystems during the Holocene (Douarin et al., 2015). Live coral samples seem preferentially distributed on the top and flank of the mounds from Mingulay Reef 1 and Mingulay Reef 5 (North and South).

Figure 3 shows the schematic model of cold-water coral reef build-up presented by Douarin *et al.* (2014). This model explains the systematic sedimentary sequence observed in vibrocores, suggesting cyclic depositional environments that can be subdivided into four major steps: reef initiation, framework expansion, collapse of the framework and coral rubble. Each step characterised by changes in the relative biodiversity, sedimentological regime and changes in erosional processes.

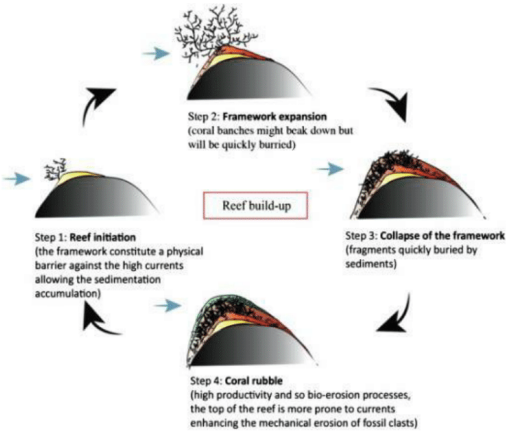

Figure 3 - Schematic model of cold-water coral reef build-up, extract from Douarin *et al.* (2014).

3 Data

In early summer 2003, multibeam surveys were carried out in four areas to the west of Scotland where the coral *Lophelia pertusa* had previously been recorded. The surveys used a 200 kHz Kongsberg EM2000 MBES with approximately 50% overlap between survey lines. East of the island of Mingulay a total of five areas between 2 and 21 km^2 were surveyed (Figure 2). A further survey in 2006, on board of the RV 'Pelagia' equipped with the 30 kHz Kongsberg EM300 MBES, covered some of the reefs and identified previously unknown reefs (Davies *et al.*, 2009). These are the elongate reef named "Banana Reef" and a series of mounds called "Four Mounds".

Additionally, during mid-July 2013, a surface-towed boomer shallow seismic survey (BGS cruise 2013/7) took place in the area, and its main objective was to determine the thickness and extent of the coral layers (Wallis, 2013). It showed that the mounds sit on a relatively smooth rock head (Figure 4).

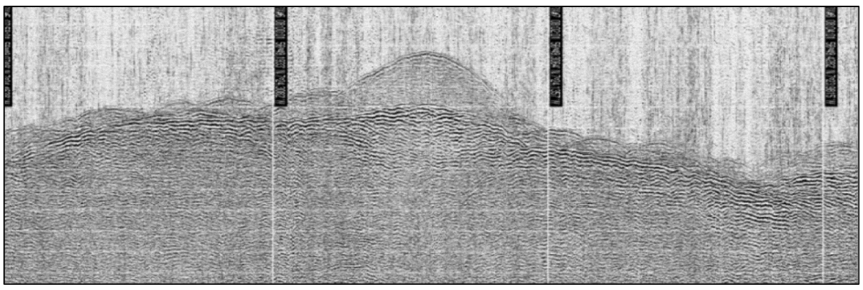

Figure 4 - Boomer line across one of the Mingulay's cold-water coral mound, showing its internal structure and how it sits on top of underlying rock head.

4 Semi-automated mapping

A semi-automated mapping tool was previously developed for mapping and attributing pockmarks from multibeam datasets (Gafeira *et al.*, 2012). This has since been adapted for mapping cold-water corals mounds, often termed 'mini-mounds', found on the Celtic Margin. However, due to the preferential development of cold-water coral mounds in areas of irregular topography, the application of the semi-automated mapping tool directly from the bathymetric data is not possible. Therefore, it was decided to attempt to map this features using a derived dataset, the Bathymetric Position Index (BPI) map.

4.1 BATHYMETRIC POSITION INDEX

The BPI was originally derived from topographic data to characterising watersheds and was called topographic position index (TPI) (Weiss, 2001). It is a measure of where a certain location is relative to its surrounding (*i.e.* compares the water depth of each cell in a DEM to the mean water depth of the neighbourhood cells). Positive BPI values represent locations that are shallower than the average of their surroundings, as defined by the neighbourhood (ridges). Negative BPI values represent locations that are deeper than their surroundings (depressions). BPI values near zero are either flat areas or areas of constant slope (Figure 5).

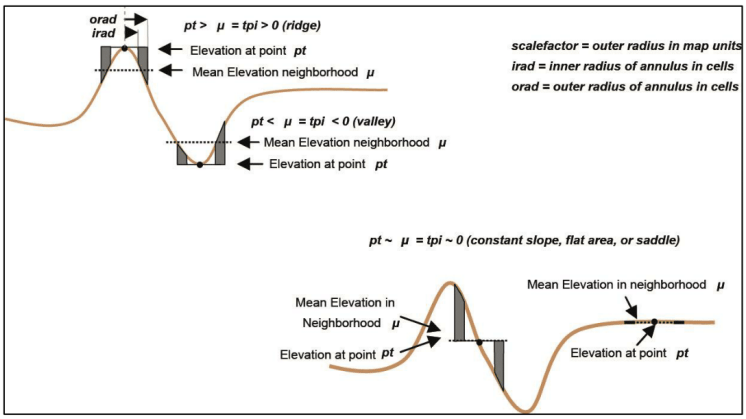

Figure 5 - Topographic Position Index (TPI) illustration taken from Weiss' poster (2001).

To develop and test the new method, a small area of the Mingulay Reef Complex was assessed (Figure 6). The use of a smaller area allows short processing time and faster rate of iterations during the process of writing the scripts.

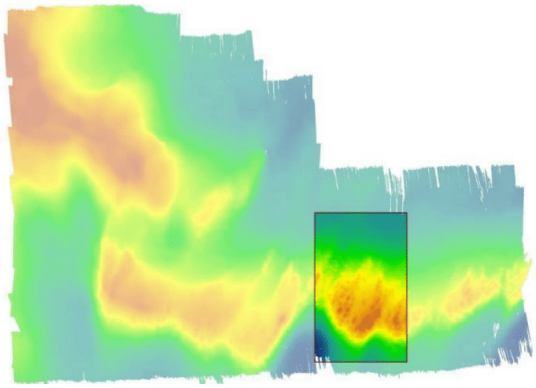

Figure 6 – Location of the clipped area used for this mapping exercise.

By using the BPI values it is possible to delineate the coral mounds, however, the delineation will depend dramatically on how the BPI map was calculated. The BPI is calculated from the bathymetrical digital elevation model (DEM) but if can be calculated at different scales. The BPI algorithm compares each cell's elevation to the mean elevation of the surrounding cells within a user-defined analysis neighbourhood. The analysis neighbourhood can have the shape of a rectangle, an annulus (doughnut shape) or a circle and any size defined by the interpreter. The BPI value for a given cell will depend on of the geometry and size of the analysis neighbourhood used in its calculation. Smaller analysis neighbourhood will allow the detection of smaller, localised variations in the terrain. BPI maps with different analysis neighbourhood were generated using Benthic Terrain Modeller (BTM) and compared (Figure 7 and Figure 8).

The BTM toolbox contains a set of customised scripts that allow users to create, from a multibeam bathymetry input grid, additional grids of slope, bathymetric position index or BPI and seafloor rugosity. It can be downloaded from the ArcGIS website:

http://www.arcgis.com/home/item.html?id=b0d0be66fd33440d97e8c83d220e7926

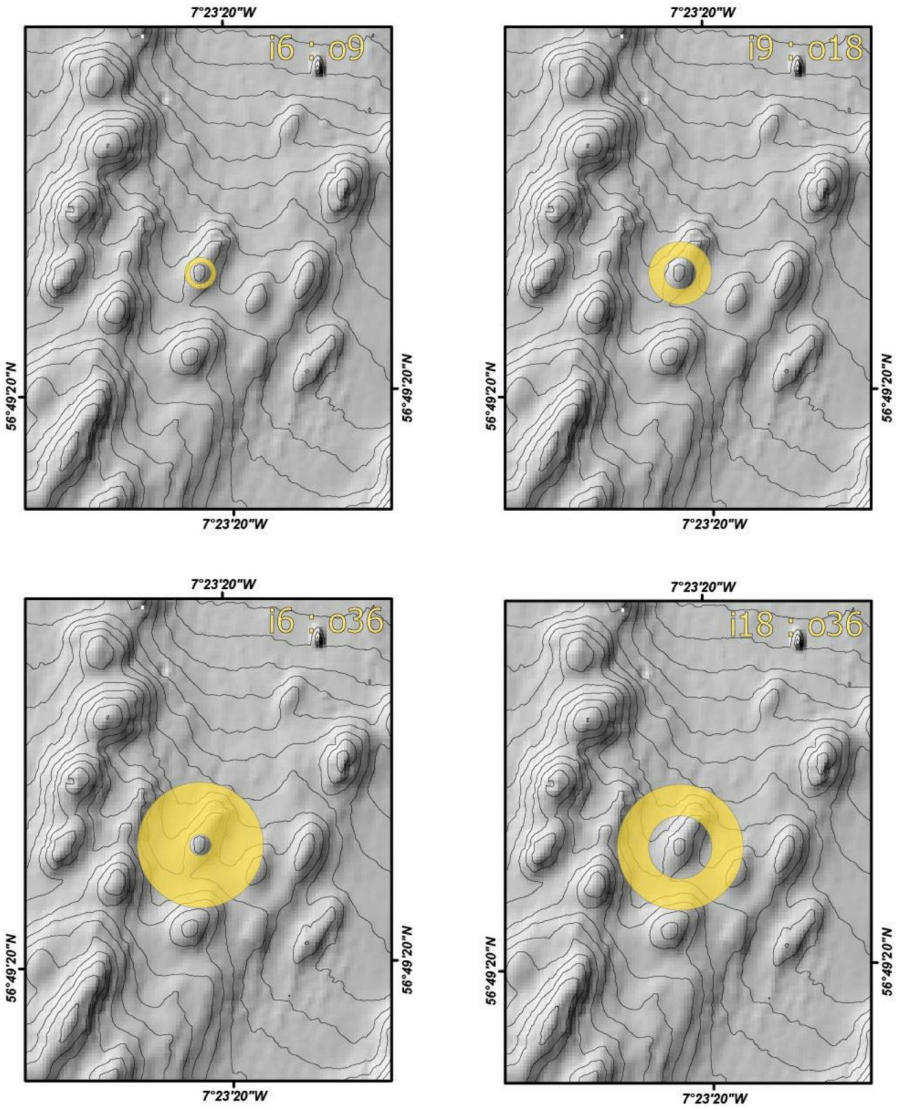

Figure 7 – Illustration of the analysis neighbourhood used to create the four different BPI maps. From with the finest scale map (i6:o9) with an inner radius of 6 cells and outer radius of 9 cells, and the broader scale (i18:o36) with an inner radius of 18 cells and outer radius of 36 cells.

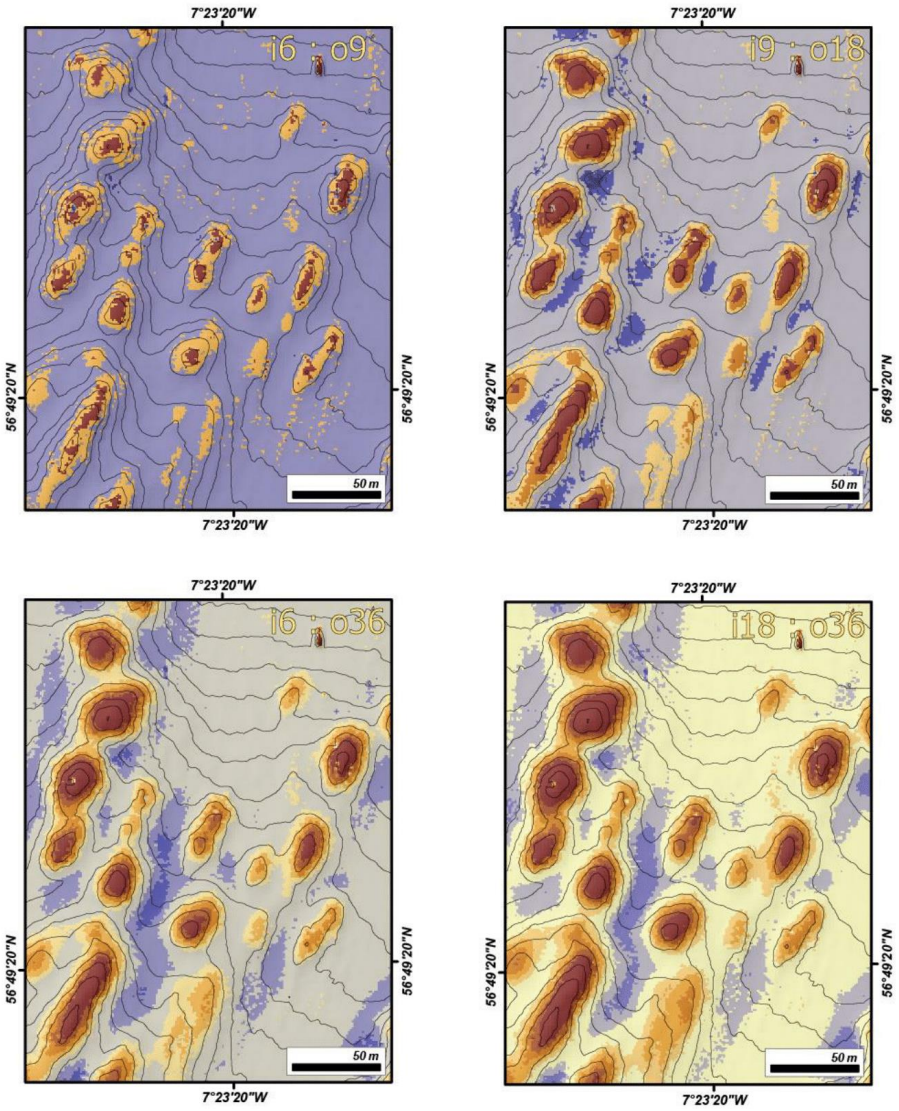

Figure 8 – Clip of the four different BPI maps created using different analysis neighbourhood. From with the finest scale map (i6:o9) with an inner radius of 6 cells and outer radius of 9 cells, and the broader scale (i18:o36) with an inner radius of 18 cells and outer radius of 36 cells. Note that the areas identify as topographic highs (in brown) change depending on the scale used.

Additionally to the visual assessment of the BPI map generated, profiles across some of the mounds assisted the selection of BPI map used as input dataset and also to define the threshold value for the automated method (Figure 9).

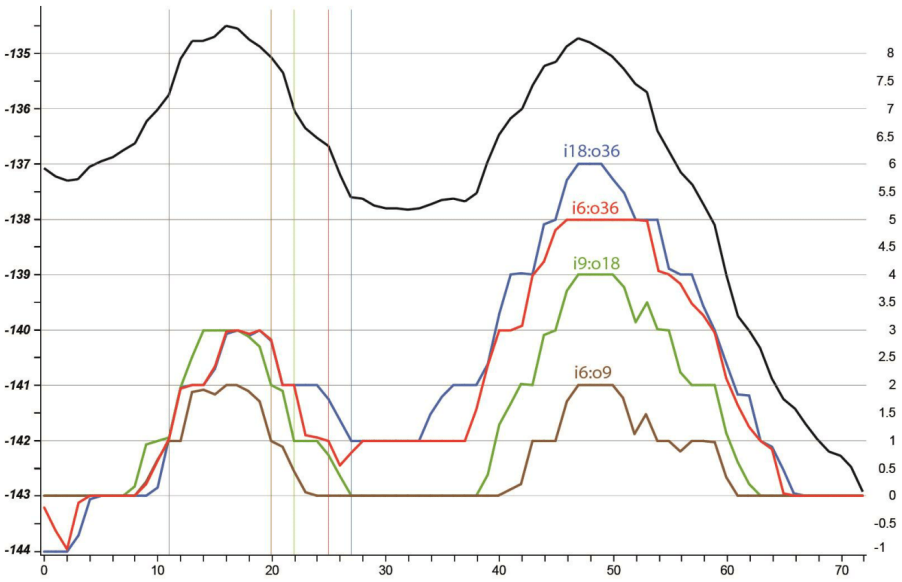

Figure 9 –The bathymetric profile (black) and four corresponding BPI profiles (in brown, green, red and blue).

4.2 BGS CORAL MOUND TOOLS

Two scripts were written in Python during this work: "*BPI Feature Delineation"* and *"Feature Description"*. These were added to an ArcGIS Tool Box named BGS Coral Mound tools.

4.2.1 BPI Feature Delineation

If we consider a coral mound as a confined bathymetric high capable to be identified within a BPI map and invert the BPI map, it is possible to employ hydrological algorithms developed to identify sinks on digital elevation models. Sinks, in this context, are cells with an undefined drainage direction since no cells surrounding it are lower. BPI Feature Delineation script follows a similar logic to the script developed for mapping pockmarks and described by (Gafeira et al., 2012). By creating a script tool dialogue box (Figure 10) any user can run the script as a normal ArcGIS tool and read the description for the individual parameters (Table 1). The output of this script is a polygons shapefile delineating all the mounds respecting the dimensions and BPI values set by the thresholds defined by the used. The table of attributes of the output shapefile will capture varies characteristics of the mapped features (e.g. Area, Perimeter, Maximum BPI value, Minimum Bounding Geometry box's length, …).

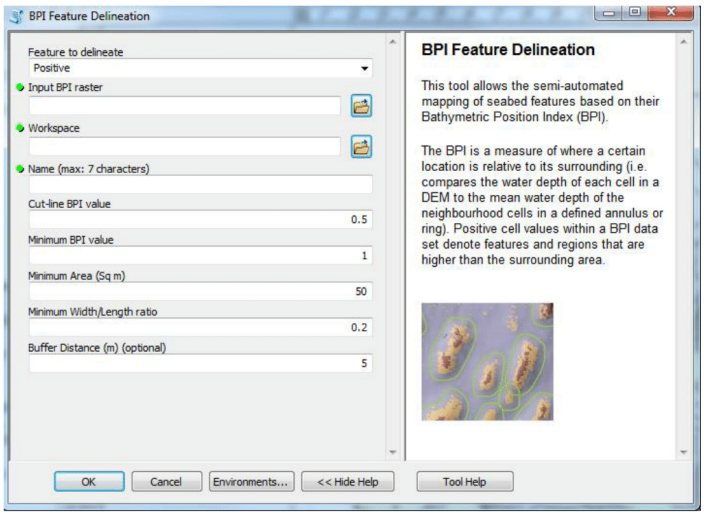

Figure 10 – "*BPI Feature Delineation"* script tool dialogue box.

Table 1- Parameter set for the *"BPI Feature Delineation"* script tool.

Parameter	Explanation	Data Type
Feature to delineate	Pockmarks (negative BPI values) or Mounds (positive BPI values).	String
Input BPI raster	File with the BPI map.	Raster Dataset
Workspace	Folder where the final shapefile and temporary files will be stored.	Workspace
Name	Shapefile name: without extension and should not be longer than 7 characters.	String
Cut-line BPI value	Threshold defined to delineate the features. Only areas with a BPI value higher than the Cut-line BPI value will be mapped.	Double
Minimum BPI value	Features with a maximum BPI value lower than this threshold will be excluded. The *Minimum BPI value* has to be the same or higher than the *Cut-line BPI value.*	Double
Minimum Area (Sq m)	*Minimum Area* threshold excludes features smaller than a given area.	Double
Minimum Width/Length ratio	*Minimum Width/Length Ratio* threshold allows excluding features based on their shape.	Double
Buffer Distance (m) (Optional)	A buffer is applied to the polygons created to compensate for the fact that the delineation process was based on the Minimum BPI threshold. The Buffer Distance should reflect approximately the distance, in plan view, from the initially delineated polygon to the actual rim of the feature.	Double

With the *"BPI Feature Delineation"* script tool and using the finest scale BPI map created (i6:o9) a total of 354 coral reefs were delineated within the study area. Figure 11 illustrate the results of this mapping exercise (polygons in light green) and also compare it to the automated mapping previous obtain by using directly the DEM dataset (purple). The application of the "*Feature Delineation*" tool with DTM dataset tends to underestimate the coral mounds' area.

A certain degree of manual editing would be recommended before proceeding to the extraction of further morphological attributes. However, for the aim of this exercise (test-of-concept) the second script "*Feature Description*" was run using the initially generated shapefile.

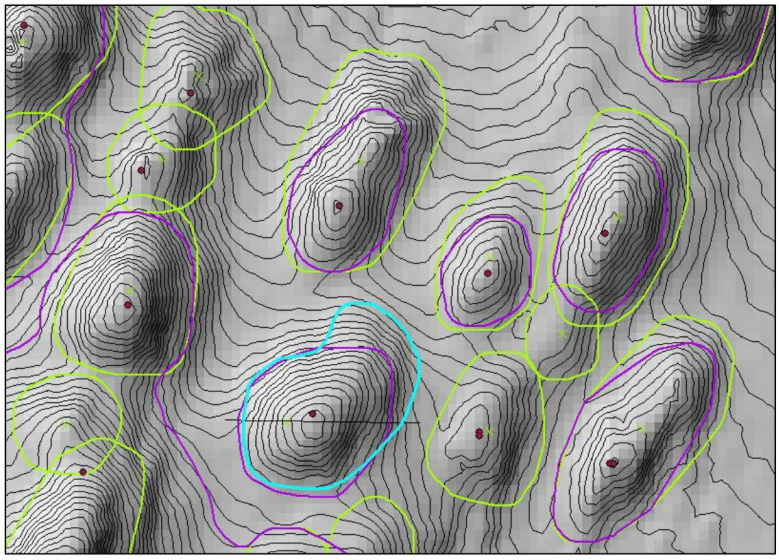

Figure 11 – Detail view of the differences between the mapping based on the BPI map (green) and the mapping based directly on the DEM (purple). Note that some degree of manual editing may be required (polygon highlighted in bright blue).

4.2.2 Feature Description

After manually editing the outline of some of the polygons generated by the first script, the geometry of some polygons may have changed but the attribute table will still be the same. Therefore, the information on it could be partially incorrect. The *"Feature Description*" script recalculates the attribute values for each feature and adds new attribute fields with additional information. After various conversations with members of the Coral Ecosystems Lab at Heriot-Watt University, it was decided to incorporate information from different datasets, when available. At this point, the "*Feature Description"* script tool (Figure 12) allows the extract information from the original DEM and from the BPI, Backscatter and Rugosity Map (Table 2). Plus, this tool can also calculate the original seabed slope before the development of the coral mound.

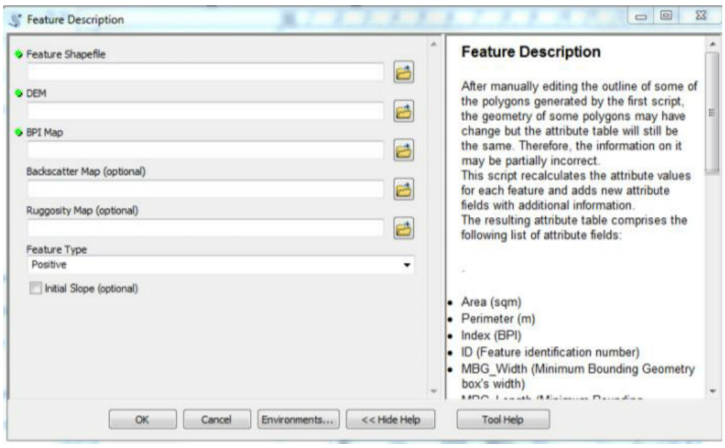

Figure 12 - "*Feature Description"* script tool dialogue box.

Table 2 - Parameter set for the *"Feature Description"* script tool.

Parameter	Explanation	Data Type
Feature Shapefile	Shapefile delineating the features	Shapefile
DEM	DEM from where the water depth will be extracted.	Raster Dataset
BPI Map	BPI Map previously used to delineate the features mapped.	Raster Dataset
Backscatter Map (Optional)	Backscatter data from where the backscatter values will be extracted.	Raster Dataset
Rugosity Map (Optional)	Rugosity maps from where the rugosity values will be extracted.	Raster Dataset
Feature Type	Positive features: features with a positive vertical relief, like mounds. Negative features: features with a negative vertical relief, like pockmarks.	String
Initial Slope (Optional)	The initial slope will be calculated by erasing the bathymetric data of the features mapped and recreating an initial surface.	Boolean

In addition to the polygon shapefile that delineates the mapped coral mounds, two other shapefiles are generated: *1)* a point shapefile that shows the centroid of the referred polygons ('shapefile'_C), and *2)* a point shapefile that marks the shallower point within each mound ('shapefile'_M). The table of attributes of both point shapefiles also includes the X and Y fields with the location of each point.

All of the shapefiles are completed with the full attribute table that comprises the following list of attribute fields:

Area (sq m)
Perimeter (m)
Index (BPI)
ID (Feature identification number)
MBG_Width (Minimum Bounding Geometry box's width)
MBG_Length (Minimum Bounding Geometry box's length)
MBG_Orient (Minimum Bounding Geometry box's orientation)
MBG_W_L (MBG_Width / MBG_Lenght)
MinWD (Minimum Water Depth)
MaxWD (Maximum Water Depth)
MeanWD (Mean Water Depth)
MaxVRelief (Maximum Vertical Relief)
MinVRelief (Minimum Vertical Relief)
ConfCL_WD (Water Depth of 1st Confined Contour Line)
MaxSlope (Maximum Slope)
MeanSlope (Mean Slope)
Min_Rug (Minimum Rugosity Value)
Max_Rug (Maximum Rugosity Value)
Mean_Rug (Mean Rugosity Value)
Min_BS (Minimum Backscatter Value)
Max_BS (Maximum Backscatter Value)
Mean_BS (Mean Backscatter Value)
InitialSlp (Mean Slope of the assumed initial seabed surface)

5 Conclusions

This work demonstrates that there is significant potential to support expert data analysis through the application of a range of automated steps, which accelerate mapping and feature characterization process as well as bring more rigour and consistency to the process.

The mapping based on the BPI values is better adjusted to the morphology of cold-water coral mounds whereas the direct application of the "*Feature Delineation*" tool, that use DTM as input data, tends to underestimate the coral mounds area.

The collaboration with potential external end-users during this work led to the expansion of the type of attributes extract automatically (Figure 13).

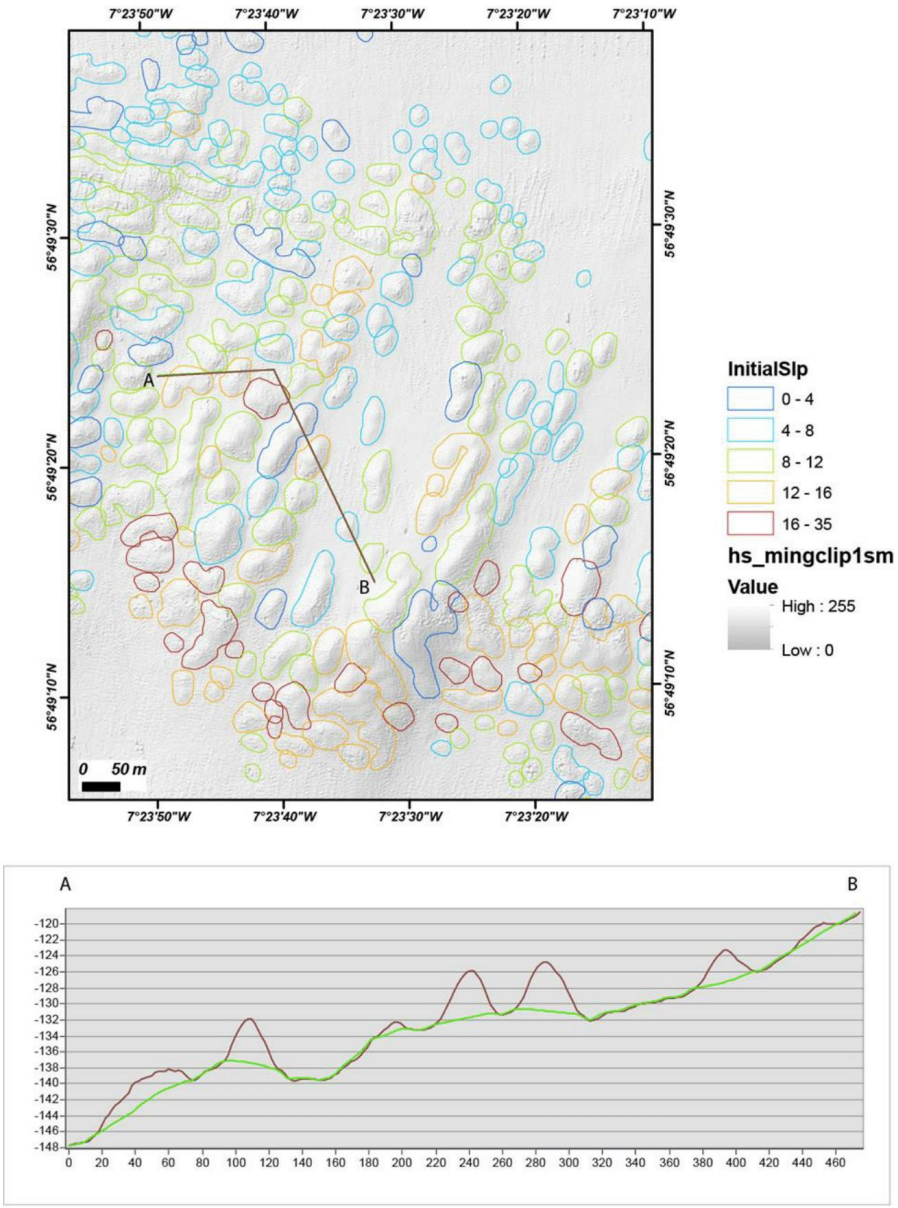

Figure 13 –*Top:* Map showing the coral mounds mapped within the study area, classified according to the steepness of the calculated original seabed. *Bottom*: Profile showing the present day bathymetry (in brown) and the assumed seabed morphology previous to the development of the cold-water coral mounds.

References

British Geological Survey holds most of the references listed below, and copies may be obtained via the library service subject to copyright legislation (contact libuser@bgs.ac.uk for details). The library catalogue is available at: http://geolib.bgs.ac.uk.

Davies, A.J., Green, S.L., Long, D., Roberts, J.M., 2009. SNH Commissioned Report 306: Developing the necessary data layers to inform the development of a site boundary for the East Mingulay dSAC - Phase II. Edinburgh.

Douarin, M., Elliot, M., Noble, S.R., Sinclair, D., Henry, L.A., Long, D., Moreton, S.G., Murray Roberts, J., 2013. Growth of north-east Atlantic cold-water coral reefs and mounds during the Holocene: A high resolution U-series and 14C chronology. Earth Planet. Sci. Lett. 375, 176–187. doi:10.1016/j.epsl.2013.05.023

Douarin, M., Sinclair, D.J., Elliot, M., Henry, L.A., Long, D., Mitchison, F., Roberts, J.M., 2014. Changes in fossil assemblage in sediment cores from Mingulay Reef Complex (NE Atlantic): Implications for coral reef build-up. Deep. Res. Part II Top. Stud. Oceanogr. 99, 286–296. doi:10.1016/j.dsr2.2013.07.022

Gafeira, J., Long, D., Diaz-Doce, D., 2012. Semi-automated characterisation of seabed pockmarks in the central North Sea. Near Surf. Geophys. 10, 303–314. doi:10.3997/1873-0604.2012018

Long, D., Wilson, C.K., 2003. Geological background to coldwater coral occurrences in the Minch. Edinburgh.

Roberts, J.M., Brown, C.J., Long, D., Bates, C.R., 2005. Acoustic mapping using a multibeam echosounder reveals cold-water coral reefs and surrounding habitats. Coral Reefs 24, 654–669. doi:10.1007/s00338-005-0049-6

Roberts, J.M., Davies, A.J., Henry, L.A., Dodds, L.A., Duineveld, G.C.A., Lavaleye, M.S.S., Maier, C., Soest, R.W.M. Van, Bergman, M.J.N., Hühnerbach, V., Huvenne, V.A.I., Sinclair, D.J., Watmough, T., Long, D., Green, S.L., Haren, H. Van, 2009. Mingulay reef complex : an interdisciplinary study of cold-water coral habitat , hydrography and biodiversity. Mar. Ecol. Prog. Ser. 397, 139–151. doi:10.3354/meps08112

Wallis, D., 2013. Surface Tow Boomer over Mingulay Reef - BGS Internal Report OR/13/033. Edinburgh.

Weiss, A., 2001. Topographic position and landforms analysis (Poster presentation), in: ESRI User Conference, San Diego, CA, July 9-13. pp. 227 – 245.

REFERENCES

Aerts LAM and van Soest RWM (1997) Quantification of sponge/coral interactions in a physically stressed reef community, NE Colombia. Marine Ecology Progress Series 148: 125-134

Aitchison J (1986) The statistical analyses of compositional data. Chapman and Hall, London

Althaus F, Williams A, Schlacher TA, Kloser RJ, Green MA, Barker BA, Bax NJ, Brodie P, Schlacher-Hoenlinger MA (2009) Impacts of bottom trawling on deep-coral ecosystems of seamounts are long-lasting. Marine Ecology Progress Series 397: 279-294

Andrews AH, Cordes EE, Mahoney MM, Munk K, Coale KH, Cailliet GM and Heifets J (2001) Age and growth of a deep-sea, habitat-forming octocorallian (*Primnoa* sp.) from the Gulf of Alaska, with radiometric age validation. NPMR meeting, UAF, October 2001, extended abstract pp 101-110

Andrews AH, Stone RP, Lundstorm CC, DeVogelaere AP (2009) Growth rate and age determination of bamboo corals from the norteastern Pacific Ocean using refined 210Pb dating. Marine ecology Progress Series 397: 173-185

Aronson RB and Precht WF (2001) White-band disease and the changing face of Caribbean coral reefs. Hydrobiologia 460: 25-38

Artioli Y, Blackford JC, Butenschön M, Holt JT, Wakelin SL, Thomas H, Borges AV, Allen JI (2012) The carbonate system in the North Sea: Sensitivity and model validation. Journal of Marine Systems 102: 1-13

Baillon S, Hamel J-F, Wareham VE and Mercier A (2012) Deep cold-water corals as nurseries for fish larvae. Frontiers in Ecology and the Environment 10(7): 351-356

Barnes DJ (1973) Growth in colonial scleractinians. Bulletin of Marine Science 23: 280-298

Barsby T and Kubanek J (2005) Isolation and structure elucidation of feeding deterrent diterpenoids from the sea pansy, *Renilla reniformis*. Journal of Natural Products 68: 511-516

Bayer FM (1981) Key to the genera of Octocorallia exclusive of Pennatulacea (Coelenterata: Anthozoa), with diagnosis of new taxa. Proceedings of the Biological Society of Washington 94: 902-947

Beijbom O, Edmunds PJ, Kline DI, Mitchell BG, Kriegman D (2012) Automated Annotation of Coral Reef Survey Images. Computer Vision and Pattern Recognition (CVPR), IEEE Conference pp 1170-1177

Bell JJ (2008) Connectivity between island Marine Protected Areas and the mainland. Biological Conservation 141: 2807-2820

Bell JJ and Barnes DKA (2001) Sponge morphological diversity: a qualitative predictor of species diversity? Aquatic Conservation: Marine and Freshwater Ecosystems 11: 109-121

Bell N and Smith J (1999) Coral growing on North Sea oil rigs. Nature 402: 601

Bellwood DR and Hughes TP (2001) Regional-scale assembly rules and biodiversity of coral reefs. Science 292: 1532-1535

Berger WH (2016) "Calcite Compensation Depth (CCD)" In Harff J, Martin M, Petersen S, Thiede J. Encyclopedia of Marine Geosciences. Encyclopedia of Earth Sciences Series. Springer Netherlands pp 71-73 ISBN 978-94-007-6238-1

Berntsen J (2000) USERS GUIDE for a Modesplit σ-Coordinate Numerical Ocean Model. Technical Report, vol. 135. Department of Applied Mathematics, University of Bergen, Johannes Bruns gate 12, N-5008 Bergen, Norway pp 48

Best BA (1988) Passive suspension feeding in a sea pen: effects of ambient flow on volume flow rate and filtering efficiency. Biology Bulletin 175: 332-342

Beuck L and Freiwald A (2005) Bioerosion patterns in a deep-water *Lophelia pertusa* (Scleractinia) thicket (propeller Mound, northern Porcupine Seabight) Cold-water corals and ecosystems pp 915-936

Birkeland C (1997) Life and death of coral reefs. New York: Chapman and Hall.

Bo M, Bavestrello G, Canese S, Giusti M, Salvati E, Angiolillo M, Greco S (2009) Characteristics of a black coral meadow in the twilight zone of the central Mediterranean Sea. Marine Ecology Progress Series 397: 53-61

Bo M, Lavorato A, Di Camillo CG, Poliseno A, Baquero A, Bavestrello G, Irei Y and Davis J (2012) Black coral assemblages from Machalilla National Park (Ecuador). Pacific Science 66(1): 63-81

Boerdoom CM, Smith JE and Risk MJ (1998) Bioerosion and micritization in the deep-sea coral *Desmophyllum cristagalli*. An international Journal of Paleabiology 13(1): 53-60

Bopp L, Aumont O, Cadule P, Alvain S and Gehlen M (2005) Response of diatoms distribution to global warming and potential implications: A global model study. Geophysical Research Lett 32: L19606

Bopp L, Monfray P, Aumont O, Dufresne J-L, Le Treut H, Madec G, Terray L and Orr JC (2001) Potential impact of climate change on marine export production. Global Biogeochemical Cycles 15: 81-89

Bosence D (1979) The factors leading to aggregation and reef formation in *Serpula vermicularis*. In Biology and systematics of colonial Organisms, ed. G. Larwood and B. Rosen. London and New York: Academic Press pp 299-318

Braga-Henriques A, Carreiro-Silva M, Tempera F, Porteiro FM, Jakobsen K, Jakobsen J, Albuquerque M and Serrão Santos R (2012) Carrying behavior in the deep-sea crab *Paromola cuvieri* (Northeast Atlantic). Marine Biodiversity 42(1): 37-46

Breiman L (2001) Random forests. Machine Learning 45: 5-32

Brooke SD, Holmes MW and Young CM (2009) Sediment tolerance of two different morphotypes of the deep-sea coral *Lophelia pertusa* from the Gulf of Mexico. Marine Ecology Progress Series 390: 137-144

Bruckner AW (2001) Tracking the trade in ornamental coral reef organisms: the importance of CITES and its limitations. Aquarium Sciences and Conservation 3(1): 79-94

Bryan TL and Metaxas A (2007) Predicting suitable habitat for deep-water gorgonian corals on the Atlantic and Pacific continental margins of North America. Marine Ecology Progress Series 330: 113126

Bryan TL and Metaxas A (2006) Distribution of deep-water corals along the North American continental margins: relationships with environmental factors. Deep-Sea Research I 53: 1865-1879

Buhl-Mortensen L, Bøe R, Dolan MFJ, Buhl-Mortensen P, Thorsnes T, Elvenes S, Hodnesdal H (2012) Chapter 51: Banks, throughs and canyons on the continental margin off Lofoten, Vesterålen, and Troms, Norway. In Harris PT and Baker EK (2012) Seafloor Geomorphology as Benthic Habitat: GeoHab Atlas of seafloor geomorphic features and benthic habitats. Elsevier

Buhl-Mortensen L and Mortensen PB (2004) Crustaceans associated with the deep-water gorgonian corals *Paragorgia arborea* (L., 1758) and *Primnoa resedaeformis* (Gunn., 1763). Journal of Natural History 38(10): 1233-1247

Buhl-Mortensen L and Mortensen PB (2005) Distribution and diversity of species associated with deep-sea gorgonian corals off Atlantic Canada, Cold-water Corals and Ecosystems. Springer-Verlag, Berlin Heidelberg pp. 849-879

Buhl-Mortensen L, Buhl-Mortensen P, Dolan MJF, Gonzalez-Mirelis G (2015) Habitat mapping as a tool for conservation and sustainable use of marine resources: Some perspectives from the MAREANO Programme, Norway. Journal of Sea Research 100: 46-61

Buhl-Mortensen L, Vanreusel A, Gooday AJ, Levin LA, Preide IG, Buhl-Mortensen P, Gheerardyn H, King NJ and Raes M (2010) Biological structures as a source of habitat heterogeneity and biodiversity on the deep ocean margins. Marine Ecology- an Evolutionary Perspective 31(1): 21-50

Buhl-Mortensen P, Buhl Mortensen L, Purser A (2017) Trophic Ecology and habitat provision in cold-water coral ecosystems. Marine Animal Forests ISBN 978-3-319-21011-7

Butman CA and Carlton JT eds. (1995) Understanding marine biodiversity: A research agenda for the nation. Washington DC: National Academy Press.

Byrne RH, Mecking S, Feely RA, Liu X (2010) Direct observations of basin-wide acidification of the North Pacific Ocean. Geophysical Research Letters 37: L02601

Cairns SD (2007) Deep Water Corals: An overview with special reference to diversity and distribution of deep water scleractinian corals. Bulletin of Marine Science 81: 311-322

Caldeira K and Wickett ME (2003) Anthropogenic carbon and ocean pH. Nature 425: 365

Capezzuto F, Maiorano P, Indennidate A and Sion L (2012) Occurrence and behaviour of *Paromola cuvieri* (Crustacea, Decapoda) in the Santa Maria di Leuca cold-water coral community (Mediterranean Sea). Deep-Sea Research I 59:1-7

CBD Secretariat (2012) COP 11 Decision XI/17. Marine and coastal biodiversity: ecologically or biologically significant marine areas.

Cedhagen T (1994) Taxonomy and biology of *Hyrrokkin sarcophaga* gen. et sp. n., a parasitic foraminiferan (Rosalinidae). Sarsia 79: 65-82

Chamberlain JA and Graus RR (1975) Water-flow and hydromechanical adaptations of branched reef corals. Bulletin of Marine Science 25(1): 112-125

Chindapol N, Kaandorp JA, Cronemberger C, Mass T, Genin A (2013) Modelling growth and form of the Scleractinian coral *Pocillopora verrucosa* and the influence of hydrodynamics. Plos Computational Biology 9(1): e1002849

Clark MR, Althaus F, Schlacher TA, Williams A, Bowden DA, Rowden AA (2016) The impacts of deep-sea fisheries on benthic communities: A review. ICES Journal Marine Science 73: i51-i69

Clarke KR and Warwick RM (2001) Change in marine communities: an approach to statistical analysis and interpretation, 2nd edn. National Environment Research Council, Cambridge, UK

Clode PL, Lenna K, Saunders M, Weiner S (2010) Skeletal mineralogy of newly settling *Acropora millepora* (Scleractinia) coral recruits. Coral Reefs 30:1-8

Cnaan A, Laird NM, Slasor P (1997) Tutorial in biostatistics: using the general linear mixed model to analyse unbalanced repeated measures and longitudinal data. Statistics in Medicine 16(2349): 80.

Cole AJ, Pratchett MS and Jones GP (2008) Diversity and functional importance of coral-feeding fishes on tropical coral reefs. Fish and Fisheries 9: 286-307

Colin C, Frank N, Copard K, Douville E (2010) Neodymium isotopic composition of deep sea corals from the NE Atlantic: implications for past hydrological changes during the Holocene. Quaternary Science Review 29: 2509-2517

Coll JC, La Barre S, Sammarco PW, Williams WT, Bakus GJ (1982) Chemical defences of soft corals (Coelenterata: Octocorallia) of the great barrier reef: a study of comparative toxicities. Marine Ecology Progress Series 8: 271-278

Convention on Biological Diversity Secretariat (2014) An Updated Synthesis of the Impacts of Ocean Acidification on Marine Biodiversity (Eds: S. Hennige, JM Roberts and P Williamson). Montreal, Technical Series No. 75: 99

Corbera Pascual G (2015) The role of gorgonians as engineering species, in the structure and diversity of benthic communities, Ms Thesis, Faculty of natural and environmental sciences, oceans and earth sciences, University of Southampton

Cordes EE, Jones DO, Schlacher TA, Amon DJ, Bernardino AF, Brooke S, Carney R, DeLeo DM, Dunlop KM, Escobar-Briones EG, Gates AR (2016) Environmental impacts of the deep-water oil and gas industry: a review to guide management strategies. Frontiers in Environmental Science

Cordes EE, McGinley MP, Podowski EL, Becker EL, Lessard- Pilon S, Viada ST, Fisher CR (2008) Coral communities of the deep Gulf of Mexico. Deep-Sea Res I 55: 777-787

Costello MJ, McCrea M, Freiwald A, Lundälv T, Jonsson L, Bett BJ, Weering TCE, Haas H, Roberts JM, Allen D (2005) Role of cold-water *Lophelia pertusa* coral reefs as fish habitat in the NE Atlantic. In: Freiwald A, Roberts JM (eds) Cold-water corals and ecosystems. Springer, Berlin Heidelberg pp 771–805

Cowen RK and Sponaugle S (2009) Larval dispersal and marine population connectivity. Annual Review of Marine Science 1: 443-466

Craig RE (1959) Hydrography of Scottish coastal waters. Marine Research 1958(2): 33

Cutler DR, Edwards TC, Beard KH, Cutler A, Hess KT (2007) Random forests for classification in ecology. Ecology 88: 783-2792

Cyr F, Van Haren H, Mienis F, Duineveld G. and Bourgault D (2016) On the influence of cold-water coral mound size on flow hydrodynamics, and vice versa. Geophysical Research Letters 43

Dahlgren T, Wiklund H, Kallstrom B, Lundalv T, Smith C and Glover A (2006) A shallow-water whale-fall experiment in the North Atlantic. Cahiers De Biologie Marine 47: 385-389

Dai CF and Lin MC (1993) The effects of flow on feeding of three gorgonians from southern Taiwan. Journal of Experimental Marine Biology 173: 57-69

Davies AJ and Guinotte JM (2011) Global habitat suitability for framework-forming cold-water corals. PLoS One 6(4): e18483

Davies AJ, Duineveld GC, Lavaleye MSS, Bergman MJN, Van Haren H, Roberts JM (2009) Downwelling and deep-water bottom currents as food supply mechanisms to the cold-water coral *Lophelia pertusa* (Scleractinia) at the Mingulay Reef complex. Limnology and Oceanography 54: 620-629

Davies AJ, Roberts JM, Hall-Spencer J (2007) Preserving deep-sea natural heritage: emerging issues in offshore conservation and management. Biological Conservation 138(3): 299-312

Davies AJ, Wisshak M, Orr JC, Roberts JM (2008) Predicting suitable habitat for the cold-water coral *Lophelia pertusa* (Scleractinia). Deep Sea Research Part 1: Oceanography Research Papers 55: 1048-1062

De Clippele LH, Buhl-Mortensen P and Buhl-Mortensen L (2015) Fauna associated with cold water gorgonians and sea pens. Continental Shelf Research 105: 67-78

de Haas H, Mienis F, Frank N, Richter TO, Steinacher R, de Stigter H, van der land C, van Weering TCE (2009) Morphology and sedimentology of (clustered) cold-water coral mounds at the south Rockall Trough margins, NE Atlantic Ocean. Facies 55(1): 1-26

De Mol B, Amblas D, Alvarez G, Busquets P, Calafat A, Canals M, Duran R, Lavoie C, Acosta J, Muñoz A, Party HS (2012a) Chapter 45: Cold-water coral distribution in an erosional environment: the Strait of Gibraltar gateway. In Harris PT and Baker EK (2012) Seafloor Geomorphology as Benthic Habitat: GeoHab Atlas of seafloor geomorphic features and benthic habitats. Elsevier

De Mol L, Hilario A, van Rooij D, Henriet J-P (2012b) Chapter 46: Habitat mapping of a cold-water coral mound on Pen Duick Escarpment (Gulf of Cadiz). In Harris PT and Baker EK (2012) Seafloor Geomorphology as Benthic Habitat: GeoHab Atlas of seafloor geomorphic features and benthic habitats. Elsevier

De'ath G, Fabricius KE, Sweatman H, Puotinen M (2012) The 27-year decline of coral cover on the Great Barrier Reef and its causes. Proceedings of the National Academy of Science of the USA 109: 17995-17999

Diaz RJ and Rosenberg R (1995) Marine benthic hypoxia; a review of its ecological effects and the behavioural responses of benthic macrofaunal. Oceanography and Marine Biology. An annual review 33: 245-03

Dobson AJ, Barnett AG (2008) Introduction to Generalized Linear Models (3rd ed.). Boca Raton, FL: Chapman and Hall/CRC. ISBN 1-58488-165-8

Dodds LA, Black KD, Orr H, Roberts JM (2009) Lipid biomarkers reveal geographical differences in food supply to the cold-water coral Lophelia pertusa (Scleractinia). Marine Ecology Progress Series 397: 113-114

Dodds LA, Roberts JM, Taylor AC and Marubini F (2007) The cold-water coral *Lophelia pertusa* (Scleractinia) reveals metabolic tolerance to temperature and dissolved oxygen change. Journal of Experimental Marine Biology and Ecology 349: 205-214

Dolan MFJ, Grehan AJ, Guinan JC, Brown C (2008) Modelling the local distribution of cold-water corals in relation to bathymetric variables: adding spatial context to deep-sea video data. Deep-sea Research part I- Oceanic Research Papers 55(11): 1564-1579

Dorschel B, Hebbeln D, Foubert A, White M and Wheeler AJ (2007) Hydrodynamics and cold-water coral facies distribution related to recent sedimentary processes at Galway Mound west of Ireland. Marine Geology 244(1-4): 184-195

Douarin M, Elliot M, Noble SR, Sinclair D, Henry L-A, Long D, Moreton SG and Roberts JM (2013) Growth of north-east Atlantic cold-water coral reefs and mounds during the Holocene: A high resolution U-series and C-14 chronology. Earth and Planetary Science Letters 375: 176-187

Douarin M, Sinclair DJ, Elliot M, Henry L-A, Long D, Mitchison F and Roberts JM (2014) Changes in fossil assemblage in sediment cores from Mingulay Reef Complex (NE Atlantic): Implications for coral reef build-up. Deep-Sea Research Part II: Topical Studies in Oceanography 99: 286-296

Duineveld CGA, Lavaleye MSS and Berghuis EM (2004) Particle flux and food supply to a seamount cold-water coral community (Galicia Bank, NW Spain). Marine Ecology Progress Series pp 13-23

Duineveld GC, Jeffreys RM, Lavaleye MSS, Davies AJ, Bergman MJN, Watmough T, Witbaard R (2012) Spatial and tidal variation in food supply to shallow CWC reefs of the Mingulay Reef complex (Outer Hebrides, Scotland). Marine Ecology Progress Series 444: 97-115

Duineveld GC, Lavaleye MSS, Bergman MJN, Stigter H De, Mienis F, de Stigter H, Mienis F, Stigter H De, Mienis F, Duineveld, Lavaleye MSS, Bergman MJN, de Stigter H, Mienis F (2007) Trophic Structure of a Cold-Water Coral Mound Community (Rockall Bank, NE Atlantic) in Relation to the Near-Bottom Particle Supply and Current Regime. Bulletin of Marine Science 81: 449-467

Duran Munoz P and Sayago-Gil M (2011) An overview of cold-water coral protection on the high seas: The Hatton bank (NE Atlantic)-A case study. Marine Policy 35(5): 615-622

EC (1996) Interpretation manual of European Union habitats. In: Council Directive on the Conservation of Natural Habitats and of Wild Fauna and Flora, Version EUR 15, European

Commission Directorate General XI Environment, Nuclear Safety and Civil Protection, Nature Protection, Coastal Zones and Tourism, Brussels.

Elawady M (2015) Sparse Coral Classification Using Deep Convolutional Neural Networks. Ms thesis, Heriot-Watt University, UK

Elith J, Graham CH, Anderson RP, Dudik M, Ferrier S, Guisan A, Hijmans RJ, Huettmann F, Leathwick JR, Lehmann A, Li J, Lohmann LG, Loiselle BA, Manion G, Moritz C, Nakamura M, Nakazawa Y, McC. Overton J, Peterson AT, Phillips SJ, Richardson K, Scachetti-Pereira R, Schapire RE, Sobéron J, Williams S, Wisz MS, Zimmermann NE (2006) Novel methods improve prediction of species' distributions from occurrence data. Ecography 29: 129-151

Ellett DJ (1979) Some oceanographic features of Hebridean waters. Proc R Soc Edin 77B: 61-74

Ellett DJ and Edwards A (1983) Oceanography and inshore hydrography of the Inner Hebrides. Proc R Soc Edin 83B:143–160

Etiope G, Savini A, Lo Bue N, Favali P and Corselli C (2010) Deep-sea survey for the detection of methane at the "Santa Maria di Leuca" cold-water coral mounds (Ionian Sea, South Italy). Deep- Sea Research Part II: Tropical Studies in Oceanography 57(5-6): 431-440

Etnoyer P and Morgan LE (2003) Occurrences of habitat-forming, deep-sea corals in the Northeast Pacific. Final Report NOAA Off Protected Resources

Fabricius KE, Genin A and Benayahu Y (1995) Flow-dependent herbivory and growth in zooxanthellae-free soft corals. Limnology and Oceanography 40(7): 1290-1301

FAO: Report of the Technical Consultation on International Guidelines for the Management of Deep-sea Fisheries in the High Seas, Rome. 4-8 February and 25-29 August 2008. FAO Fisheries and Aquaculture Report, 881-886 (2009)

Farmer DM and Denton RA (1985) Hydraulic control of flow over the sill in Observatory Inlet. J. Geophys Res 90(C5): 9051-9068

Fielding AH and Bell JF (1997) A review of methods for the assessment of prediction errors in conservation presence/absence models. Environmental Conservation 24: 38-49

Findlay HS, Artioli Y, Moreno-Navas J, Hennige SJ, Wicks LC, Huvenne VA, Woodward EM, Roberts JM (2013) Tidal downwelling and implications for the carbon biogeochemistry of cold-water corals in relation to future ocean acidification and warming. Global change biology19(9): 2708-19

Fleming J (1846) On the recent Scottish Madrepores, with remarks on the climatic character of the extinct races. Proceedings of the Royal Society of Edinburgh 2: 82-83

Fosså JH, Mortensen PB, Furevik DM (2002) The deep-water coral *Lophelia pertusa*. Norwegian waters: distribution and fishery impacts. Hydrobiologia: 471: 1-12

Fosså JH, Skjoldal HR, Grafton RQ, Hilborn R, Squires D, Tait M, Williams M (2010) Handbook of Marine Fisheries Conservation and Management. Oxford University Press, New York

Foster AB (1979) Phenotypic plasticity in the reef corals *Montastrea annularis* and *Siderastrea sideria*. Journal of Experimental Marine Biology and Ecology 39: 25-54

Fox A, Henry L-A, Corne DW, Roberts JM (2016) Sensitivity of marine protected area network connectivity to atmospheric variability. Royal Society Open Science 3: 160494

Frank KT, Petrie B, Fisher JA, Leggett WC (2011) Transient dynamics of an altered large marine ecosystem. Nature 477: 86-89

Frank N, Freiwald A, López Correa M, Wienberg C, Eisele M, Hebbeln D, Van Rooij D, Henriet J-P, Colin C, van Weering T, de Haas H, Buhl-Mortensen P, Roberts JM, De Mol B, Douville E, Blamart D, Hatté C (2011) Northeastern Atlantic cold-water coral reefs and climate. Geology 39: 743-746

Frederiksen R, Jensen A and Westerberg H (1992) The distribution of the scleractinian coral *Lophelia pertusa* around the Faroe Islands and the relation to internal tidal mixing. Sarsia 77: 157-171

Freiwald A (1998) Geobiology of *Lophelia Pertusa* (Scleractinia) Reefs in the North Atlantic. Universitat Bremen, Bremen

Freiwald A (2002) Reef-forming cold-water corals. In: Wefer G, Billett D, Hebbeln D, Jorgensen BB, Schluter M, van Weering T (eds) Ocean margin systems. Springer, Berlin pp 365-385

Freiwald A and Schönfeld J (1996) Substrate pitting and boring pattern *of Hyrrokkin sarcophaga* Cedhagen, 1994 (Foraminifera) in a modern deep-water coral reef mound. Marine Micropaleontology 28: 199-207

Freiwald A, Fosså JH, Grehan A, Koslow T, Roberts JM (2004) Cold-water coral reefs. UNEP-WCMC, Cambridge, UK, Biodiversity Series 22: 84

Freiwald A, Henrich R and Patzold J (1997) Anatomy of a deep-water coral reef mound from Stjernsund, west Finnmark, Northern Norway. In James NP and Clarke JAD, eds. Cool water carbonates. Tulsa: Society for Sedimentary Geology, pp 141-162

Freiwald A, Rogers A, Hall-Spencer J, Guinotte JM, Davies AJ, Yesson C, Martin CS, Weatherdon LV (2017). Global distribution of cold-water corals (version 3.0). Second update to the dataset in Freiwald et al. (2004) by UNEP-WCMC, in collaboration with Andre Freiwald and John Guinotte. Cambridge (UK): UNEP World Conservation Monitoring Centre

Freiwald A and Wilson JB (1998) Taphonomy of modern deep, cold-temperate water coral reefs. History of Biology 13: 37-52

Freiwald A, Wilson JB and Henrich R (1999) Grounding Pleistocene icebergs shape recent deep-water coral reefs. Sedimentary Geology 125: 1-8

Fujita T and Ohta S (1988) Photographic observations of the life-style of a deep- sea ophiuroid *Asteronyx loveni* (Echinodermata). Deep-Sea Research Part a-Oceanographic Research Papers 35(12): 2029-2043

Fuller SD, Murillo Perez FJ, Wareham V and Kenchington E (2008) Vulnerable Marine Ecosystems Dominated by Deep-Water Corals and Sponges in the NAFO Convention Area, Serial No N5524

Fyfe JA, Long. D, Evands D (1993) The geology of the Malin-Hebrides sea area: The Stationery Office/Tso

Gafeira J, Diaz-Doce D, Long D (2015) Semi-automated mapping and characterisation of coral reef mounds: Mingulay Reef proof of concept. British Geological Survey, Marine Geosciences Programme: Internal report IR/15/042

Gafeira J, Long D, Diaz-Doce D (2012) Semi-automated characterisation of seabed pockmarks in the central North Sea. Near Surface Geophysics 10: 303-315

Gage JD (1996) Why are there so many species in deep-sea sediments? Journal of Experimental Marine Biology and Ecology 200: 257-286

Gass and Roberts (2006) The occurrence of the cold-water coral *Lophelia pertusa* (Scleractinia) on oil and gas platforms in the North Sea: Colony growth, recruitment and environmental controls on distribution. Marine Pollution Bulletin 52: 549-559

Gass and Roberts (2010) Growth and branching patterns of *Lophelia pertusa* (Scleractinia) from the North Sea. Journal of the Marine Biological Association of the United Kingdom pp 1-5

Gehlen M, Séférian R, Jones DOB, Roy T, Roth R, Barry J, Bopp L, Doney SC, Dunne JP, Heinze C, Joos F, Orr JC, Resplandy L, Segschneider J, Tjiputra J (2014) Projected pH reductions by 2100 might put deep North Atlantic biodiversity at risk. Biogescience 11: 6955-6967

Genin A, Dayton PK, Lonsdale PF and Spiess FN (1986) Corals on seamounts peaks provide evidence of current acceleration over deep sea topography. Nature 322(6074): 59-61

Gillibrand PA, Sammes PJ, Slesser G, Adams RD (2003) Seasonal water column characteristics in the Little and North Minches and the Sea of the Hebrides. I. Physical and chemical parameters. 08/03. Fisheries Research Services Marine Laboratory, Aberdeen

Glecker PJ, Durack PJ, Stouffer RJ, Johnson GC and Forest CE (2016) Industrial-era global ocean heat uptake doubles in recent decades. Nature Climate Change 6: 394-398

Glynn PW (1997) Bioerosion and coral reef growth: a dynamic balance. In 'Life and Death of Coral Reefs' (Ed. C. Birkeland) pp 68-95

Glynn PW and Manzello DP (2015) Bioerosion and Coral Reef growth: a dynamic balance. Coral reefs in the Anthropocene pp 67-97

Gori A, Orejas C, Madurell T, Bramanti L, Martins M, Quintanilla E, Marti-Puig P, Lo Iacono C, Puis P, Requena S, Greenacre M and Gili JM (2013) Bathymetrical distribution and size structure of cold-water coral populations in the Cap de Creus and Lacaze-Duthiers canyons (northwestern Mediterranean). Biogeosciences 10: 2049-2060

Gori A, Reynaud S, Orejas C and Ferrier-Pagès (2015) The influence of flow velocity and temperature on zooplankton capture rates by the cold-water coral *Dendrophyllia cornigera*. Journal of Experimental Marine Biology and Ecology 466: 92-97

Gosse PH (1860) Actinologica Britannica. A History of the British Sea-Anemones and Corals. xi, Van Voorst, London p 362

Gotelli NJ and Ellison AM (2004) A primer of ecological statistics. Sinauer Associates, Sunderland, Massachusetts p 510

Grassle JF (1989) Species diversity in deep-sea communities. Trends in Ecology and Evolution, 4(1):12-15

Grassle JF, Brown-Leger LS, Morse-Porteous L, Petrecca R, Williams I (1985) Deep-sea fauna of sediments in the vicinity of hydrothermal vents. Bulletin of the Biological Society of Washington (6): 443-452

Gray JS (2001) Marine diversity: the paradigms in patterns of species richness examined. Scientia marina, 65(S2):41-56

Gray JS, Poore GC, Ugland KI, Wilson RS, Olsgard F, Johannessen Ø (1997) Coastal and deep-sea benthic diversities compared. Marine ecology progress series pp 97-103

Grigg RW (1965) Ecological Studies of Black Coral in Hawaii. Pacific Science 19: 244-260

Grigg RW (2001) Black coral: History of a sustainable fishery in Hawaii. Pacific Science 55: 91-299

Guihen D, White M, Lundälv T (2012) Temperature shocks and ecological implications at a cold-water coral reef. Marine Biodiversity Records 5: e68

Guihen D, White M, Lundälv T (2013) Boundary layer flow dynamics at a CWC reef. Journal of Sea Research 78: 36-44

Guinan J, Brown C, Dolan MFJ and Grehan AJ (2009) Ecological niche modelling of the distribution of cold-water coral habitat using underwater remote sensing data. Ecological Informatics 4(2): 83-92

Guinan J, Grehan AJ, Dolan MFJ, Brown C (2009) Quantifying relationships between video observations of cold-water coral cover and seafloor features in Rockall Trough, west of Ireland. Marine Ecology Progress Series 375: 125-138

Guinan J, Leahy Y, Furey T, Verbruggen K (2012) Chapter 47: Habitats at the Rockall Bank slope failure features, Northeast Atlantic Ocean. In Harris PT and Baker EK (2012) Seafloor Geomorphology as Benthic Habitat: GeoHab Atlas of seafloor geomorphic features and benthic habitats. Elsevier

Guinot D, Doumenc D and Chintiroglou CC (1995) A review of the carrying behaviour in Brachyuran crabs, with additional information on the symbioses with sea anemones. Raffles Bulletin of Zoology 43: 377-416

Guinotte J, Orr JC, Cairns S, Freiwald A, Morgan L and George R (2006) Will human-induced changes in seawater chemistry alter the distribution of deep-sea scleractinian corals? Frontiers in Ecology and the Environment 4(3): 141-146

Gunnerus JE (1768) Om nogle Norske coraller. Norske entomologisk forening 4: 38-73

Gustafsson B (1999) High frequency variability of the surface layers in the Skagerrak during SKAGEX. Continental Shelf Research 19: 1021-1047

Häkkinen S and Rhines PB (2004). Decline of subpolar North Atlantic circulation during the 1990s. Science 304: 555–559

Hall MM and Bryden HL (1982) Direct estimates and mechanisms of ocean heat transport. Deep-Sea Research Part A-Oceanographic Research Papers 29: 339- 359

Hallock P (1997) Reefs and reef limestones in Earth history. In 'Life and Death of Coral Reefs' (Ed. C Birkeland) pp 13-42

Hall-Spencer J, Allain V, Fosså JH (2001) Trawling damage to Northeast Atlantic ancient coral reefs. Proceedings of the Royal Society of London B 269: 507-511

Halpern BS, Walbridge S, Selkoe KA, Kappel CV, Micheli F, D'Agrosa C, Bruno JF, Casey KS, Ebert C, Fox HE, Fujita R, Heinemann D, Lenihan HS, Madin EMP, Perry MT, Selig ER, Spalding M, Steneck R and Watson R (2008) A global map impact on marine ecosystems. Science 319: 948-952

Hannah CG, Shore JA and Loder JW (2001) Seasonal circulation on the Western and Central Scotian Shelf. American Meteorological Society pp 591-615

Harris PT and Baker EK (2012) Chapter 4: Biogeography, benthic ecology and habitat classification schemes. In Harris PT and Baker EK (2012) Seafloor Geomorphology as Benthic Habitat: GeoHab Atlas of seafloor geomorphic features and benthic habitats. Elsevier

Harris PT and Baker EK (2012a) Chapter 1: Why map benthic habitats? In Harris PT and Baker EK (2012) Seafloor Geomorphology as Benthic Habitat: GeoHab Atlas of seafloor geomorphic features and benthic habitats. Elsevier

Harris PT and Baker EK (2012b) Chapter 2: Habitat mapping and marine management In Harris PT and Baker EK (2012) Seafloor Geomorphology as Benthic Habitat: GeoHab Atlas of seafloor geomorphic features and benthic habitats. Elsevier

Hátún H, Olsen B, Pacariz S (2017) The Dynamics of the North Atlantic Subpolar Gyre introduces predictability to the breeding success of Kittiwakes. Frontiers in Marine Science 4: 123

Hátún H, Payne M, Beaugrand G, Reid PC, Sandø AB, Drange H, Hansen B, Jacobsen JA, Bloch D (2009) Large bio-geographical shifts in the north-eastern Atlantic Ocean: from the sub-polar gyre, via plankton, to blue whiting and pilot whales. Progress in Oceanography 80: 149-162

Hátún H**,** Sandø AB, Drange H, Hansen B, Valdimarsson H (2005) Influence of the Atlantic subpolar gyre on the thermohaline circulation. Science 309: 1841-1844

Heinrich R and Freiwald A, Shipboard Party (1997) *Lophelia* reef on Sula Ridge, mid-Norwegian shelf. Cruise Report No. 288/97, IFM-GEOMAR, Kiel

Helama S, Fauria MM, Mielikäinen K, Timonen M and Eronen M (2010) Sub-Milankovitch solar forcing of past climates: Mid- and late Holocene perspectives. Geological Society of America Bulletin 122: 1981-1988

Helm KP, Bindoff NL and Church JA (2011) Observed decreases in oxygen content of the global ocean. Geophysical Research Letteers 38: L23602

Hennige S (2016) Abstract: How corals apply the goldilocks principle to engineer habitat. 6th International Symposium on Deep-Sea Corals, Boston, MA, USA, 11-16 September

Hennige S, Morrison CL, Form AU, Buscher J, Kamenos NA, Roberts JM (2014) Self-recognition in corals facilitates deep-sea habitat engineering. Scientific Reports 4: 6782

Hennige SJ, Wicks LC, Kamenos NA, Bakker DCE, Findlay HS, Dumousseaud C, Roberts JM (2014) Short-term metabolic and growth responses of the cold-water coral *Lophelia pertusa* to ocean acidification. Deep Sea Research Part II: Topical Studies in Oceanography 99: 27-35

Hennige SJ, Wicks LC, Kamenos NA, Perna G, Findlay HS, Roberts JM (2015) Hidden impacts of ocean acidification to live and dead coral framework. Proceedings of the Royal Society B. Biological Sciences 282: 10

Henry L-A and Roberts JM (2007) Biodiversity and ecological composition of macrobenthos on cold-water coral mounds and adjacent off-mound habitat in the bathyal Porcupine Sea bight, NE Atlantic. Deep Sea Research Part I 54: 654-672

Henry L-A and Roberts JM (2016) Global biodiversity in CWC reefs. Marine Animal Forests. Meteor Springer

Henry L-A, Davies AJ and Roberts JM (2010) Beta diversity of cold-water coral reef communities off western Scotland. Coral Reefs 29: 427-436

Henry L-A, Frank N, Hebbeln D, Wienberg C, Robinson L, van de Flierdt T, Dahl M, Douarin M, Morrison CL, López Correa M, Rogers AD, Ruckelshausen M, Roberts JM (2014) Global ocean conveyor lowers extinction risk in the deep sea. Deep-Sea Research Part I 88: 8-16

Henry L-A, Moreno-Navas JM, Hennige SJ, Wicks LC, Vad J and Roberts JM (2013) Cold-water coral reef habitats benefit recreationally valuable sharks. Biological Conservation 161: 67-70

Henry L-A, Stehmann M, De Clippele LH, Golding N, Roberts JM (2016) Seamount egg-laying grounds of the deepwater skate *Bathyraja richardsoni* (Garrick 1961) Journal of Fish Biology (89): 1473-1481

Henry L-A, Vad J, Findlay HS, Murillo J, Milligan R and Roberts JM (2014) Environmental variability and biodiversity of megabenthos on the Hebrides Terrace Seamount (Northeast Atlantic). Scientific Reports 4: 5589

HERMES: Hotspot Ecosystem Research on the Margins of the European Seas. FP6 Integrated project. Sustainable development, global change and ecosystems. Periodic Activity Report: Month 36 (EC Contract No. GOCE-CT-2005-511234) (2008)

Higuchi T, Fujimura H, Yuyama I, Harii S, Agostini S, Oomori T (2014) Biotic control of skeletal growth by scleractinian corals in aragonite–calcite seas. PloS one 9(3): e91021.

Hill AE, Horsburgh KJ, Garvine RW, Gillibrand PA, Slesser G, Turrell WR, Adams RD (1997) Observations of a density-driven recirculation of the Scottish coastal current in the Minch. Estuarine Coastal and Shelf Science 45 (4): 473-484

Hill MS and Hill AL (2002) Morphological plasticity in the tropical sponge *Anthosigmella varians*: responses to predators and wave energy. Biological Bulletin 202: 86-95

Hill MS, Lopez NA and Young KA (2005) Anti-predator defences in western North Atlantic sponges with evidence of enhanced defence through interactions between spicules and chemicals. Marine Ecology Progress Series 291: 93-102

Hill TM, Spero HJ, Guilderson T, LaVigne M, Clague D, Macalello S and Jang N (2011) Temperature and vital effect controls on bamboo coral (Isididae) isotope geochemistry: A test of the "lines method." Geochemistry, Geophysics, Geosystems 12(4): 1-14

Hoffmann F, Radax R, Woebken D, Holtappels M, Lavik G, Rapp HT, Schlappy ML, Schleper C, Kuypers MMM (2009) Complex nitrogen cycling in the sponge *Geodia barretti*. Environmental Microbiology 11(9): 2228-2243

Hogg MM, Tendal OS, Conway KW, Pomponi SA, Van-Soest RWM, Krautter M, Roberts JM (2010) Deep-sea sponge grounds: reservoirs of biodiversity. UNEP-WCMC Biodiversity Series, Cambridge

Holliday NP (2003) Air–sea interaction and circulation changes in the northeast Atlantic. Journal of Geophysical Research 108 (C8)

Hood KA, West LM, Northcote PT, Berridge MV, Miller JH (2001) Induction of apoptosis by the marine sponge (*Mycale*) metabolites, mycalamide A and pateamine. Apostosis 6: 207-219

Houck JE, Buddemeier RW, Chave KE (1975) Skeletal low-magnesium calcite in living scleractinian corals. Science 189: 997-999

Hovland M (1990) Do carbonate reefs form due to fluid seepage? Terra Nova 2: 8-18

Hovland M, Buhl-Mortensen P, Brattegard T, Strass P, Rokoengen K (1998) Ahermatypic coral banks off Mid-Norway: evidence for a link with seepage of light hydrocarbons. Palaios 13: 189-200

Hovland M, Ottesen D, Thorsnes T, Foss JH, Bryn P (2005) Occurrence and implications of large *Lophelia*-reefs offshore Mid Norway. Norwegian Petroleum Society Special Publications 12: 265-270

Howell KL, Holt R, Endrino IP, Stewart H (2011) When the species is also a habitat: Comparing the predictively modelled distributions of *Lophelia pertusa* and the reef habitat it forms. Biological Conservation 144: 2656-2665

Hunter T (1989) Suspension feeding in oscillating flow: the effect of colony morphology and flow regime on plankton capture by the hydroid *Obelia longissimi*. Biological Bulletin 176(1): 41-49

Hunter T (1989) Suspension feeding in oscillating flow: the effect of colony morphology and flow regime on plankton capture by the hydroid *Obelia longissimi*. Biological Bulletin 176: 41-49

Huthnance JM (1986) The Rockall slope current and shelf-edge processes. Proceedings of the Royal Society of Edinburgh 88B: 83-101

Huvenne VAI, Tyler P, Masson DG, Fisher EH, Hauton C, Huhnerbach V, Le Bas T, Wolff G (2011) A picture on the wall: innovative mapping reveals cold-water coral refuge in submarine canyon. PLos One 6(12): e28755

Inall M, Gillibrand P, Griffiths C, MacDougal N, Blackwell K (2009) On the oceanographic variability of the north-west European shelf to the west of Scotland. Journal of Marine Systems 77 (3): 210-226

IUCN (2003) Recommendations of the Vth IUCN Worlds Parks Congress, Gland: IUCN

Jenness J (2002) Surface areas and ratios from elevation grid (surfgrids.avx) extension for ArcView 3.x version 1.2. Jenness Enterprises

Jenness J, Brost B, Beier P (2013) Land facet corridor designer: Extension for ArcGIS. Jenness Enterprises

Jensen A and Frederiksen R (1992) The fauna associated with the bank-forming deep water coral *Lophelia pertusa* (Scleractinaria) on the Faroe shelf. Sarsia 77: 53-69

Johnson C, Inall M, Häkkinen S (2013) Declining nutrient concentrations in the northeast Atlantic as a result of a weakening Subpolar Gyre. Deep-Sea Research I 82: 95-107

Jones CG, Lawton JH and Shachak M (1997) Positive and negative effects of organisms as physical ecosystem engineers. Ecology 78(7): 1946-1957

Jones CG, Lawton JH, Shachak M (1994) Organisms as ecosystem engineers. Oikos 69: 373-386

Jonsson LG, Nilsson PG, Floruta F, Lundälv T (2004) Distributional patterns of macro- and megafauna associated with a reef of the CWC *Lophelia pertusa* on the Swedish west coast. Marine Ecology Progress Series 284: 163-171

Kaandorp JA (1999) Morphological analysis of growth forms of branching marine sessile organisms along environmental gradients. Marine Biology 134: 295-306

Kaandorp JA (1999) Morphological analysis of growth forms of branching marine sessile organisms along environmental gradients. J Mar Biol 134: 295-306

Keeling RF, Körtzinger A and Gruber N (2010) Ocean deoxygenation in a warming world. Annual Review of Marine Science 2: 199-229

Kenyon NH, Akhmetzhanov Am, Wheeler AJ, van Weering TCE, de Haas H and Ivanov MK (2003) Giant carbonate mud mounds in the southern Rockall Trough. Marine Geology 195(1-4): 5-30

Kitidis V, Hardman-Mountford NJ, Litt E, Brown I, Cummings D, Hartman S, Hydes D, Fishwick JR, Harris C, Martinez-Vicente V, Woodward EMS (2012) Seasonal dynamics of the carbonate system in the Western English Channel. Continental Shelf Research 42: 30-40

Knowlton N and Jackson JBC (2008) Shifting Baselines, Local Impacts, and Global Change on Coral Reefs. PLoS Biol6(2): e54

Kohler KE and Gill SM (2006) Coral Point Count with Excel extensions (CPCe): A Visual Basic program for the determination of coral and substrate coverage using random point count methodology. Computers & Geosciences 32(9): 1259-1269

Koslow JA, Boehlert GW, Gordon JDM, Haedrich RL, Lorance P, Parin N (2000) Continental slope and deep-sea fisheries: implications for a fragile ecosystem. ICES Journal of Marine Science 57: 548-557

Kostylev VE, Todd BJ, Fader GBJ, Courtney RC, Cameron GDM, Pickrill RA (2001) Benthic habitat mapping on the Scotian Shelf based on multibeam bathymetry, surficial geology and sea floor photographs. Marine Ecology Progress Series 219: 121-137

Larsson AI, Jarnegren J, Stromberg SM, Dahl MP, Lundälv T, Brooke S (2014) Embryogenesis and Larval Biology of the CWC *Lophelia pertusa*. PLoS One 9: 14

Larsson AI, Purser A (2011) Sedimentation on the cold-water coral Lophelia pertusa: Cleaning efficiency from natural sediments and drill cuttings. Marine Pollution Bulletin 62(6):1159-68

Lavaleye M, Duineveld G, Lund*ä*lv T, White M, Guihen D, Kiriakoulakis K, Wolff GA (2009) CWCs on the Tisler reef Preliminary observations on the dynamic reef environment. Oceanography 22: 76-84

Le Bas TP and Huvenne VAI (2009) Acquisition and processing of backscatter data for habitat mapping - Comparison of multibeam and sidescan systems. Applied Acoustics 70: 1248-1257

Lenihan HS, Holbrook SJ, Schmitt RJ, Brooks AJ (2011) Influence of corallivory, competition and habitat structure on coral community shifts. Ecology 92(10): 1959-1971

Levin LA and Gage JD (1998) Relationships between oxygen, organic matter and the diversity of bathyal macrofauna. Deep Sea Research Part II: Topical Studies in Oceanography 45(1-3): 129-163

Levin LA, Etter RJ, Rex MA, Gooday AJ, Smith CR, Pineda J, Stuart CT, Hessler RR, Pawson D (2001) Environmental influences on regional deep-sea species diversity. Annual Review of Ecology and Systematics 32(1): 51-93

Levin LA, Gage J, Lamont P, Cammidge L, Martin C, Patience A, Crooks J (1997) Infaunal community structure in a low-oxygen, organic-rich habitat on the Oman continental slope, NW Arabian Sea. In Responses of Marine Organisms to Their Environments; Proceedings of the 30th European Marine Biological Symposium, eds. L. Hawkins and S. Hutchinson. Southampton, UK: University of Southampton pp 223

Liaw A and Wiener M (2002) Classification and regression by random forest. R News 2(3): 18-22

Linnaeus C (1758) Systema Naturae per regna tria naturae, secundum classes, ordines, genera, species, cum characteribus, differentiis, synonymis, locis. Editio decima, reformata. Laurentius Salvius: Holmiae. ii, 824 pp.

Long D and Wilson CK (2003) Geological background to cold-water coral occurrences in the Minch. British Geological Survey, Continental Shelf and Margins Programme, Internal Report IR/03/149

Long MC, Deutsch C, Ito T (2016) Finding forced trends in oceanic oxygen. Global Biogeochemical Cycles 30: 381-397

Lundälv T and Jonsson L (2003) Mapping of deep-water corals and fishery impacts in the north-east Skagerrak, using acoustical and ROV survey techniques. Proceedings 6th Underwater Science Symposium, Aberdeen

Lundälv T, Fossa JH, Buhl Mortensen P, Jonsson L, Unnithan V (2008) Development in a trawl-damaged coral habitat (Tisler reef, NE Skagerrak during four years of trawl protection), Geohab

Lunden JJ, Georgian SE, Cordes EE (2013) Aragonite saturation states at cold- water coral reefs structured by *Lophelia pertusa* in the northern Gulf of Mexico. Limnology and Oceanography 58: 354-362

Lurton X (2002) An Introduction to Underwater Acoustics: Principles and Applications, Springer, Chichester

Mah C, Nizinski M and Lundsten L (2010) Phylogenic revision of the Hippasterinae (Goniasteridae; Asteroidae): systematics of deep sea corallivores, including one new genus and three new species. Zoological Journal of the Linnean Society 160(2): 266-301

Maier C, Hegeman J, Weinbauer MG and Gattuso JP (2009) Calcification of the cold-water coral *Lophelia pertusa* under ambient and reduced pH. Biogeosciences 6(8): 1671-1680

Masson D, Bett B, Billett D, Jacobs C, Wheeler A, Wynn R (2003) The origin of deep-water, coral-topped mounds in the northern Rockall Trough, Northeast Atlantic. Marine Geology 194(3-4): 159-180

McCullagh P and Nelder J (1989) Generalized Linear Models, Second Edition. Boca Raton: Chapman and Hall/CRC. ISBN 0-412-31760-5

McFadden CS and Collins AG (2007) The Phylum Cnidaria: A Review of Phylogenetic Patterns and Diversity 300 Years After Linnaeus 182: 127-182

McKinley IG, Baxter MS, Ellett DJ, Jack W (1981) Tracer applications of radiocaesium in the Sea of the Hebrides. Estuarine, Coastal and Shelf Science 13: 69-82

Mienis F, de Stigter HC, White M, Duineveld G, de Haas H, van Weering TCE (2007) Hydrodynamic controls on cold-water coral growth and carbonate-mound development at the SW and SE Rockall Trough Margin, NE Atlantic Ocean. Deep-Sea Research I 54(9): 1655-1674

Mienis F, van de Land C, de Stigter HC, van de Vorstenbosch M, de Haas H, Richter T, van Weering TCE (2009) Sediment accumulation on a cold-water carbonate mound at the Southwest Rockall Trough margin. Marine Geology 265(1-2): 40-50

Mienis F, van Weering T, de Haas H, de Stigter H, Huvenne VAI and Wheeler A (2006) Carbonate mound development at the SW Rockall Trough margin based on high resolution TOBI and seismic recording. Marine Geology 233(1-4): 1-1

Millennium Ecosystem Assessment: Ecosystems and Human Wellbeing: Synthesis Washington DC: World Resources Institute (2005)

Milne-Edwards H and Haime J (1857) Histoire naturelle des Coralliaires ou polypes proprement dits. Tome, 1-3 Paris

Mohn C and Beckmann A (2002) Numerical studies on flow amplification at an isolated shelf break bank, with application to Porcupine Bank. Continental Shelf Research 22: 1325-1338

Mora C, Wei CL, Rollo A, Amaro T, Baco AR, Billett D, Bopp L, Chen Q, Collier M, Danovaro R, Gooday AJ (2013) Biotic and human vulnerability to projected changes in ocean biogeochemistry over the 21st century. PLoS Biology 11(10): e1001682

Moreno-Navas JM, Miller PL, Henry L-A, Hennige SJ, Roberts JM (2014) Ecohydrodynamics of cold-water coral reefs: A case study of the Mingulay Reef Complex (Western Scotland). PLoS one 9(5)

Mortensen P and Fosså JH (2006) Species diversity and spatial distribution of invertebrates on deep water *Lophelia* reefs in Norway. Proceedings of 10th International Coral reef symposium pp 1849-1868

Mortensen P, Hovland M, Fosså J and Furevik DM (2001) Distribution, abundance and size of *Lophelia pertusa* coral reefs in mid-Norway in relation to seabed characteristics. Journal of the Marine Biological Association of the United Kingdom 81(4): 581-597

Mortensen P, Roberts JM and Sundy RC (2000) Video-assisted grabbing: a minimally destructive method of sampling azooxanthellate coral banks. Journal of the marine biological association of the UK. 80: 365-366

Mortensen PB (2001) Aquarium observations on the deep-water coral *Lophelia pertusa* (L., 1758) (Scleractinia) and selected associated invertebrates. Ophelia 54: 83-104

Mortensen PB and Buhl-Mortensen L (2004) Distribution of deep-water gorgonian corals in relation to benthic habitat features in the Northeast Channel (Atlantic Canada). Marine Biology 144(6): 1223-1238

Mortensen PB and Buhl-Mortensen L (2005) Morphology and growth of the deep-water gorgonians *Primnoa resedaeformis* and *Paragorgia arborea*. Marine Biology 147(3): 775-788

Mortensen PB and Fosså JH (2006) Species diversity and spatial distribution of invertebrates on deep-water *Lophelia* reefs in Norway. Proceedings of 10th International Coral Reef Symposium pp 1849-1868

Mortensen PB and Rapp HT (1998) Oxygen and carbon isotope ratios related to growth line patterns in skeletons of *Lophelia pertusa* (L) (Anthozoa, Scleractinia): implications for determination of linear extension rates. Sarsia 83: 433-446

Mortensen PB, Buhl-Mortensen L, Gebruk AV, Krylova EM (2008) Occurrence of deep-water corals on the Mid-Atlantic Ridge based on MAR-ECO data. Deep Sea Research Part II Topical Studies of Oceanography 55: 142-152

Mueller CE, Larsson AI, Veuger B, Middelburgh JJ, van Oevelen D (2014) Opportunistic feeding on various organic food sources by the cold-water coral *Lophelia pertusa*. Biogeosciences, 11(1): 123-133

Naumann MW, Orejas C, Wild C and Ferrier-Pages C (2011) First evidence for zooplankton feeding sustaining key physiological processes in a scleractinian cold-water coral. Journal of Experimental Biology 214: 3570-3576

Noé S, Titschack J, Freiwald A, Dullp W-C (2006) From sediment to rock: diagenetic processes of hardground formation in deep-water carbonate mounds of the NE Atlantic. Facies 52: 183-208

Norse EA ed. (1993) Global Marine Biological Diversity: A strategy for building conservation into decision making. Washington DC: Island Press

Nybø S, Certain G, Skarpaas O (2011) The Norwegian Nature Index 2010. DN-report 2011-1

Opresko DM (2001) Revision of the Antipatharia (Cnidaria: Anthozoa). Part I: establishment of a new family, Myriopathidae. Zoologische Mededelingen (Leiden) 75: 147-174

Opresko DM (2002) Revision of the Antipatharia (Cnidaria: Anthozoa). Part II: Schizopathidae. Zoologische Mededelingen (Leiden) 76: 411-442

Opresko DM (2003) Revision of the Antipatharia (Cnidaria: Anthozoa). Part III: Cladopathidae. Zoologische Mededelingen (Leiden) 77: 495-536

Opresko DM (2004) Revision of the Antipatharia (Cnidaria: Anthozoa). Part IV: establishment of a new family, Aphanipathidae. Zoologische Mededelingen (Leiden) 78: 209-240

Opresko DM (2005a) New genera and species of antipatharian corals (Cnidaria: Anthozoa) from the North Pacific. Zoologische Mededelingen (Leiden) 79-2: 129-165

Opresko DM (2005b) A new species of antipatharian coral (Cnidaria: Anthozoa: Antipatharia) from the southern California Bight. Zootaxa 852: 1-10

Opresko DM (2006) Revision of the Antipatharia (Cnidaria: Anthozoa). Part V. Establishment of a new family, Stylopathidae. Zoologische Mededelingen Leiden 80-4: 109-138

Opresko DM and de Laia Loiola L (2008) Two new species of *Chrysopathes* (Cnidaria: Anthozoa: Antipatharia) from the Western Atlantoc. Zootaxa 1707: 49-59

Orejas C and Jiménez (2017) Marine Animal Forests: The builders of the Oceans- Part I: Coral architecture from the tropics to the poles, from the shallow to the deep. ISBN: 9783319210131

Orejas C, Ferrier-Pages C, Reynaud S, Gori A, Beraud E, Tsounis G, Allemand D and Gili JM (2011) Long-term growth rates of four Mediterranean cold-water coral species maintained in aquaria. Marine Ecology Progress Series 398: 149-155

Orejas C, Gori A and Gili JM (2008) Growth rates of live *Lophelia pertusa* and *Madrepora oculata* from Mediterranean Sea maintained in aquaria. Coral Reefs 27: 255-255

Orejas C, Gori A, Rad- Menédez C, Last KS, Davies AJ, Beveridge CM, Sadd D, Kiriakoulakis K and White U (2016) The effect of flow speed and food size on the capture efficiency and feeding behaviour of the cold-water coral *Lophelia pertusa.* Journal of Experimental Marine Biology and Ecology 481: 34–40

Orr JC, Fabry VJ, Aumont O, Bopp L, Doney SC, Feely RA, Gnanadesikan A, Gruber N, Ishida A, Joos F, Key RM, Lindsay K, Maier-Reimer E, Matear R, Monfray P, Mouchet A, Najjar RG, Plattner G-K, Rodgers KB, Sabine CL, Sarmiento JL, Schlitzer R, Slater RD, Totterdell IJ, Weirig M-F, Yamanaka Y and Yool A (2005) Anthropogenic ocean acidification over the twenty-first century and its impact on calcifying organisms, Nature 437: 681-686

Ottersen G, Olsen E, van der Meeren GI, Dommasnes A, Loeng H (2011) The Norwegian plan for integrated ecosystem-based management of the marine environment in the Norwegian Sea. Marine Policy 35: 389-398

Pachauri RK, Allen MR, Barros VR, Broome J, Cramer W, Christ R, Church JA, Clarke L, Dahe Q, Dasgupta P and Dubash NK (2014) Climate Change 2014: Synthesis Report. Contribution of Working Groups I, II and III to the Fifth Assessment Report of the Intergovernmental Panel on Climate Change, Pachauri, R, Meyer, L, eds., Geneva, Switzerland: IPCC p 151

Palardy JE, Grottoli AG, Matthews KA (2005) Effects of upwelling, depth, morphology and polyp size on feeding in three species of Panamanian corals. Marine Ecology Progress Series 300: 79-89

Patterson MR (1984) Patterns of prey capture in the soft coral *Alcyonium siderium*. Biological Bulletin 167: 613-629

Pauly DC, Dalsgaard J, Froese R, Torres F (1998) Fishing down the marine food webs. Science 279: 860-863

Phillips SJ, Dudik M, Elith J, Graham CH, Lehmann A, Leathwick J, Ferrier S (2009) Sample selection bias and presence-only distribution models: implications for background and pseudo-absence data. Ecological Applications 19(1): 181-197

Pontoppidan E (1755) The natural history of Norway. A Linde, London. Roberts, M. 1997. Coral in deep water. New Scientist 2100: 40-43

Porter JW (1976) Autotrophy, heterotrophy, and resource partitioning in Caribbean reef-building corals. The American Naturalist 110: 731-742

Primack RB (2006) Essentials of conservation biology. Chapter 3: Where is the world's biological diversity found? Sunderland, Mass: Sinauer Associates.

Purkey SG and Johnson GC (2010) Warming of global abyssal and deep Southern Ocean waters between the 1990s and 2000s: Contributions to global heat and sea level rise budgets. Journal of Climate 23: 6336-6351

Purser A and Thomsen L (2012) Monitoring strategies for drill cutting discharge in the vicinity of cold-water coral ecosystems. Marine Pollution Bulletin, 64(11): 2309-2316

Purser A, Bergmann M, Lundälv T, Ontrup J, Nattkemper TW (2009) Use of machine-learning algorithms for the automated detection of CWC habitats: a pilot study. Marine Ecology Progress Series 397: 241-251

Purser A, Larsson AI, Thomsen L, van Oevelen D (2010) The influence of flow velocity and food concentration on *Lophelia pertusa* (Scleractinia) zooplankton capture rates. Journal of Experimental Marine Biology and Ecology 395: 55-62

Purser A, Orejas C, Gori A, Unnithan V, Thomsen L (2013) Local variation in the distribution of benthic megafauna species associated with CWC reefs on the Norwegian margin. Continental Shelf Research 54: 37-51

Purser A, Thomsen L (2012) Monitoring strategies for drill cutting discharge in the vicinity of cold-water coral ecosystems. Marine pollution bulletin 64(11):2309-16

R Development Core Team (2013) R: A language and environment for statistical computing. R Foundation for Statistical Computing, Vienna, Austria

Raes M and Vanreusel A (2005) The metazoan meiofauna associated with a cold-water coral degradation zone in the Porcupine Seabight (NE Atlantic). In Cold-water Corals and Ecosystems, ed. Freiwald A and Roberts JM. Berlin Heidelberg: Springer pp 821-847

Read JF (2001) CONVEX-91: Water masses and circulation of the Northeast Atlantic subpolar gyre, Progress in Oceanography 48: 461-510

Reidenbach MA, Monismith SG, Koseff JR, Yahek G and Genin A (2006) Boundary layer turbulence and flow structure over a fringing coral reef. Limnology and Oceanography 51(5): 1956-1968

Reitner J (2005) Calcifying extracellular mucus substances (EMS) of *Madrepora oculata* - a first geobiological approach. CWCs and Ecosystems pp 731-744

Rengstorf AM, Grehan A, Yesson C, Brown C (2012) Towards High-Resolution Habitat Suitability Modelling of Vulnerable Marine Ecosystems in the Deep-Sea: Resolving Terrain Attribute Dependencies. Marine Geodesy 35: 343-361

Rengstorf AM, Yesson C, Brown C, Grehan AJ (2013) High-resolution habitat suitability modelling can improve conservation of vulnerable marine ecosystems in the deep sea. Journal of Biogeography 40: 1702-1714

Resolution adopted by the General Assembly. 61/105. Sustainable fisheries, including through the 1995 Agreement for the Implementation of the Provisions of the United Nations Convention on the Law of the Sea of 10 December 1982 relating to the Conservation and Management of Strad- dling Fish Stocks and Highly Migratory Fish Stocks, and related instruments. Ref.: A/Res/61/105. United Nations, New York, 2006

Ritchie JD, Gatliff RW, Richards PC (1999) "Early Tertiary magmatism in the offshore NW UK margin and surrounds". In Fleet AJ and Boldy SAR Petroleum geology of Northwest Europe: Proceedings of the 5th conference, held at the Barbician Centre, London Geological Society. Pp 581 ISBN 978-1-86239-039-3

Roark EB, Guilderson TP, Dunbar RB, Fallon SJ and Mucciarone DA (2009) Extreme longevity in proteinaceous deep- sea corals. Proceedings of the National Academy of Sciences of the United States of America 106: 5204-5208

Robert K, Jones DOB, Roberts JM and Huvenne VAI (2016) Improving predictive mapping of deep-water habitats: Considering multiple model outputs and ensemble techniques. Deep-Sea research part I 113: 80-89

Roberts CM (2002) Deep impact: the rising toll of fishing in the deep sea. Trends in Ecology and Evolution 17: 242-245

Roberts J, Brown C, Long D, Wilson C, Bates C, Mitchell A, Service M (2004) Mapping inshore coral habitats, the MINCH project. Scottish Association for Marine Science, Oban 115

Roberts JM (2005) Reef-aggregation behaviour by symbiotic eunicid polychaetes from cold-water corals: Do worms assemble reefs? Journal of the Marine Biological Associations of the United Kingdom 85: 813-819

Roberts JM (2013) Changing Oceans Expedition 2013. RRS James Cook 073 Cruise Report 224

Roberts JM and Anderson RM (2002) A new laboratory method for monitoring deep-water coral polyp. Hydrobiologia 471: 143-148

Roberts JM and Cairns SD (2014) Cold-water corals in a changing ocean. Current opinion in Environmental Sustainability 7: 188-126

Roberts JM, Brown CJ, Long D, Bates CR (2005) Acoustic mapping using a multibeam echosounder reveals cold-water coral reefs and surrounding habitats. Coral Reefs 24: 654-669

Roberts JM, Davies AJ, Henry L-A, Dodds LA, Duineveld GCA, Lavaleye MSS, Maier C, van Soest RWM, Bergman MJN, Huehnerbach V, Huvenne VAI, Sinclair DJ, Watmough T, Long D, Green SL, van Haren H (2009b) Mingulay reef complex: an interdisciplinary study of cold-water coral habitat, hydrography and biodiversity. Marine Ecology Progress Series 397: 139-151

Roberts JM, Henry L-A, Long D and Hartley JP (2008) Cold-water coral reef frameworks, megafaunal communities and evidence for coral carbonate mounds on the Hatton Bank, north east Atlantic. Facies 54(3): 297-316

Roberts JM, Long D, Wilson JB, Mortensen PB, Gage JD (2003) The cold-water coral *Lophelia pertusa* (Scleractinia) and enigmatic seabed mounds along the north-east Atlantic margin: are they related? Marine Pollution Bulletin 46: 7-20

Roberts JM, Wheeler A, Freiwald A and Cairns SD (2009a) Cold-water corals: the biology and geology of deep-sea coral habitats, Cambridge University Press.

Rodhe J. (1996) On the dynamics of the large-scale circulation of the Skagerrak. Journal of Sea Research 35, 9–21.

Rogan J, Franklin J, Stow D, Miller J, Woodcock C, Roberts D (2008) Mapping land-cover modifications over large areas: A comparison of machine learning algorithms. Remote Sensing of Environment 112: 2272-2283

Rogers A. (2004) The biology, ecology and vulnerability of deep-water coral reefs. International Union for Conservation of Nature pp 13

Rogers AD (1999) The biology of *Lophelia pertusa* (Linnaeus 1758) and other deep-water reef-forming corals and impacts from human activities. International Review of Hydrobiology 84: 315-406

Rogers AD and Gianni M (2010) The implementation of UNGA Resolutions 61/ 105 and 64/72 in the management of deep-sea fisheries on the high seas. Report Prepared for the Deep-Sea Conservation Coalition, International Programme on the State of the Ocean 97

Rosenberg R, Dupont S, Lundalv T, Skold HN, Norkko A, Roth J, Stach T and Thorndyke M (2005) Biology of the basket star *Gorgonocephalus caputmedusa* (L.). Marine Biology 1: 43-50

Ross R and Howell K (2013) Use of predictive habitat modelling to assess the distribution and extent of the current protection of 'listed' deep-sea habitats. Diversity and Distributions 19: 433-445

Rossi S, Bramanti L, Gori A, Orejas C (2017) An overview of the Animal forests of the world. Marine Animal Forests ISBN 978-3-319-21011-7

Rotjan RD and Lewis SM (2008) Impact of coral predators on tropical reefs. Marine Ecology Progress Series 367: 73-91.

Ruhl HA and Smith KL 2004 Shifts in deep-sea community structure linked to climate and food supply. Science 305: 513-515

Rützler K and Muzik K (1993) *Terpios hoshinota*, a new cyanobacteriosponge threatening Pacific reefs. Sci Mar 57: 395-403

R*ü*tzler K and Muzik K (1993) *Terpios hoshinota*, a new cyanobacteriosponge threatening Pacific reefs. Scientia Marina 57: 395-403

Salcedo-Sanz S, Cuadra L, Vermeij MJA (2016) A review of computational intelligence techniques in coral reef-related applications. Ecological Informatics 32: 107-123

Sanders HL and Hessler RR (1969) Ecology of the deep-sea benthos. Science, 163(3874): 1419-1424

Santavy DL, Courtney LA, Fisher WS, Quarles RL and Jordan SJ (2013) Estimating surface area of sponges and gorgonians as indicators of habitat availability on Caribbean coral reefs. Hydrobiologia 707(1): 1-16

Savidge G, Lennon HJ (1987) Hydrography and phytoplankton distribution in north-west Scottish waters. Continental Shelf Research 7: 45–66

Sayago-Gil M, Durán-Muñoz P, Murillo FJ, Díaz-del-Río-Español V, Serrano-López A (2012) Chapter 55: A study of geo-morphological features of the sea bed and the relationship to deep sea communities on the western slope of Hatton Bank (NE Atlantic Ocean). In Harris PT and Baker EK (2012) Seafloor Geomorphology as Benthic Habitat: GeoHab Atlas of seafloor geomorphic features and benthic habitats. Elsevier

Schlacher TA, Rowden AA, Dower JF, Consalvey M (2010) Recent advances in seamount ecology: A contribution to the census of marine life. Marine Ecology 31: 1-241

Sebens KP (1997) Adaptive responses to water flow: morphology, energetics and distribution of reef corals. Proceedings 8th International Coral Reef Symposium 2: 1053-1058

Sebens KP, Grace SP, Helmuth B, Maney EJ and Miles JS (1998) Water flow and prey capture by three scleractinian corals, *Madracis mirabilis*, *Montastrea cavernoss* and *Porites porites* in a field enclosure. Marine Biology 131(2): 347-360

Sebens KP, Johnson AS (1991) Effects of water-movement on prey capture and distribution of reef corals. Hydrobiologia 226:91–101

Sgubin G, Swingedouw D, Drijfhout S, Mary Y, Bennabi A (2017) Abrupt cooling over the North Atlantic in modern climate models. Nature Communications 8: 14375

Sherwood O and Edinger E (2009) Ages and growth of some deep-sea gorgonian and antipatharian corals of Newfoundland and Labrador. Canadian Journal of Fisheries and Aquatic sciences 66: 142-152

Shihavuddin ASM, Gracias N, Garcia R, Gleason ACR, Gintert B (2013) Image-based coral reef classification and thematic mapping. Remote Sensing 5: 1809-1841

Simpson JH and Hill AE (1986) The Scottish coastal current. In, The Role of Freshwater Outflow in Coastal Marine Ecosystems (Skreslet, S., ed.) NATO ASI Series. Springer-Verlag, Berlin, Heidelberg. G7: 295-308

Smith KL, Ruhl HA, Kahru M, Huffard CL and Sherman AD (2013) Deep ocean communities impacted by changing climate over 24 y in the abyssal northeast Pacific Ocean. Proceedings of the National Academy of Science of the USA 110: 19838-19841

Smith LW, Barshis D and Birkeland C (2007) Phenotypic plasticity for skeletal growth, density and calcification of *Porites lobata* in response to habitat type. Coral Reefs 26: 559-567

Soetaert K, Mohn C, Rengstorf A, Grehan A and van Oevelen D (2016) Ecosystem engineering creates a direct nutritional link between 600-m deep cold-water coral mounds and surface productivity. Scientific Reports 6: 35057

Spalding MD and Greenfell Am (1997) New estimates of global and regional coral reef areas. Coral Reefs 16:225-230

Squires DF (1959) Deep-sea corals collected by the Lamont Geological Observatory. 1. Atlantic corals. American Museum Novitates 1965: 1-42

Stevenson A and Rocha C (2013) Evidence for bioerosion of deep-water corals by echinoids in the Northeast Atlantic. Deep Sea research part I: Oceanographic research papers 71: 73-78

Stigebrandt A (1983) A model for the exchange of water and salt between the Baltic and the Skagerrak. Journal of Physical Oceanography 13: 411-427

Stockwell DRB and Peterson AT (2002) Effects of sample size on accuracy of species distribution models. Ecological Modelling 148: 1-13

Stokes MD and Deane GB (2009) Automated processing of coral reef benthic images. Limnology and Oceanography 7: 157-168

Stramma L, Johnson GC, Sprintall J and Mohrholz V (2008) Expanding oxygen-minimum zones in the tropical oceans. Science 320: 655-658

Stramma L, Prince ED, Schmidtko S, Luo J, Hoolihan JP, Visbeck M, Wallace DW, Brandt P, Körtzinger A (2012) Expansion of oxygen minimum zones may reduce available habitat for tropical pelagic fishes. Nature Climate Change 2: 33-37

Stramma L, Schmidt S, Levin LA and Johnson GC (2010) Ocean oxygen minima expansions and their biological impacts. Deep-Sea Research 210: 587595

Strömberg SM (2016) Early life history of the cold-water coral *Lophelia pertusa*—with implications for dispersal. PhD thesis, University of Gothenburg.

Stuiver M and Becker B (1993) High precision decadal calibration of the radiocarbon time scale, AD 1950-6000 BC. In Stuiver M, Long A and Kra RS, eds. Calibraion 1993. Radiocarbon 35(1): 35-65

Suchanek TH, Carpenter RC, Witman JD, Harvell CD (1983) Sponges as important space competitors in deep Caribbean coral reef communities. In: Reaka ML (ed) the ecology of deep and shallow coral reefs. Symposia series for undersea research 1 NOAA/ NURP, Rockville, MD, p 55-60

Sullivan B, Faulkner DJ, Webb L (1983) Siphonodictine, a metabolite of the burrowing sponge *Siphonodictyon sp.* that inhibits coral growth. Science 211: 1175-1176

Sutherland DS (editor) (1982). Igneous Rocks of the British Isles. Chichester: John Wiley and Sons. ISBN 0-471-27810-6.

Sweetman AK, Thurber AR, Smith CR, Levin LA, Mora C, Wei C-L, Gooday AJ, Jones DOB, Rex M, Yasuhara M, Ingels J, Ruhl HA, Frieder CA, Danovaro R, Würzberg L, Baco A, Grupe BM, Pasulka A, Meyer KS, Dunlop KM, Henry L-A, Roberts JM (2017) Major impacts of climate change on deep-sea benthic ecosystems. Elementa Science of the Anthropocene 5: 4

Taviani M, Remia A, Corselli C, Freiwald A, Malinverno E, Mastrototaro F, Savini A and Tursi A (2005) First geo-marine survey of living cold-water *Lophelia* reefs in the Ionian Sea (Mediterranean basin). Facies 50: 409-417

Tazioli S, Bo M, Boyer M, Rotinsulu H and Bavestrello G (2007) Ecological observations of some common antipatharian corals in the marine park of Bunaken (North Sulawesi, Indonesia). Zoological Studies 46: 227-241

Thiagarajan N, Gerlach D, Roberts ML, Burke A, McNichol A, Jenkins WJ, Subhas AV, Thresher RE and Adkins JF (2013) Movement of deep-sea coral populations on climatic timescales. Paleoceanography 28: 227-236

Thiem O, Rvagnan E, Fosså JH, Berntsen J (2006) Food supply mechanisms for cold water corals along a continental shelf edge. Journal of Marine Systems 60: 207-219

Thomas E and Gooday AJ (1996) Cenozoic deep-sea benthic foraminifers: Tracers for changes in oceanic productivity? Geology 24: 355-358

Todd BJ, Fader GBJ, Courtney RC, Pickrill R.A (1999) Quaternary geology and surficial sediment processes, Browns Bank, Scotian Shelf, based on multibeam bathymetry. Marine Geology 162: 165-172

Todd PA (2008) Morphological plasticity in scleractinian corals. Biological Reviews 83(3): 315-337

Tong R, Purser A, Guinan J, Unnithan V (2013) Modelling the habitat suitability for deep-water gorgonian corals based on terrain variables. Ecological Informatics 13: 123-132

Troffe PM, Levings CD, Piercey GE, Keong V (2005) Fishing gear effects and ecology of the sea whip (*Halipteris willemoesi* (Cnidaria: Octocorallia: Pennatulacea)) in British Columbia, Canada: preliminary observations. Aquatic Conservation of Freshwater Ecosystems 15:523-533

Tsounis G, Orejas C, Reynaud S, Gili JM, Allemand D, Ferrier-Pages C (2010) Prey-capture rates in four Mediterranean cold-water corals. Marine Ecology Progress Series 398: 149-155

Turley C, Blackford J, Widdicombe S, Lowe D, Nightingale P (2006) Reviewing the impact of increased atmospheric CO_2 on oceanic pH and the marine ecosystem. Avoiding dangerous climate change 8: 65-70

Turley CM, Roberts JM, Guinotte JM (2007) Corals in deep-water: will the unseen hand of ocean acidification destroy cold-water ecosystems? Coral Reefs 26: 445-448

United Nations, Department of Economic and Social Affairs, Population Division (2017) World Population Prospects: The 2017 Revision, Key Findings and Advance Tables. Working Paper No. ESA/P/WP/248

Vad J, Orejas C, Moreno-Navas J, Findlay HS, Roberts JM (2017) Assessing the living and dead proportions of cold-water coral colonies: implications for deep-water Marine Protected Area monitoring in a changing ocean. PeerJ *5*: e3705

van den Hove S and Moreau V (2007) Ecosystems and Biodiversity in Deep Waters and High Seas: A scoping report on their socio-economy, management and governance. Switzerland: UNEP-WCMC

Van Haren H, Mienis F, Duineveld G and Lavaleye M (2014) High-resolution temperature observations of a trapped nonlinear diurnal tide influencing cold-water corals on the Logachev mounds. Progress in oceanography 125: 16-25

van Oevelen F, Duineveld G, Lavaleye M, Mienis F, Soetaert K and Heip CHR (2009) The cold-water coral community as a hot spot for carbon cycling on continental margins: A food-web

analysis from Rockall Bank (northeast Atlantic). Limnology and Oceanography 54(6): 1829-1844

Van Soest RWM and De Voogd NJ (2015) Sponge species composition of north-east Atlantic cold-water coral reefs compared in a bathyal to inshore gradient. Journal of the Marine Biological Association of the United Kingdom 95(7): 1461-1474

Van Soest RWM, Cleary DFR, de Kluijver MJ, Lavaleye MS, Maier C, van Duyl FC (2007) Sponge diversity and community composition in Irish bathyal coral reefs. Contributions to Zoology 76: 121-142

Van Weering TCE, de Haas H, de Stigter HC, Lykke-Andersen H and Kouvaev I (2003) Structure and development of giant carbonate mounds at the SW and SE Rockall Trough margins, NE Atlantic Ocean. Marine Geology 198(1-2): 67-81

Victorero L, Blamart D, Pons-branchu E, mavrogordato MN, Huvenne VAI (2016) reconstruction of the formation history of the Darwin Mounds, N Rockall trough: How the dynamics of a sandy contourite affected cold-water coral growth. Marine Geology 378: 186-195

Wagner D, Luck DG, Toonen RJ (2012) The Biology and Ecology of Black Corals (Cnidaria: Anthozoa: Hexacorallia: Antipatharia). Advances in Marine Biology 63: 67

Wagner D, Pochon X, Irwin L, Toonen RJ and Gates RD (2011). Azooxanthellate? Most Hawaiian black corals contain Symbiodinium. Proceedings of the Royal Society B 278: 1323-1328.

Wagner H, Purser A, Thomsen L, Jesus CC, Lundälv T (2011) Particulate organic matter fluxes and hydrodynamics at the Tisler CWC reef. Journal of Marine Systems 85: 19-29

Wahab MAA, de Nys R, Whalan S (2011) Larval behaviour and settlement cues of a brooding coral reef sponge. Coral Reefs 30: 451-460

Wainwright S, Dillon JR (1969) On orientation of sea fans (Genus Gorgonia). Biological Bulletin 136(1): 130-139

Wainwright S, Dillon JR (1969) On orientation of sea fans (Genus Gorgonia). Biological Bulletin 136(1): 130-139

Wang Y-P, Tew KS, Kuo J, Ko F-C and Meng P-J (2012) The effect of coral polyp sizes and coral exudates on picoeukaryote dynamics in a controlled environment. Scientia Marina 76(3): 455-461

Watling L (2005) The global destruction of bottom habitats by mobile fishing gear. Marine conservation biology: the science of maintaining the sea's biodiversity. Island Press, Washington, DC pp 198-210

Watling L and Norse EA (1998) Disturbance of the seabed by mobile fishing gear: a comparison to forest clear-cutting. Conservation Biology 12: 1180-1197

Watling L, France SC, Pante E and Simpson A (2011) Biology of Deep-Water Octocorals. Advances in Marine Biology 60: 41-122

Weaver PP, Boetius A, Danovaro R, Freiwald A, Gunn V, Heussner S, Morato T, Schewe I and van den Hove S (2009) The future of integrated deep-sea research in Europe: the HERMIONE Project. Oceanography 22(1): 178-191

Weiss AD (2001) Topographic positions and landforms analysis (Conference poster) ESRI International User Conference, San Diego, USA

Wheeler AJ, Beyer A, Freiwald, de Haas H, Huvenne VAI, Kozachenko M, Olu-Le Roy K and Opderbecke (2007) Morphology and environment of cold-water coral carbonate mounds on the NW European margin. International Journal of Earth Science 96(1): 37-56

Wheeler AJ, Kozachenko M, Beyer A, Foubert A, Huvenne VAI, Klages M, Masson DG, Olu-Le Roy K, Thiede J, (2005) Sedimentary processes and carbonate mounds in the Belgica mound province, Porcupine Seabight, NE Atlantic, in: Freiwald, A., Roberts, J.M. (Eds), Cold-water corals and Ecosystems. Springer-Verlag, Berlin Heidelberg pp 571-603

White M, Mohn C, Stigter H, Mottram G (2005) Deep-water coral development as a function of hydrodynamics and surface productivity around the submarine banks of the Rockall Trough, NE Atlantic. CWCs and ecosystems pp 503-514

White M, Roberts JM and van Weering T (2007) Do bottom-intensified diurnal tidal currents shape the alignment of carbonate mounds in the NE Atlantic? Geo-Marine Letters 27(6): 391-397

White MC, de Stigter H, de Haas H and van Weering T (2003) Physical dynamics at the Rockall Trough margin that influence the carbonate mound and coral reef ecosystem. Final Report ACES program, deliverable 11-1: 46

Wicksten MK (1985) Carrying behavior in the family Homolidae (Decapoda: Brachyura). Journal of Crustacean Biology 5(3): 476-479

Wijgerde T, Spijkers P, Larruppannan E, Verreth JAJ and Singa R (2012) Water flow affects zooplankton feeding by the scleractinian coral *Galaxea fascicularis* on a polyp and colony level. Journal of Marine Biology ID 854849

Wild C, Hoegh-Guldberg O, Naumann MS, Colombo-Pallotta MF, Ateweberhan M, Fitt, WK, Iglesias-Prieto R, Palmer C, Bythell JC, Ortiz J-C, Loya Y, van Woesik R. (2011) *Climate change impedes scleractinian corals as primary reef ecosystem engineers.* Marine and Freshwater Research 62(2): 205-215

Wild C, Huettel M, Klueter A, Kremb SG, Rasheed MY, Jørgensen BB (2004) Coral mucus functions as an energy carrier and particle trap in the reef ecosystem. Nature 428(6978): 66-70

Wild C, Wehrmann LM, Mayr C, Schottner SI, Allers E, Lundälv T (2009) Microbial degradation of CWC-derived organic matter: potential implication for organic C cycling in the water column above Tisler Reef. Aquatic Biology 7(1-2): 71-80

Wild C, Woyt H and Huettel M (2005) Influence of coral mucus on nutrient fluxes in carbonate sands. Marine Ecology Progress Series 287: 87-98

Williams B, Risk MJ, Ross SW, Sulak KJ (2006) Deep-water antipatharians: proxies of environmental change. Geology 34: 773-776

Wilson JB (1979) 'Patch' development of the deep-water coral *Lophelia pertusa* (L.) on Rockall Bank. Journal of the Marine Biological Association of the United Kingdom 59(1): 165-177

Wilson JB (1979) Distribution of the coral *Lophelia pertusa* (L) Prolifera (Pallas) in the northeast Atlantic. Journal of the Marine Biology Association of the United Kingdom 59: 149-164

Wilson MFJ, O'Connel B, Brown C, Guinan JC and Grehan AJ (2007) Multiscale Terrain Analysis of Multibeam Bathymetry Data for Habitat Mapping on the Continental Slope. Marine Geodesy 30: 3-35

Winther N and Johannessen J (2006) North Sea circulation: Atlantic inflow and its destination. Journal of Geophysical Research-Oceans 111, C12018

Wisshak and *Rüggeberg* (2005) Colonisation and bioerosion of experimental substrates by benthic formainiferans from euphotic to aphotic depths (Kosterfjord, SW Sweden) Facies 52(1): 1-17

Wisshak M, Freiwalkd A, Lundälv T, Gektidis M (2005) The physical niche of the bathyal *Lophelia pertusa* in a non-bathyal setting: environmental controls and palaeoecological implications. CWCs and Ecosystems. Springer, berlin Heidelberg pp 979-1001

Wood (1993) Nutrients, predation and the history of reef-building. Palaios 8: 526-543

Yamamoto A, Abe-Ouchi A, Shigemitsu M, Oka A, Takahashi K, Ohgaito R, Yamanaka Y (2015) Global deep ocean oxygenation by enhanced ventilation in the Southern Ocean under long-term global warming. Global Biogeochemical Cycles 29: 1801-1815

Yasuhara M, Cronin TM, deMenocal PB, Okahashi H and Linsley BK (2008) Abrupt climate change and col- lapse of deep-sea ecosystems. Proceedings of the National Academy of Science of the USA 105: 1556-1560

Yasuhara M, Doi H, Wei CL, Danovaro R and Myhre SE (2016) Biodiversity-ecosystem functioning relationships in long-term time series and palaeoecological records: deep sea as a test bed. Philosophical Transactions of the Royal Society B 371: 20150282

Zhang C (2015) Applying data fusion techniques for benthic habitat mapping and monitoring in a coral reef ecosystem. ISPRS Journal of Photogrammetry and Remote Sensing 104: 213-223

Zibrowius H (1980) Les scleractinaires de la Mediterranee et de l'Atlantique nord- oriental. Memoires de la Institut Oceanographique, Monaco 11: 284